Doctoral Thesis Dissertation


Università degli Studi della Tuscia
Dipartimento DAFNE
Corso di Dottorato di Ricerca in Scienze delle Produzioni Vegetali e Animali – XXX ciclo
Settore scientifico disciplinare BIO/04

Aix-Marseille Université
UFR Sciences ISM2, Équipe BioSciences
École doctorale des Sciences de la Vie et de la Santé ED62
Doctorat: Biologie - Spécialité Biologie Végétale


# Reinforcing and broadening wheat resistance against *Fusarium* diseases by a barley deoxynivalenol detoxifying UDP-glucosyltransferase and its pyramiding with ectopic glycosidase inhibitors


Candidate: Giulia Mandalà



Dissertation submitted April 24, 2018


Pr. Francesco Favaron, Università degli Studi di Padova (Reviewer)

Dr. Isabelle Oswald, INRA Toulouse (Reviewer)

Pr. Daniela Bellincampi, Università degli Studi La Sapienza (Examiner)

Pr. Renato D'Ovidio, Università degli Studi della Tuscia (Thesis director)

Pr. Carla Ceoloni, Università degli Studi della Tuscia (Thesis director)

Pr. Thierry Giardina, Aix-Marseille Université (Thesis co-director)

Dr. Marc Maresca, Aix-Marseille Université (Thesis co-director)

PhD Course coordinator: Pr. Stefania Masci

**In memory of Professor Renato D'Ovidio**

We all miss your guidance,
but your teachings will always light our paths.
Thank you, Renato.

Ai miei nonni.

A nonno Marco,
che ha sempre spronato i nostri studi perché
li riteneva importanti per il nostro futuro,
la sua preoccupazione e gioia più grande.

A nonno Delis,
che con la sua fantasia animava la mia creatività
e con la sua pazienza mi insegnava la bontà.
Grazie per essere rimasto a darmi coraggio quel primo giorno.

A nonna Lia,
che ha sempre creduto nelle mie potenzialità
e nel raggiungimento di grandi traguardi;
spero di portartene sempre di nuovi.
(E chissà se il tempo non ti darà ragione…!)

A nonna Pina,
che gioiva con orgoglio ad ogni nuovo successo,
incoraggiava con amore ad ogni difficoltà
e soffriva in silenzio la lontananza dei suoi 'gioielli'.
Sei stata tu il nostro tesoro più grande.

# Acknowledgement

Firstly, I would like to thank Professor Renato D'Ovidio, my thesis director, for all the knowledge and experience he has imparted to me. My passion and fascination for research is in a large part down to him. He was not only an excellent researcher, but also a great mentor and a fantastic person. I am grateful for the opportunity of being his student over the course of my studies. With great sorrow for us all, he passed away on March 2, 2017.

My gratitude to Pr. Carla Ceoloni, who kindly agreed to step in to supervise the final part of my studies. She supported me in this difficult period, showing compassion and expertise that enabled me to complete my work. Her dedication to research is an inspiration and I am extremely thankful.

Furthermore, I would like to thank Pr. Thierry Giardina and Dr. Marc Maresca, my thesis co-directors in France, who gave me the opportunity to join their laboratories and improve my skills.

I would also like to acknowledge Pr. Stefania Masci, coordinator of the PhD course, for her help whenever needed and for the excellent organization of the PhD course.

My immense and sincere appreciation to my colleagues from the laboratory of Plant Physiology and Biotechnology, who made this PhD experience great: Dr. Silvio Tundo, Dr. Ilaria Moscetti, Dr. Alessandra Zega and Dr. Raviraj Kalunke. And also to Mr. Claudio Perani for his technical support.

In addition, I would like to address my thanks also to Dr. Michela Janni and Dr. Chiara Volpi, for critically reviewing my manuscript. I deeply appreciated their willingness to help and to share their expertise with me.

My gratitude must also go to the current and past members of the research teams at Tuscia University: Pr. Domenico Lafiandra, Dr. Francesco Sestili, Dr. Anna Pucci, Dr. Ljiljiana Kuzmanovic, Sandra Bitti, Dr. Linda Botticella, Dr. Rocco Caracciolo, Alessandro Riccini, Dr. Davide Santagati, Dr. Francesca Imperatori, Sara Francesconi, and all the other members.

Many thanks also to the members of the Équipe BiosCiences and the Platforme AVB, especially Dr. Cendrine Nicoletti and Dr. Ange Pujol.

Moreover, I would like to thank Pr. Francesco Favaron (University of Padova), for kindly providing the *F. graminearum* strains used in this work, and all the members of the Proteomics and Mass Spectrometry laboratory, especially its director Pr. Lello Zolla, for metabolite analyses.

Thanks to the University of Tuscia ('Bando Dottorato XXX ciclo'), for supporting this research, and to French-Italian University (Grant 'Bando Vinci 2016, Cap. II: Contributi di mobilità per tesi di Dottorato in cotutela') for supporting my staying in France.

I would also like to take this opportunity to show my gratitude to all my friends at home, in Viterbo and all around the world, for always being by my side. An additional thanks to my friend Roberta, the best friend one could ever imagine, and to "my girls" Martina, Franca and Roberta, who can make the distance of more than 2,000 km between us disappear.

A special thanks to my partner and friend Silvio: thank you for your patience and for supporting me over the years.

Finally, thanks to my incredible family, who have always supported me and believed in me.

Last, but first for me, my immense gratitude to my parents, Filippo and Concetta, and my sister Roberta: none of this would have been possible without your love and encouragement. Thank you.

# Abstract

*Fusarium* diseases, including Fusarium head blight (FHB) and Fusarium crown rot (FCR) represent major agricultural problems worldwide, causing reduction of grain yield and quality and food safety. The latter issue is associated with grain contamination by mycotoxins, particularly deoxynivalenol (DON), responsible for health problems in humans and animals. DON is a protein synthesis inhibitor, acting as a virulence factor during pathogenesis. DON glycosylation, forming DON-3-β-D-glucoside (D3G) by specific UDP-glucosyltransferases (UGTs), is the main mechanism involved in enhancing plant tolerance to DON. Improvement of FHB resistance is a major target in both bread and durum wheat, the latter being especially vulnerable, as effective resistance sources are particularly limited. Previous studies demonstrated that the expression of the barley *HvUGT13248* gene confers resistance to FHB in bread wheat (Li et al. 2015, MPMI 28:1237-46), reducing disease symptoms of almost 60% as compared to control plants.

To highlight DON-detoxification potential in FHB control, we produced transgenic durum wheat plants constitutively expressing the *HvUGT13248* gene (Ubi-UGT) and bread wheat plants expressing it in flower tissues (Lem-UGT). Transgenic plants were used in infection experiments with *F. graminearum* for evaluating FHB severity, as compared to wild-type plants. Our results showed that the *HvUGT13248* gene determines in durum wheat Ubi-UGT plants a significant reduction of FHB symptoms (up to 30%) during early to mid stages of infection progress. Notably, Ubi-UGT plants showed much higher DON-to-D3G conversion ability (100x D3G/DON ratio) and a considerably reduced total DON content in semolina. Lem-UGT bread wheat plants also showed reduction of FHB severity. In particular, the floral-specific expression highlighted a dose-dependent efficacy of the UGT detoxification mechanism. Indeed, two transgenic lines with different levels of transcript expression showed that, while the higher expressing line determined a significant reduction of FHB symptoms (up to 40%) at all infection stages, only a slight reduction of FHB severity was observed in the lower expressing line, as compared to non-transgenic plants. Although DON-to-D3G conversion increased (10x) in transgenic plants, total DON in flours resulted not different or even higher than the control. This possibly reflects the importance of timing and control of transgene expression in toxin detoxification and thus in restraining DON production.

In addition, we verified for the first time the possible involvement of the DON-detoxifying approach in limiting FCR disease induced by *F. culmorum*. When challenged with the pathogen at the seedling stage, Ubi-UGT durum wheat plants demonstrated significant reduction of almost 50% of FCR symptoms throughout the infection timing, as compared to non-transgenic plants. This result represents the first report of FCR resistance improvement associated with overexpression of an UGT involved in DON-detoxification.

Finally, in order to investigate if the combination of different mechanisms could further improve *Fusarium* disease resistance, we stacked transgenes controlling the DON-to-D3G conversion and the inhibition of cell wall degrading enzymes by glycosidase inhibitors in the same wheat genotype. To this aim, in the cross progeny of separate transgenic lines, durum

wheat UGT+PMEI and bread wheat UGT+PGIP double-transgenic genotypes were selected. UGT+PMEI plants constitutively express the genes *HvUGT13248* and *AcPMEI*, coding for a kiwi pectin methylesterase inhibitor. UGT+PGIP plants express in floral tissues the *HvUGT13248* gene and constitutively the *PvPGIP2* gene, coding for a bean polygalacturonase inhibiting protein. The PMEI contribution in UGT+PMEI plants resulted ineffective against FCR disease, the double-transgenic seedlings exhibiting similar level of symptom reduction to the UGT single transgenic line. On the other hand, both UGT+PMEI and UGT+PGIP plants exhibited increased resistance against FHB, further reducing FHB symptoms during infection, as compared to the separate transgenic lines.

In conclusion, our results demonstrate that DON-detoxification confers a broad-spectrum resistance against DON-producing fungi. Moreover, pyramiding genes controlling different resistance mechanisms can further reinforce the host response. This approach may be particularly attracting for breeding programs aimed at improving and broadening the plant reaction to pathogen attacks in a sustainable manner.

Key words: FHB, FCR, transgenic plants, *HvUGT13248,* DON-detoxification, gene pyramiding.

# Riassunto

Le malattie causate dai funghi del genere *Fusarium*, comunemente chiamate fusariosi, includono la fusariosi della spiga (FHB) e il marciume del colletto (FCR). Le fusariosi rappresentano uno dei maggiori problemi in agricoltura a livello mondiale, in quanto causano sia una riduzione della resa e della qualità della granella, sia problemi di sicurezza alimentare. Quest'ultimi sono associati soprattutto alla contaminazione dei semi da parte di micotossine, principalmente deossinivalenolo (DON), responsabile di problemi alla salute umana e animale. Il DON è un inibitore della sintesi proteica che agisce inoltre come fattore di virulenza nella patogenesi. Il meccanismo principale per aumentare la tolleranza della pianta al DON è considerato la detossificazione mediante glicosilazione, effettuata da specifiche UDP-glucosiltransferasi (UGT) che portano alla formazione della molecola D3G (DON-3-β-D glucoside). Il miglioramento della resistenza alla FHB è uno dei principali obiettivi sia per il frumento tenero che per il frumento duro; quest'ultimo risulta particolarmente vulnerabile in quanto risorse naturali di resistenza sono decisamente limitate. È stato dimostrato in studi precedenti (Li et al. 2015, MPMI 28:1237-46) che l'espressione costitutiva in frumento tenero del gene *HvUGT13248* di orzo conferisca resistenza alla FHB, riducendo i sintomi tipici della malattia circa del 60% rispetto alle piante controllo.

Al fine di mettere in luce le potenziali proprietà della detossificazione del DON nel miglioramento della resistenza alla FHB, in questo lavoro sono state prodotte delle piante transgeniche sia di frumento duro, esprimenti in maniera costitutiva il gene *HvUGT13248* (piante Ubi-UGT), sia di frumento tenero, esprimenti lo stesso gene nei tessuti fiorali (piante Lem-UGT). Le prime sono state inizialmente utilizzate per valutare la sintomatologia di FHB rispetto alle piante non transgeniche, dopo infezione col fungo *F. graminearum*. I risultati ottenuti mostrano una significativa riduzione dei sintomi (fino al 30%) durante gli stadi iniziali ed intermedi della progressione dell'infezione e inoltre le piante Ubi-UGT hanno dimostrato non solo una notevole capacità di conversione del DON in D3G (rapporto D3G/DON in farine aumentato di 100 volte), ma anche un significativo abbassamento del contenuto totale di DON nella semola. Anche le piante di frumento tenero Lem-UGT hanno mostrato una riduzione dei sintomi di FHB, evidenziando inoltre un'efficacia del meccanismo di detossificazione di tipo dose-dipendente. Infatti, in questo caso le due linee transgeniche utilizzate mostravano livelli di espressione dell'UGT ectopica differenti e, mentre la linea con maggiore espressione ha ridotto fino al 40% la sintomatologia di FHB rispetto al controllo non transgenico durante tutte le fasi di infezione, la linea che mostrava un minore livello di espressione l'ha ridotta solo parzialmente e solo in alcuni stadi. In entrambi i casi, nelle linee transgeniche la conversione del DON in D3G è risultata notevolmente aumentata (circa 10 volte) ma il contenuto totale di DON nelle farine non è risultato differente rispetto alle farine derivate dalle piante non transgeniche, possibilmente riflettendo l'importanza del controllo e della tempistica di espressione del transgene per detossificare la micotossina al fine di contenerne efficacemente la produzione.

Inoltre, per la prima volta in questo lavoro è stato valutato il possibile coinvolgimento del meccanismo di detossificazione del DON per limitare la FCR causata dal fungo *F. culmorum*. A

tal fine, le piante Ubi-UGT di frumento duro sono state infettate col suddetto fungo allo stadio di plantule, dimostrando una riduzione circa del 50% dei sintomi di FCR durante tutti gli stadi dell'infezione. Questo lavoro costituisce dunque la prima osservazione del coinvolgimento della detossificazione del DON ad opera di UGT, associato al miglioramento della resistenza alla malattia FCR.

Infine, allo scopo di valutare se la combinazione di meccanismi di difesa differenti potessero ulteriormente migliorare la resistenza alle fusariosi, abbiamo combinato nello stesso genotipo transgeni coinvolti nella conversione del DON in D3G e nell'inibizione degli enzimi fungini che degradano la parete cellulare, tramite inibitori delle glicosidasi. A questo scopo sono state incrociate differenti linee con singoli transgeni, ottenendo genotipi con i doppi transgeni UGT+PMEI in frumento duro, e UGT+PGIP in frumento tenero. In particolare, le piante UGT+PMEI esprimono costitutivamente i geni *HvUGT13248* e *AcPMEI* (un inibitore di kiwi delle pectin metil esterasi), mentre le piante UGT+PGIP esprimono i geni *HvUGT13248* e *PvPGIP2* (un inibitore di fagiolo delle poligalatturonasi), rispettivamente nei tessuti fiorali e in maniera costitutiva. I risultati delle analisi di infezione hanno mostrato che la PMEI non è efficace nel contrastare la malattia FCR in quanto le piante UGT+PMEI presentano livelli di resistenza simili alla linea parentale Ubi-UGT. D'altra parte, entrambi i genotipi con doppi transgeni UGT+PMEI e UGT+PGIP hanno invece dimostrato una resistenza alla malattia FHB superiore rispetto alle linee parentale con singoli transgeni.

In conclusione, i risultati ottenuti dimostrano sia che la detossificazione del DON può conferire un ampio spettro di resistenza contro funghi che producono questa micotossina, che la piramidazione di geni coinvolti in meccanismi di resistenza differenza può ulteriormente contribuire nel migliorare la risposta dell'ospite. Questi approcci possono inoltre essere particolarmente interessanti per programmi di miglioramento genetico volti, in maniera sostenibile, all'incremento e all'ampliamento dello spettro di resistenza a diversi patogeni.

Parole chiave: FHB, FCR, piante transgeniche, *HvUGT13248*, detossificazione del DON, piramidazione genica.

# Résumé

Les maladies du blé causées par *Fusarium* sont communément appelées fusarioses. Parmi ces dernières, la brulure de l'épi (Fusarium head blight (FHB)) et la pourriture de la tige (Fusarium crown rot (FCR)), entrainent une réduction du rendement de production et de la qualité du blé. Ces infections posent mais également des problèmes de sécurité alimentaire liés à la présence dans les grains infectés de molécules affectant la santé de l'Homme et des animaux appelées mycotoxines, le plus représenté étant le déoxynivalénol (DON). Le DON est un inhibiteur de la synthèse protéique qui agit comme un facteur de virulence durant l'infection du blé par *Fusarium*. La glycosylation du DON en D3G (DON-3-β-D-glicoside) catalysée par des UDP-glycosyltransférases (UGTs) est le principal mécanisme de protection des plantes vis-à-vis de sa toxicité. Améliorer la résistance du blé aux fusarioses que ce soit le blé panifiable (bread wheat) ou le blé dur (durum wheat) est de première importance, essentiellement pour le blé dur qui est particulièrement vulnérable aux fusarioses du fait d'un nombre limité de sources de résistance. Des études antérieures ont montrées que l'expression du gène d'orge *HvUGT13248* confère une résistance du blé panifiable à la fusariose (Li et al. 2015, MPMI 28:1237-46) réduisant les symptômes de la maladie d'approximativement 60 % par rapport aux plantes contrôles non infectées.

Pour confirmer le rôle potentiel de la détoxification du DON dans la lutte contre les fusarioses du blé, nous avons produit des plants de blé durs exprimant de manière ubiquitaire et constitutive le gène *HvUGT13248* (Ubi-UGT) ainsi que des plants de blé panifiables exprimant ce gène uniquement au niveau du tissu floral (Lem-UGT). Les plantes transgéniques ont ensuite été utilisées au cours d'expériences d'infection par *F. graminearum* avant évaluation de la sévérité des symptômes et comparaison avec les symptômes observés sur plantes sauvages. Nos résultats montrent que l'expression du gène *HvUGT13248* réduit significativement les symptômes de fusariose de l'épi (jusqu'à 30 %) pour le blé dur durant les stades précoces et médians de l'infection. Cette résistance est associée à une capacité accrue des plantes Ubi-UGT à convertir le DON en D3G (100 fois plus que les plantes sauvages) associée à une réduction notable du niveau de DON dans la semoule obtenue à partir de ces grains. Une diminution de la sévérité de la fusariose de l'épi a également été observée avec Les blés panifiables transgéniques Lem-UGT. Nos résultats ont montré une corrélation entre les niveaux d'expression de l'UGT et le niveau de protection observé. Ainsi, alors qu'une expression élevée du gène réduit de 40% les symptômes de la fusariose de l'épi à tous les stades de l'infection, seule une faible réduction des symptômes a été observée pour les plantes exprimant faiblement le gène. De manière surprenante, alors que la capacité de conversion des plantes transgéniques Lem-UGT est multipliée par 10, le niveau de DON dans la farine issue de leurs grains n'est pas diminué, voir augmenté, comparé au blé sauvage, montrant l'importance du moment et du lieu d'expression de l'UGT dans la détoxification du DON et le contrôle de sa production.

Outre l'effet de l'expression de l'UGT sur la fusariose de l'épi causée par *F. graminearum*, nous avons également évalué l'effet de l'expression du transgène sur la fusariose des tiges causée par *F. culmorum*. Nos résultats montrent que l'expression transgénique

constitutive/ubiquitaire de l'UGT par le blé dur (Ubi-UGT) au stade de plantule réduit de près de 50 % les symptômes de la fusariose des tiges à tous les stades de l'infection comparé aux plantes sauvages. Ce résultat montre, pour la première fois, que l'expression transgénique d'UGT est associée à une résistance à la fusariose des tiges.

Finalement, afin d'évaluer si l'expression de plusieurs facteurs de résistance pouvait améliorer la résistance du blé aux fusarioses, nous avons généré des plants de blé exprimant à la fois l'enzyme de conversion du DON en D3G mais également des inhibiteurs de glycosidases qui sont impliquées dans la dégradation de la paroi cellulosique. Ont été générés des plants de blés durs UGT+PMEI et des plants de blés panifiables UGT+PGIP. Les plantes UGT+PMEI expriment de manière constitutive / ubiquitaire le gène *HvUGT13248* codant pour l'UGT d'orge et le gène *AcPMEI* qui code pour un inhibiteur protéique de pectine méthylestérase de kiwi. Les plantes UGT+PGIP quant à elles expriment dans leur tissu floral le gène *HvUGT13248* et de manière constitutive / ubiquitaire le gène *PvPGIP2* codant pour un inhibiteur protéique de polygalacturonase d'haricot. Nos résultats montrent que l'expression du PMEI par les plantes UGT+PMEI n'a pas amélioré la résistance du blé à la fusariose de la tige ; les plantules doubles transgènes montrant les mêmes niveaux de symptômes que les plantules de blé n'exprimant que l'UGT. Par contre, les plantes UGT+PMEI et UGT+PGIP ont montré une résistance accrue à la fusariose de l'épi, réduisant de manière plus importante les symptômes comparés aux souches simple transgène.

En conclusion, nos résultats démontrent que l'expression de système de détoxification du DON confère une résistance à large spectre contre les moisissures productrices de DON. De plus, la co-expression de plusieurs gènes associés à des mécanismes de résistance différents peut renforcer la résistance de l'hôte à l'infection. Cette approche pourrait être particulièrement attractive au cours de programmes de sélection de plantes visant à améliorer et élargir la résistance des plantes aux attaques de pathogènes.

Mots clés: FHB, FCR, plants transgéniques, *HvUGT13248*, détoxification du DON, pyramidation des gènes

# Index

# List of abbreviations

**Simbols**

§: Paragraph.

♀: Female.

♂: Male.

**#**

15ADON: 15-Acetyl deoxynivalenol.

2,4-D: 2,4-dichlorophenoxyacetic acid.

3ADON: 3-Acetyl deoxynivalenol.

4ANIV: 4-Acetyl nivalenol.

**A**

AB: Alamar Blue.

ABC: ATP-binding cassette.

AcPMEI: *Actinidia chinensis* pectin methylesterase.

AMP: antimicrobial peptide

ANOVA: Analysis of variance.

*AtPDF*: *Arabidopsis thaliana* plant defensin

AVR: Avirulence.

AX: Arabinoxylans.

**B**

BR: brassinosteroid.

BW: *Triticum aestivum* cultivar Bobwhite.

**C**

CAZymes: Carbohydrate activity enzymes.

CE: Carbohydrate esterase.

cv: cultivar.

CWDE: Cell wall degrading enzymes.

**D**

D3G: deoxynivalenol-3-β-D-glucoside.

DAMP: Danger associated molecular pattern.

DH: Doubled haploid.

DNA: Deoxyribonucleic acid.

DOM-1: De-epoxy deoxynivalenol.

DON: Deoxynivalenol.

dpi: days post-infection.

**E**

ET: Ethylene.

ETI: Effector trigger immunity.

ETS: Effector trigger susceptibility.

**F**

F: Filial generation.

FAO: Food and Drug Administration.

*Fc*iRNA*Tri6*: *F. culmorum* iRNA *TRI6* mutant.

FCR: Fusarium Crown Rot.

Fg: Homogenate of *Fusarium graminearum* mycelium.

Fg 3827: *Fusarium graminearum* strain 3827.

Fg 8/1: *Fusarium graminearum* strain 8/1.

Fg PH1: *Fusarium graminearum* strain PH1.

*FgΔfgl1*: lipase-deficient mutant *Δfgl1.*

FGL1: *Fusarium graminearum* lipase 1.

*FgΔpg1*: *F. graminearum Δpg1* mutant.

*FgΔpme1*: *F. graminearum Δpme1* mutant.

*FgΔpgΔxyr*: *F. graminearum Δpg1* and *Δpme1* double mutant.

*FgΔTri5*: *F. graminearum Δtri5* or trichothecene- or DON- deficient mutant.

Fig: Figure.

FHB: Fusarium Head Blight.

*FpΔTri5*: *F. pseudograminearum* DON-nonproducing mutant.

*Fp*PG: *Fusarium phyllophilum* polygalacturonase

**G**

GalA: Galacturonic acid.

GAX: Glucuronoarabinoxylan.

GFP: Green fluorescent protein.

GH: Glycoside hydrolase.

GM: Genetically modified.

GSH: Glutathione.

GT: Glycosyltransferase.

GX: Glucuronoxylans.

**H**

h: hour.

HG: homogalacturonan.

HR: Hypersensitive response.

HvUGT13248: *Hordeum vulgare* UDP-glucosyltransferase 13248.

**J**

JA: Jasmonic acid.

**L**

LTP: Lipid transfer protein.

**M**

M: mean.

MAMP: microbe associated molecular pattern.
MeJa: Methyl jasmonate.
min: minute.
MS: Murashige and Skoog.
Mt: Million tonnes.

**N**

NAA: 1-Naphthaleneacetic acid.
NB-LRR: Nucleotide-binding leucine-rich repeat.
NIL: Near-isogenic line.
NIV: Nivalenol.

**O**

OG: Oligogalacturonide.

**P**

PBS: Phosphate Buffer Solution.
PCD: Plant cell death.
PCR: Polymerase chain reaction.
PDA: Potato Destrose Agar.
PDF: Plant defensin.
PFT: Pore-forming toxin.
PG: Polygalacturonase.
PGIP: Polygalacturonase inhibitor protein.
PL: Polysaccharide lyase.
PME: pectin-methylesterase.
PMEI: Pectin-methylesterase inhibitor.
ppm: parts per million.
PPT: phosphinotricin.
PR: Pathogenesis-related.
*PR1*: *Pathogenesis-related 1* gene.
PRR: Pattern recognition receptors.
PSPG: Plant secondary product glycosyltransferase.
PTI: PAMP-triggered immunity.
PvPGIP2: *Phaseolus vulgaris* polygalacturonase inhibiting protein 2.

**Q**

*q*RT-PCR: quantitative real-time PCR
QTL: Quantitative trait loci.

**R**

R: Resistance gene/protein.
RG: Rhamnogalacturonan.
Rha: Rhamnose.
RNA: Ribonucleic acid.
RNAi: RNA interference.
ROS: Reactive oxygen species.
RT-PCR: Reverse Transcriptase PCR.

**S**

SA: Salicylic acid.
SAR: Systemic immunity.
SDS-PAGE: Sodium dodecyl sulphate polyacrylamide gel electrophoresis.
SE: Standard error.
spp.: species.
subsp.: subspecie.
SV: *Triticum durum* cultivar Svevo.

**T**

T: Transgenic generation.
*TaPDR1*: *Triticum aestivum* pleiotropic drug resistance 1.
*TaUGT12887*: *Triticum aestivum* UDP-glucosyltransferase 12887.
*TaUGT3*: *Triticum aestivum* UDP-glucosyltransferase 3.
TAXI: Triticum aestivum xylanase inhibitor.
TLP: Thaumatin-like protein.
TLXI: Thaumatin-like xylanase inhibitor.

**U**

UDP: Uridine diphosphate.
UGT: UDP-dependent glucosyltransferase.

**V**

VIGS: Virus-induced gene silencing.
vs: versus.

**W**

wt*Fc*: *F. culmorum* wild-type.
wt*Fg*: *F. graminearum* wild-type.
wt*Fp*: *F. pseudograminearum* wild-type.

**X**

XI: Xylanase inhibitor.

# List of figures

# List of tables

# 1. Introduction

## 1.1 The wheat plant

Wheat and human history began since remote time; indeed, wild wheat was one of the first cereals to be domesticated in the Fertile Crescent, between 12,000 and 10,000 years ago, during the transition from hunting-gathering of food to settled agriculture. Nowadays, wheat, together with maize and rice, is the most important food grain source for humans, providing almost 20% of food calories worldwide, and its cultivation occupies more land than any other commercial crop.

FAO's forecast for global wheat production in 2017 stands at 743 million tonnes (Mt), more than the latest record of nearly 724 million tonnes in 2014 (FAO 2017). The five major wheat producing countries in 2013 were China (almost 121 Mt), India (93 Mt), United States of America (58 Mt), Russia (52 Mt) and France (38 Mt) (FAOSTAT 2014).

After the "Green revolution" (1960s), annual wheat production has gained over 400% in the developing world. Currently, with global human population expected to exceed 9 billion by 2050, the new challenge is to increase wheat production by about 70% to meet future demands. However, intensive crop production often leads to loss of soil fertility, declining input use-efficiency, increasing environments that are highly favourable to pests, leading to an ever increasing need for effective pesticides (FAO 2016).

Wheat grains are composed by around 70% carbohydrates, 13% water, 10-13% proteins, vitamins and minerals. Even if wheat proteins have a low quality for human nutrition, due to deficiency of some essential amino acids, they confer to the gluten, made of wheat flour and water, exceptional viscoelastic proprieties, essential for processing wheat in a broad range of products, from bread to pasta and many others. This is one of the essential key factors for wheat success worldwide, together with its adaptability to a wide range of pedo-climatic conditions, the use of mechanical supports from production to transformation and the possibility to easily harvest and store grains.

Today, mainly two wheat species are cultivated all over the world: the hexaploid wheat *Triticum aestivum* and the tetraploid wheat *Triticum turgidum* ssp. *durum* (or *T. durum*).

### 1.1.1 Origin

Wheat (*Triticum* spp.) belongs to the Triticeae tribe of the *Pooideae* subfamily of grasses, together with rye (*Secale* spp.) and barley (*Hordeum* spp.), from which it diverged 11 and 7 million years ago, respectively (Huang et al. 2002).

During domestication, the selection from wild populations gave advantage to genetic traits leading to superior yield (e.g., larger seeds and spikes), free-threshing state (seeds released from the glumes at threshing) and tough rachis (no disarticulation of dried inflorescence at maturity) (Kilian et al. 2007). The origin of cultivated wheats is based on interspecific hybridization events between different species belonging to *Triticum* and *Aegilops* genera, followed by spontaneous chromosome doublings, leading to the cultivated allopolyploid *Triticum* species. The wild and cultivated wheats include diploid (einkon), tetraploid (emmer and durum wheat) and, more recently, hexaploid species (bread wheat). The *Triticum* and *Aegilops* genera contain 13 diploid and 18 polyploid species. The diploid ones contain eight distinct genomes, named: A (A and $A^b$/$A^m$), D, S (S, $S^s$, $S^b$, $S^l$, $S^{sh}$), M, C, U, N, and T. Moreover, two additional genomes, named B and G, are present in polyploid wheats, whose diploid progenitors are not known (Huang et al. 2002).

Among *Triticum* genus, the diploid wheats are *T. monococcum* ($A^mA^m$; wild form: *T. boeoticum*, $A^bA^b$) and *T. urartu* (AA; only wild form). The tetraploid wheats include two species: *T. turgidum* (AABB), which includes the wild ssp. *dicoccoides* and several cultivated subspecies, among which *T. turgidum* ssp. *durum* (syn. durum wheat), and *T. timopheevii* (AAGG). Finally, the hexaploid wheats are *T. aestivum* (AABBDD; syn. bread wheat), with many subspecies, and *T. zhukovskyi* ($A^mA^mAAGG$) (Huang et al. 2002).

Bread wheat (AABBDD) has no direct wild hexaploid progenitor; it arose from allopolyploidization occurred only 8,000 years ago between *T. turgidum* ssp. *dicoccoides* (AABB) and the wild diploid *Ae. tauschii* (DD). The AABB donor, in turn, arose from hybridation occurred less than 0.5 million year ago between the wild diploid *T. urartu* (AA) and a wild diploid from the *Sitopsis* section of the *Aegilops* genus. The donor species of the B genome is still debated, but many evidences indicate *Ae. speltoides* (SS) as the main candidate (Dvorak and Zhang 1990). Moreover, also the D genome origin has been reconsidered in recent studies, which indicate a homoploid hybridization between A and B genomes leading to the rise of the modern *Ae. tauschii* ancestor (Marcussen et al. 2014; Sandve et al. 2015), and hybridization(s) with *Sitopsis* genome(s) (Li et al. 2015b, 2015a).

### 1.1.2 Phenological phases and morphology

Wheat is a monocot cereal; it is usually classified as winter or spring type depending on cold request for flowering. Winter wheat development is promoted by exposure of the seedlings to temperatures between 3°/8° C; instead, spring wheat does not require exposure to cold temperatures for normal development. The life cycle of wheat can be divided into different phenological phases: germination, seedling establishment and leaf production, tillering and head differentiation, stem and head growth, head emergence and flowering, grain filling, and maturity (Fig. **1**).

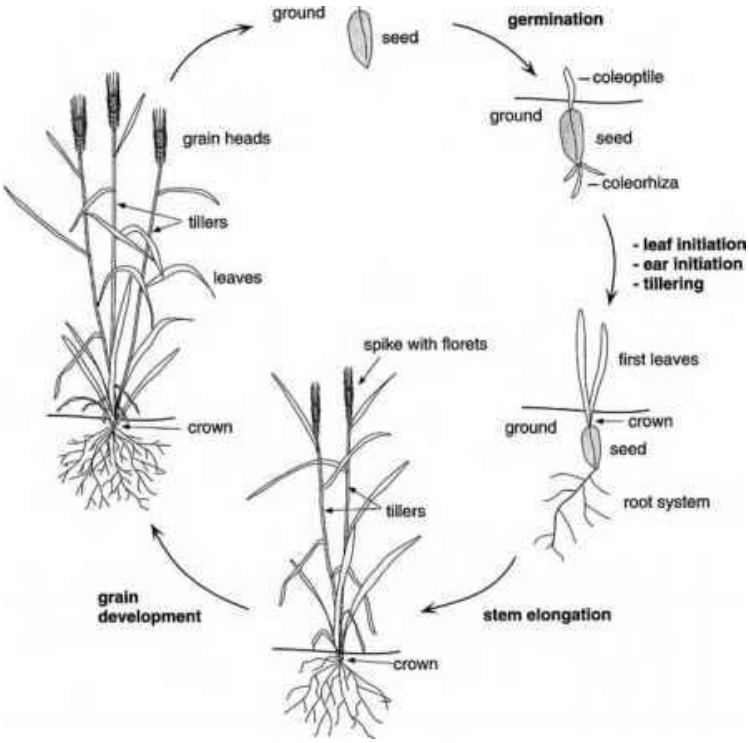


Fig. **1**. Schematic illustration of wheat life cycle.
Adapted from Kirby et al. (1987). Line drawing by Tim F. Knight.

Among the available developmental classifications, the Freak, Zadoks and Haun scales are usually employed. All scales describe growth and developmental stages by a numerical code. Here, Zadoks scale (Zadoks et al. 1974) is adopted, since it provides the most detailed and precise description of wheat growth stages. The scale uses a two-digit code, in which the first digit describes the nine main stages of development, from germination to kernel ripening, and the second one further subdivides each main growth stage (Table **1**).

Table **1.** Condensed summary of the Zadoks two-digit code system for growth staging in wheat (Zadoks et al. 1974).
Adapted from: Simmons et al., available at: http://www.extension.umn.edu/agriculture/small-grains/growth-and-development/spring-wheat/index.html.

| Zadoks code | | Description |
|---|---|---|
| **Principal stage** | **Secondary stage** | |
| **0** | | **Germination** |
| | 0 | Dry kernel |
| | 1 | Start of imbibition (water absorption) |
| | 5 | Radicle emerged |
| | 7 | Coleoptile emerged |
| | 9 | Leaf just at coleoptile tip |
| **1** | | **Seeding development** |
| | 0 | First leaf through coleoptile |
| | 1 | First leaf at least 50% emerged |
| | 2 | Second leaf at least 50% emerged |
| | 3 | Third leaf at least 50% emerged |
| | 4 | Fourth leaf at least 50% emerged |
| | 5 | Fifth leaf at least 50% emerged |
| **2** | | **Tillering** |
| | 0 | Main shoot only |
| | 1 | Main shoot plus 1 tiller visible |
| | 2 | Main shoot plus 2 tillers |
| | 3 | Main shoot plus 3 tillers |
| | 4 | Main shoot plus 4 tillers |
| | 5 | Main shoot plus 5 tillers |
| **3** | | **Stem elongation** |
| | 1 | First node detectable |
| | 2 | Second node detectable |
| | 3 | Third node detectable |
| | 7 | Flag leaf just visible |
| | 9 | Flag leaf collar just visible |
| **4** | | **Boot** |
| | 1 | Flag leaf sheath extending |
| | 3 | Boot just beginning to swell |
| | 5 | Boot swollen |
| | 7 | Flag leaf sheath opening |
| | 9 | First awns visible |
| **5** | | **Head emergence** |
| | 1 | First spikelet of head just visible |
| | 3 | One-fourth of head emerged |
| | 5 | One-half of head emerged |
| | 7 | Three-fourths of head emerged |
| | 9 | Head emergence complete |

| Zadoks code | | Description |
|---|---|---|
| **Principal stage** | **Secondary stage** | |
| **6** | | **Flowering** |
| | 1 | Beginning of flowering |
| | 5 | Half of florets have flowered |
| | 9 | Flowering complete |
| **7** | | **Milk development in kernel** |
| | 1 | Kernel watery ripe |
| | 3 | Early milk |
| | 5 | Medium milk |
| | 7 | Late milk |
| **8** | | **Dough development in kernel** |
| | 3 | Early dough |
| | 5 | Soft dough |
| | 7 | Hard dough, head losing green colour |
| | 9 | Approximate physiological maturity |
| **9** | | **Ripening** |
| | 1 | Kernel hard (difficult to divide with thumbnail) |
| | 2 | Kernel cannot be dented by thumbnail, harvest ripe |

Germination begins when water is available to the caryopsis. It absorbs the 35-40% of its weight and, if temperature and oxygenation are favourable, it germinates. First, the central embryonic radicle protrudes from the kernel, followed by the coleoptile and other primary roots. After emergence, the first leaf breaks the coleoptile and expands, followed by leakage of the remaining leaves (Baldoni and Giardini 2000).

Tillering is a phenomenon of branching, starting from the 4-5 leaves stage and consists of the development of secondary shoots, called tillers. Tillers develop from buds present in the crown area of the main stem. The number of tillers depends on many factors, including the genotype, cultivation conditions, sowing date and temperatures. However, usually only two to four tillers are able to produce fertile spikes.

Wheat inflorescence, the spike (syn. head or ear), begins differentiation before stem elongation, when internodes increase in length thanks to the proliferation of meristematic tissue at the base of each node. When all lower internodes are developed, the spike, already fully formed, is pushed through the sheath of the last leaf, called flag leaf, resulting in an enlargement, which identifies the boot stage.

A few days after ear emergence, or heading, the flowering stage occurs, starting from the central spikelet, moving upwards and downwards. The major axis of the spike is called rachis and it holds two rows of spikelets in alternating order and a single terminal one. Spikelets are placed on a short axis, the rachilla, which joins them to the rachis. The spikelet can present from 3 to 8 floret, included between two external glumes at the base of each spikelet. A pair of flowering glumes encloses each floret; the outer is called lemma and the inner palea (Fig. **2**). The floret presents three stamens with bilobed anthers, and the ovary, with a bifid style and a feathery stigma (Fig. **2**). At its base, two membranous pads, called lodicules, are present. Lodicules swell at the time of anthesis, pulling back the glumes and allowing the stamens and the stigmas to protrude. During the self-pollinating fertilization, the yellow anthers and the swollen ovary with an open feathery stigma are observed in the closed flower.

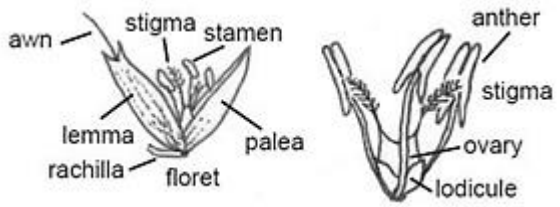


Fig. **2.** Wheat floret.
Adapted from: (Rauh) https://www.asba-art.org/article/science-botanical-art-grasses.

The kernel development, or caryopsis filling, occurs in three main phases: first, in the milk phase, the endosperm cells accumulate secondary starch granules, reaching the maximum volume and a humidity of about 70%. Then, in the dough phase, the kernel begins a progressive accumulation of starch and protein, becoming waxy and yellow. In the last phase, the ripening, water content decreases, reaching 30-45%. Maturation of the caryopsis is completed when the starch granules entirely fill the endosperm cells, its moisture content is 30% and the plant is almost completely yellowed. Moreover, maturation is characterized by the fact that endosperm stops accumulating reserve substances. It follows a gradual and further loss of water, which leads the grain moisture content to 13%, determining the full maturation.

The wheat caryopsis (Fig. **3**) is a dry indehiscent fruit characterized by two sides, with respect to the spikelet axis: the upper or dorsal side is rounded, while the lower or ventral one presents a longitudinal groove. The pericarp strictly adheres to the seed, which is composed by two different parts: the embryo and the endosperm, the latter supporting the first growth

of the embryo during germination. The embryo, or germ, is situated at the point of attachment of the spikelet axis and is composed by the plumule (the coleoptile), the radicle (primary root), and the scutellum, an epithelial formation whose function is to transfer the nutrients from the endosperm to the embryo. The endosperm consists of cells rich in starch surrounded by the aleurone layer, made of metabolically active cells, the testa, or seed coat, and the pericarp, or fruit coat.

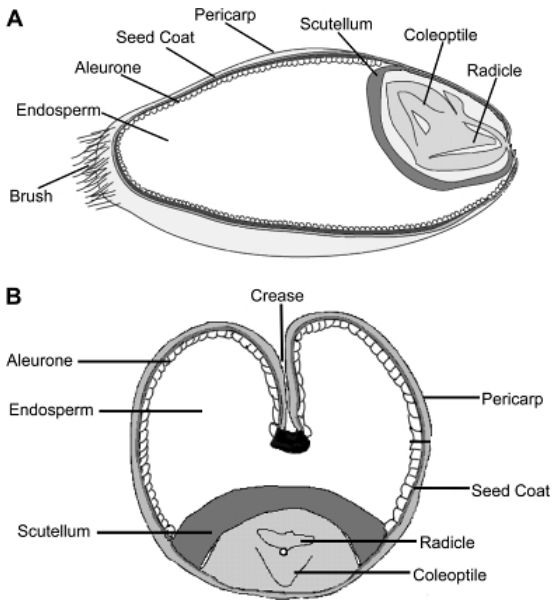


Fig. **3.** Wheat grain scheme in **A**) longitudinal and **B**) transverse sections.
From Rathjen et al. 2009

## 1.2 The plant immune system

Plants are sessile organisms, i.e. they cannot move from their location. Therefore, they have to cope with pathogens of different type by evolving effective perception and response mechanisms.

The main plant pathogens are bacteria, fungi, insects, nematodes and viruses. They can penetrate the host cell in different ways: *via* natural openings, like stomata, or through wounds. During colonization, pathogens can have different lifestyles: necrotrophs kill the host cell and live saprophytically; biotrophs, instead, need alive host cells to carry out their life cycle; finally, hemibiotrophs have an initial biotrophic stage and then switch to a necrotrophic habit. For their behaviour, necrotrophs often produce phytotoxic compounds and cell wall–degrading enzymes (CWDEs) to induce host cell death. In contrast, biotrophic pathogens evolve, complex mechanisms to maintain host viability, and so they secrete limited amounts of CWDEs and generally lack toxin production (Mengiste 2012).

Plants evolved constitutive defence mechanisms against different pathogens, including development of external cuticular layers, of the cell wall, and production of anti-microbial metabolites, like tannins, terpenoids, alkaloids, and flavonoids. However, when the pathogen overcomes these constitutive defence strategies, the host plant cells activate specific, inducible defence processes.

The 'zig-zag' model by Jones and Dangl (2006) (Fig. **4**) provides a general scheme of the plant immune system during plant-pathogen interaction and it is described below.

The first level in the plant defence arsenal is represented by transmembrane receptors called pattern recognition receptors (PRRs), which recognise microbe- or danger-associated molecular patterns (MAMPs and DAMPs), such as flagellin, chitin, oligogalacturonides (OGs), etc. PRRs trigger intracellular pathway of defence signalling, resulting in PAMP-triggered immunity (PTI), which could include accumulation of defence hormones, like salicylic acid (SA), defence signalling molecules, like reactive oxygen species (ROS), change of the intracellular calcium level, activation of signal transduction pathway, like MAPK cascades, reprogramming cell transcription and synthetizing antimicrobial compounds (Coll et al. 2011).

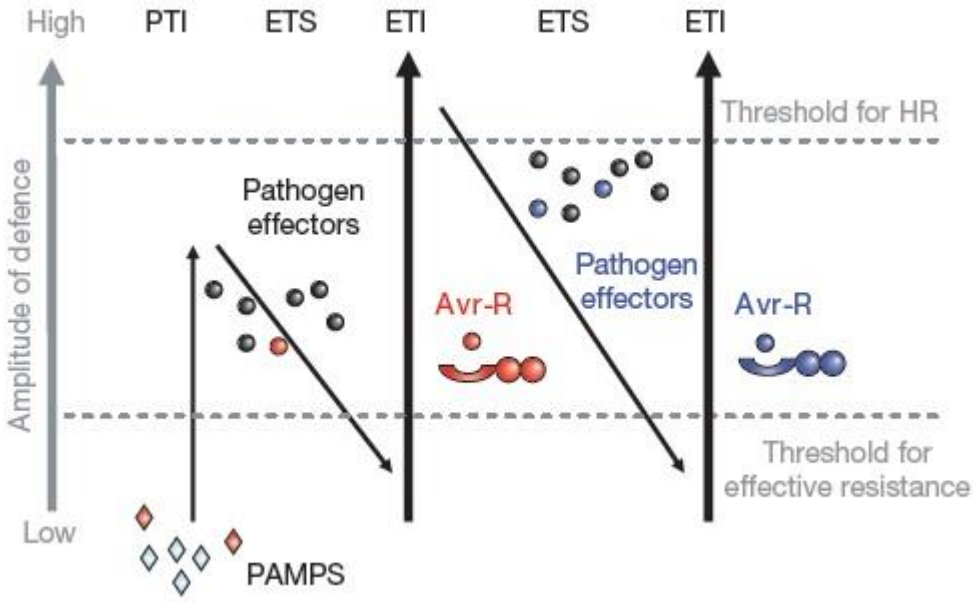


Fig. **4.** The 'zig-zag' model. From: Jones and Dangl (2006)

Pathogens can secrete effector molecules, also called avirulence (AVR) proteins, which normally act by suppressing PTI and facilitating the infection process as well as pathogen nutrition or dispersal. Effectors that enable pathogens to overcome PTI cause the so-called effector trigger susceptibility (ETS). However, plants evolve specific reaction against ETS,

allowing recognition of AVR proteins by specific disease resistance (R) proteins, such as the intracellular NB-LRR receptors.

AVR recognition is not actually an easy task, and limiting ETS depends on it. Several mechanisms can be implemented, and four, co-existing models have been proposed to this respect. In the “elicitor-receptor” model, R proteins directly recognize a specific AVR protein and trigger defence responses (Keen 1990; Jia et al. 2000). In the “guard” model, the interaction R-AVR proteins is indirect, since plant target proteins, called guardees, are detected by R proteins when modified by effectors (Dangl and Jones 2001). In the “decoy” model, specific plant proteins, called decoys, mimic the effector target and the R protein detects their modifications, trapping the AVR protein (Van Der Hoorn and Kamoun 2008). Finally, in the “integrated decoy” model, domains that mimic the effector target are integrated into the AVR NB-LRR receptors (Cesari et al. 2014; Le Roux et al. 2015).

NB-LRR receptors sense the specific effectors and trigger the effector trigger immunity (ETI), which is a stronger and amplified version of PTI. ETI often result in a hypersensitive response (HR), a programmed cell death mechanism that takes place at the site of infection, and activates systemic immunity (SAR), a mechanism alerting the whole plant of the pathogen attack.

Paradoxically, HR response could be an advantage for necrotrophic pathogens; in fact, some of them evolved strategies to use plant HR pathways, and plants have to react blocking their own death (Wang et al. 2014; Mengiste 2012). On the other hand, biotrophic pathogens need strategies to suppress HR in plant cells, since they represent their living substrate; thus, pathogens undergo a selection pressure to lose ‘susceptible’ effectors and/or evolve new ones to suppress ETI and again result in ETS (Coll et al. 2011; Jones and Dangl 2006). The ‘gene-for-gene hypothesis’ (Flor 1971) describes that for each gene that conditions resistance in the host, there is a corresponding gene that conditions pathogenicity in the pathogen. This sharp and deep down interaction between plant and pathogens will continue until natural evolution, environmental conditions and selective pressures will take place.

### 1.2.1 The plant cell wall

Without the cell wall, plants would not be as we know them. Indeed, the plant cell wall is one of the main feature of the plant cell, conferring to it many essential characteristics during all plant lifecycle. The wall surrounds the cell and its structure is continuously modified to

follow through the developmental stages and environmental changes. Its main roles are to: determine the shape and volume of different cell and tissue types, confer strength and flexibility, supply a sugar deposit in case of need, as well as provide a structural and dynamic barrier against pathogens and the environment.

Typically, the cell wall is classified in two main typologies (Table **2**): the primary wall, established in young cells and composed of approximately 10% proteins and 90% polysaccharides of three groups: cellulose, hemicellulose and pectin, present in different percentages in different plant species (Caffall and Mohnen 2009). The secondary wall, produced only by some specialized cell types like vascular cells, is laid down the plasma membrane and the primary wall once the cell has reached its final size and shape. The secondary wall is thicker and provides more support than the primary type; it is typical composed of 40–80% cellulose, 10–40% hemicellulose, 5–25% lignin, depending of cell type and cell wall proteins (Kumar et al. 2016).

Cellulose is a polymer of β-(1,4)-D-Glucose residues that associate with other cellulose chains aligned in parallel by hydrogen bonds and Van der Waals forces, forming microfibrils. Cellulose is insoluble, strong and highly resistant to enzymatic degradation, and represents the main component of both primary and secondary walls (Caffall and Mohnen 2009).

Hemicelluloses are a heterogeneous group of polysaccharides, characterized by a β-(1,4)-linked backbone with an equatorial configuration at C1 and C4, synthesized by glycosyltransferases located in the Golgi membranes. Hemicelluloses can be grouped into xyloglucans, xylans, mannans and glucomannans, and β-(1,3; 1,4)-glucans (Scheller and Ulvskov 2010).

Xyloglucan is the most abundant hemicellulose in primary walls of dicots (Table **2**). It is made of repetitive units of β-(1,4)-D-Glucose, substituted at regular sites with D-Xylose residues that can be further extended with other sugar residues. Xylan is the main hemicellulose of monocots. It is composed of a backbone of β-(1,4)-D-Xylose. Substitution with glucuronosyl and arabinose residues and esterification with ferulic acid, lead to the formation of glucuronoxylans (GX), arabinoxylans (AX) and glucuronoarabinoxylans (GAXs). The latter one is the main component of grass walls (Vogel 2008; Caffall and Mohnen 2009; Scheller and Ulvskov 2010). Mannans and glucomannans are the main hemicellulose in Charophytes (Scheller and Ulvskov 2010). When the backbone of β-(1,4)-linked polysaccharides consists entirely of mannose, hemicellulose is termed mannan. Instead, when

the backbone consists of mannose and glucose in a nonrepeating pattern, it is referred to as glucomannan. Finally, the hemicellulose β-(1,3; 1,4)-glucan is mixed linkage of β-(1,4)-linked glucans with interspersed single β-(1,3)-linkages. They are typically present in grasses, but are also present in some algae and fern species (Scheller and Ulvskov 2010).

Table **2.** Composition of grass and dicot cell walls. From: Vogel (2008)

**Approximate composition (% dry weight) of typical dicot and grass primary and secondary cell walls**

| | Primary wall | | Secondary wall | |
|---|---|---|---|---|
| | Grass | Dicot | Grass | Dicot |
| Cellulose | 20–30 | 15–30 | 35–45 | 45–50 |
| Hemicelluloses | | | | |
| Xylans | 20–40 | 5 | 40–50 | 20–30 |
| MLG | 10–30 | Absent | Minor | Absent |
| XyG | 1–5 | 20–25 | Minor | Minor |
| Mannans and glucomannans | Minor | 5–10 | Minor | 3–5 |
| Pectins | 5 | 20–35 | 0.1 | 0.1 |
| Structural proteins | 1 | 10 | Minor | Minor |
| Phenolics | | | | |
| Ferulic acid and ρ-coumaric acid | 1–5 | Minor (except order Caryophyllales) | 0.5–1.5 | Minor (except order Caryophyllales) |
| Lignin | Minor | Minor | 20 | 7–10 |
| Silica | | | 5–15 | Variable |

The network formed by cellulose and hemicellulose is combined in a jelly-like matrix of pectins. They represent almost 30% of the cell wall of dicots, gymnosperms and non-Poales monocots, and approximately 10% of the Poales cell wall (Caffall and Mohnen 2009). Pectins are the most complex class of cell wall polysaccharides, characterized by the presence of galacturonic acid (GalA). The most abundant pectin polysaccharides are homogalacturonan (HG), rhamnogalacturonan II (RG-II), and rhamnogalacturonan I (RG-I). HG is the most abundant pectic polysaccharide, constituting 65% of total pectin. It consists of a linear α-(1-4)-GalA homopolymer in which some of the carboxyl groups are methylesterified. If more than 10 consecutive unmethylesterified GalA residues in different chain are present, since the unmethylated C-6 of GalA residues is negatively charged, they can ionically interact with $Ca^{2+}$ to form a stable gel within pectic molecules. The structure of HG-$Ca^{2+}$ is known as 'egg-box' model, and explains around 70% of the pectic gel in the plant cell walls (Caffall and Mohnen 2009). RG-II has a HG backbone with substitution with glycosyl residues. RG-I is a polymer of GalA and rhamnose (Rha) disaccharide subunits.

Proteins and glycoproteins are also included in the plant cell wall. Many of them are structural proteins, but other ones have specific functions, such as polysaccharide

modification, defence, signalling, cell wall metabolism and enlargement, response to abiotic and biotic stresses.

The secondary wall also contains lignin, which essentially fills the pores between the polysaccharides. Unlike dicots, grass lignin contains substantial amounts of ferulic acid and r-coumaric acid (Table **2**). Ferulic acid residues attached to GAX may serve as nucleation sites for lignin formation (Vogel 2008).

Due to its complexity in structure and heterogeneity in functions, the plant cell wall is a complicated and arduous barrier to be overcome by pathogens.

#### 1.2.1.1 Cell wall degrading enzymes (CWDEs)

As a barrier surrounding the cell, the cell wall represents the first obstacle for pathogen entry. To this aim, pathogens evolved an arsenal of wall degrading enzymes, which are key virulence factors. Carbohydrate activity enzymes (CAZymes) are produced for the degradation of polysaccharide materials of cell wall. They have been grouped into four classes: glycoside hydrolases (GHs), glycosyltransferases (GTs), polysaccharide lyases (PLs) and carbohydrate esterases (CEs), based on their structurally-related catalytic modules or functional domains (Cantarel et al. 2009). CE, GH, and PL classes are known as cell-wall degrading enzymes (CWDEs) and all kind of pathogens produce them, including bacteria, nematodes and fungi (Zhao et al. 2013). The diversity of these enzymes is related to the structural complexity and the dynamics of the cell wall, but also to the lifestyle and host adaptation by the pathogen (King et al. 2011).

Among fungal pathogens, CWDEs play a major importance for penetration and successful infection of their hosts; moreover, carbohydrates released from plant cell wall can support fungal growth (Zhao et al. 2013). In general, hemibiotrophic and necrotrophic fungi have more CAZymes than biotrophic fungi. The number of enzymes involved in cellulose degradation shows no major differences between dicot and monocot pathogens, mirroring their similar cellulose levels in the walls (Zhao et al. 2013). Moreover, although dicot and monocot plants have different amounts of hemicelluloses in their cell wall, also in this case their pathogens exhibit no significant differences in the type or number of enzymes related to hemicellulose degradation.

Pectin degrading enzymes, such as polygalacturonases (PGs), pectin and pectate lyases and pectin esterases (PMEs), degrade the pectic homogalacturonan (HG) backbone. In particular,

HG methylesterification protects it from degradation by pectinases. The de-esterification of HG by the action of microbial PMEs enables degradation of the other enzymes (Malinovsky et al. 2014). In this context, PGs play a critical role in plant-microbe interaction, since the releasing of oligomeric fragments of HG, the oligogalacturonides (OGs), is perceived by plant specific DAMPs receptors, which monitor the integrity of pectin and activate downstream defences (Ferrari et al. 2013).

In the grasses, pectin is a minor constituent of cell wall, with hemicellulose being the main one. In fact, monocot pathogens have relatively higher hydrolytic enzymes for hemicellulose (GAX) (King et al. 2011). In particular, xylanase degrades the linear backbone of the predominant hemicellulose (arabino)xylan into xylose residues (Beliën et al. 2006).

#### 1.2.1.2 CWDEs inhibitors

Plant cells monitor the status of their cell walls with various types of sensors and membrane receptors, which detect mechanical deformations or changes in cell wall structure or composition, and therefore pathogen attacks. Plants can counter the cocktail of CWDEs by producing glycosidase inhibitors, in particular xylanase inhibitors (XIs), PG inhibitor proteins (PGIPs) and pectin-methylesterase inhibitors (PMEI). These classes of inhibitors are described below.

XIs have been studied less intensely in plant defence than other inhibitors. Three classes of XIs proteins are present in wheat: *Triticum aestivum* xylanase inhibitors (TAXIs, Debyser et al. 1999), xylanase inhibiting proteins (XIPs, McLauchlan et al. 1999) and thaumatin-like xylanase inhibitors (TLXIs, Fierens et al. 2007). All these classes are involved in plant defence, and all are effective against microbial xylanases but not against the endogenous ones (Dornez et al. 2010a). Indeed, the specificity of recognition between the different classes of inhibitors and microbial xylanases is high. For instance, TAXI-type and TLXI-type inhibitors inhibit GH11 but not GH10 xylanase families (Fierens et al. 2007; Gebruers et al. 2004). XIP-type inhibitors are able to inhibit GH10 and GH11 families, although there is variability in the inhibition efficacy against GH11 xylanases (Beliën et al. 2006).

XIs proteins are localized in the apoplast and their expression is induced during stress conditions and fungal infections (Dornez et al. 2010b; Igawa et al. 2004, 2005). For example, *F. graminearum* xylanases have the capacity to cause host cell death, both in cell suspensions and in wheat spike tissue, and TAXI-III and XIP-I prevented the enzyme activity and host cell

death (Tundo et al. 2015). Indeed, the constitutive expression in durum wheat transgenic plants of the *TAXI-III* gene delayed Fusarium head blight (FHB) symptoms (Moscetti et al. 2013).

PIGPs are leucine-rich repeat (LRR) glycoproteins that physically interacts with fungal PGs, limiting cell wall degradation and fungal growth, but promoting the formation of OGs that act as elicitors of host defense responses (Ridley et al. 2001; De Lorenzo et al. 2001; D'Ovidio et al. 2004; Ferrari et al. 2013). Different PGIPs show specific recognition capabilities against many PGs produced by fungi. Indeed, PGIPs from different plants can differ in their inhibitory activities, and PGIPs of the same species can inhibit PGs from different fungi or different PGs from the same fungus (De Lorenzo et al. 2001). The need for adaptation and counteracting different pathogens or to respond to different environmental stresses in a more efficient way, explains the redundancy and diversification of PGIP members (D'Ovidio et al. 2004).

*Pgip* families in different species show variation in their expression pattern; indeed, different members are constitutive, others are tissue-specific, and, in most cases, up-regulated following stress stimuli (Kalunke et al. 2014). Diploid and polyploid wheats contain a single copy of *pgip* gene in each genome and only the *Tapgip1* (genome B) and *Tapgip2* (genome D) are expressed (Janni et al. 2006) in the latter. Transcripts of both genes accumulate in roots, stem and spikes during normal growth (Janni et al. 2006), probably contributing to wheat development. Moreover, *Tapgip1* and *Tapgip2* are up-regulated following both fungal infection and, in particular, mechanical wounding (Janni et al. 2013). However, Janni et al. (2013) demonstrated the lack of *in vitro* PG-inhibition activity in wheat, while the possible PG-inhibition activity *in planta* was not investigated. Indeed, some PGIPs are active in PG-inhibition only in the latter environment (Joubert et al. 2007).

The involvement of PGIP in plant defence has been demonstrated. For example, the constitutive (Ferrari et al. 2012; Janni et al. 2008) and floral tissue-specific (Tundo et al. 2016a) expression of the bean *PvPGIP2* in wheat transgenic plants was found to limit symptom development following infection by *Bipolaris sorokiniana* (50% reduction) and *Fusarium graminearum* (20-30% reduction). In contrast, wheat infection with a *F. graminearum Δpg1* mutant (*FgΔpg1*), strongly impaired for PG activity, demonstrated the dispensability of the PG1 activity for fungal virulence on wheat (Paccanaro et al. 2017). The *FgΔpg1* lacks the activity of the PG1, an endo-PG that showed a strong activity and induction within the first 12 hours (h) after spike inoculation with a peak at 24 h (Tomassini et al. 2009). Although not

documented, it might be that the inhibition activity in the PvPGIP2 transgenic plants against different PG isoformes, secreted during all stages of fungal infection, contributes to the reduction of FHB symptoms. Moreover, the differential monosaccharide composition of the cell wall of transgenic plants expressing the PvPGIP2 compared to wild type susceptible plants, observed by Tundo et al. (2016b), may have also contributed to the reduction of FHB symptoms.

PMEIs inhibit the de-esterification activity of PMEs. The esterification status of pectin plays a critical role in plant-pathogen interaction, since the mechanical properties of the wall matrix depend on it (Lionetti et al. 2012). De-esterification makes pectin more susceptible to the degradation by pectic enzymes such as PGs or PLs, secreted by necrotrophic pathogens (Micheli 2001; Lionetti et al. 2012). At the same time, OGs need to be de-esterified to elicit defence responses (Osorio et al. 2008, 2011). Therefore, the degree and pattern of methylesterification is important during plant-pathogen interactions. For this reason, PMEIs and PMEs are tissue-specific and developmentally regulated. During infection, plant PMEIs that regulate PME activity are induced. However, plant PMEIs act only on plant PMEs and not on microbial ones, since the latter are structurally different and act on HG differentially. In particular, plant PMEs de-methylesterify adjacent GA residues of HG, resulting in pectin blocks of free carboxyl groups that interact with $Ca^{2+}$ ions, rigidifying the cell wall and, in turn, hindering CWDEs activities. In contrast, microbial PMEs de-methylesterify not adjacent GA residues, not allowing the cell wall rigidifycation and thus promoting the action of microbial cell wall hydrolases (Micheli 2001). However, the microbial PMEs mode-of-action releases protons (Moustacas et al. 1991), which promote endoPGs activation, and in turn the releasing of OGs (Moustacas et al. 1991; Micheli 2001; Osorio et al. 2011; Lionetti et al. 2012).

Methylesterification levels of wheat cell wall pectin was demonstrated to influence plant resistance, since highly methylesterified pectin is less vulnerable to pectic enzyme degradation. Indeed, transgenic durum wheat lines expressing the PMEI of *Actinidia chinensis* (AcPMEI) were more resistant to *B. sorokiniana* and *F. graminearum*, due to the increased degree of methylesterification of pectins (Volpi et al. 2011). On the other hand, it was demonstrated that *F. graminearum* PME contributes to fungal virulence on wheat by promoting wheat spike infection. Indeed, the *F. graminearum Δpme1* mutant (*FgΔpme1*) causes reduced FHB symptoms compared to the wild type fungus, in the initial and middle stages of infection (Sella et al. 2016). Moreover, the combined actions of inhibiting the

endogenous plant PME activity by AcPMEI in transgenic wheat and of eliminating fungal PME activity by gene disruption, did not provide any appreciable additive effect on symptom reduction (Sella et al. 2016). In contrast, PME overexpression in strawberry conferred resistance to necrotrophic fungus *Botrytis cinerea* (Osorio et al. 2008). In particular, the reduced OGs degree of esterification resulted in a stronger defence elicitation capacity (Osorio et al. 2008, 2011).

*In planta*, the synergistic effect of different CWDE inhibitors that act on different cell wall components can influence the fungal infection. Indeed, durum wheat plants expressing both PvPGIP2 and TAXI-III had improved resistance against *F. graminearum* in comparison with parental lines, expressing separately glycosidase inhibitors that act on pectin and xylan, respectively (Tundo et al. 2016b). Further confirming these data, a *F. graminearum* double mutant *FgΔpgΔxyr* was produced with disruption of the *Pg1* and *xyr1* genes, the main PG and the major regulator of xylanase production, respectively (Paccanaro et al. 2017). *FgΔpgΔxyr* showed impaired PG, xylanase and cellulose activity, the latter as further consequence of the *xyr1* mutation. Wheat infection experiments with the *FgΔpgΔxyr* mutant showed reduced FHB symptoms compared to the wild type fungus, whereas no reduced symptoms were observed with the single mutant strains (Paccanaro et al. 2017).

### 1.2.2 Detoxification systems in plant

In nature, plants are continuously exposed to natural and synthetic potentially toxic compounds, also called xenobiotics. To counteract competitors, predators or pathogens, plants produce secondary metabolites, which, in turn, need to be neutralized to avoid self-toxicity. Furthermore, plants are subject to synthetic xenobiotics such as industrial contaminants, herbicides and pesticides, continuously released in the environment (Debyser et al. 1999). To protect themselves against self- and nonself-compounds, plants evolved detoxification systems.

Detoxification of xenobiotics involves one or more enzyme-catalysed reactions that modify the initial toxic compound into a distinct molecule, usually less toxic. The majority of xenobiotics are lipophilic, therefore they are easily absorbed by cells. In general, after detoxification, the modified molecules are more hydrophilic than the original compound, which decreases their ability to cross biological membranes (Coleman et al. 1997).

Typically, the detoxification process involves three phases. In phase I, the xenobiotic is activated by hydrolysis or oxidation, mainly by the cytochrome P-450 system. This phase is important to create reactive sites in the xenobiotic, by the addition or exposure of functional groups, which will react in the next phase. In phase II, the reactive molecule is covalently bound to an endogenous hydrophilic molecule, such as glucose, malonate or glutathione, by glucosyl-, malonyl- or glutathione- transferases, depending on the reactive group (Coleman et al. 1997; Bowles et al. 2006). Finally, in phase III, the nontoxic or less toxic, water-soluble conjugate is transported to the vacuole or to the apoplast. The compartmentation is important for an effective detoxification, through confinement of the potentially harmful molecule to a subcellular structure (Coleman et al. 1997; Bowles et al. 2006).

## 1.3 *Fusarium* diseases

To the *Fusarium* genus belong many plant pathogenic, filamentous fungi. The genus *Fusarium* belongs to the *Ascomycota* phylum, while the teleomorphs of *Fusarium* species are mostly classified within the genus *Gibberella*. In general, these fungi are saprophytes and facultative parasites, able to colonize living host tissues at any time during the host life cycle, and thereby establish themselves in the senescent tissue and crop debris (Bushnell et al. 2003).

The main diseases of wheat caused by *Fusarium* fungi are Fusarium head blight (FHB or scab) and Fusarium crown rot (FCR). *Fusarium* diseases can attack different crop plants, i.e. small grain cereals, maize, vegetables and fruit trees. In wheat, both diseases cause reduction in wheat yields, quality losses, because of reduced baking, brewing and seed quality, and mycotoxin contamination, negatively associated to animal and human health (Pestka 2010). The main species associated to wheat FHB and FCR are *F. graminearum* Schw. (telomorph *Gibberella zeae* Schw. & Petch), *F. culmorum* (W.G. Smith) Sacc. and *F. pseudograminearum* Aoki & O'Donnell (telomorph *G. coronicola* Aoki & O'Donnell). All belong to the section *Discolor* of the genus and are distributed worldwide. These pathogens are well adapted to grass hosts and all are capable to produce trichothecene mycotoxins. *Fusarium* spp. differ in their typical mycotoxin profile. The most produced trichothecenes belong to type B (see § 1.4), which includes deoxynivalenol (DON), nivalenol (NIV) and their derivatives, the 3-acetyl and 15-acetyl deoxynivalenol (3ADON and 15ADON) and the 4-acetyl nivalenol (4ANIV).

Trichothecene biosynthetic enzymes in *Fusarium* spp. are encoded by genes at three loci (Fig. **5**): the single-gene *TRI101* locus, the two-gene *TRI1-TRI16* locus, and the 12-gene core *TRI* cluster (Alexander et al. 2009). Most of the biosynthetic enzymes necessary for trichothecene production are located in the core *TRI* cluster. Among them, *TRI5* encodes a trichodiene synthase, that catalyses the first reaction of the biosynthetic pathway. Four genes are important to determine the basis for the type of produced trichothecene: *TRI16* is functional only in the T-2 toxin *Fusarium* strains; *TRI7* and *TRI13* are functional only in NIV-producing strains and not in DON-producing ones; a sequence variation in *TRI8* determines the 3-ADON and 15-ADON chemotypes. *TRI6* and *TRI1* are transcription factors essential for the coordination of expression of genes at the three loci. Instead, *TRI101* encodes an acetyl-transferase that reduces the toxicity of trichothecenes, thus representing a self-protection mechanism for the fungus.

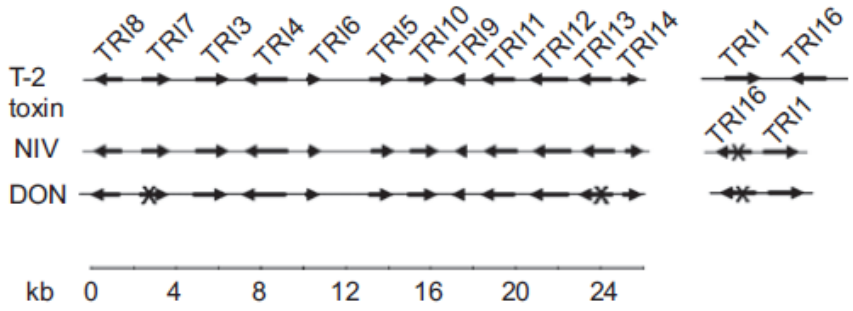


Fig. **5.** Core *TRI* trichothecene biosynthetic clusters and *TRI1-TRI16* cluster in *Fusarium* that lead to formation of T-2 toxin, nivalenol (NIV), or deoxynivalenol (DON).
Arrows indicate position and transcriptional orientation of genes. An X on an arrow indicates that a gene is non-functional. From: Alexander et al. (2009)

*Fusarium* spp. have both sexual and asexual life cycles. Both cycles result in airborne spores, which can infect floral tissues. During the asexual life cycle, the mycelial structures produce three types of mitotic spores: microconidia, macroconidia and chlamydospores. Fungi belonging to the *Discolor* section do not produce microconidia. Macroconidia have a distinctive canoe- or banana- shape. Clamydospores can overwinter and survive on crop debris and, when conditions are favourable, restart the cycle. Ascospores, produced during the sexual life cycle, are also an important source of inoculum for FHB infection in wheat (Dweba et al. 2017; Ma et al. 2013), since they represent an excellent mechanism for aerial dispersal. *Fusarium* pathogens have no specialized structures for penetration of host cells, like appressoria or haustoria.

FHB and FCR are together among the main diseases of wheat crops, causing huge economic losses and food-feed harmful contamination. *F. culmorum* is associated with cooler semiarid wheat growing regions, while *F. pseudograminearum* and *F. graminearum* are dominant in slightly warmer regions (Cook 1980). However, climate changes and crop managing practices increasingly implicate a dynamic distribution of the different species all around the world (van der Lee et al. 2015).

Because of the importance of studying and limiting the negative effects on agriculture, economy and health due to *Fusarium* diseases, the main species of *Fusarium* were subjected to genome sequencing in order to perform accurate comparative analyses and gene function studies. To date, the complete genome sequence is available for *F. graminearum* strain PH-1 (King et al. 2015) and *F. peudograminearum* strain CS3096 (Gardiner et al. 2012). A draft genome sequence was recently released for *F. culmorum* strain UK99 (Urban et al. 2016).

### 1.3.1 Fusarium head blight (FHB)

Fusarium head blight (FHB) is one of the most devastating diseases of grain crops worldwide, including wheat, barley and maize. Among *Fusarium* spp., *F. graminearum* (teleomorph *Gibberella zeae*) is found all over the world and is the main causal agent of FHB. Since *F. graminearum* isolates around the world show a geographic substructure, it should be considered as a meta-population consisting of many relatively independently developing populations (van der Lee et al. 2015).

FHB causes yield and quality losses, in particular under severe epidemics. For example, wheat yield reduction of 40–50% was reported in 1993 in north-eastern North Dakota and north-western Minnesota (Windels 2000). Moreover, even under moderate disease severity, quality losses due to mycotoxin contamination can be severe (Birzele et al. 2002; Paul et al. 2005; Champeil et al. 2004). FHB symptoms consist of both tissue necrosis, caused directly by the fungus, and bleaching, caused mainly by vessel occlusion, that can be due to the pathogen or to plant mechanisms to avoid fungal spread.

A simplified scheme of FHB is provided in Fig. **6**.

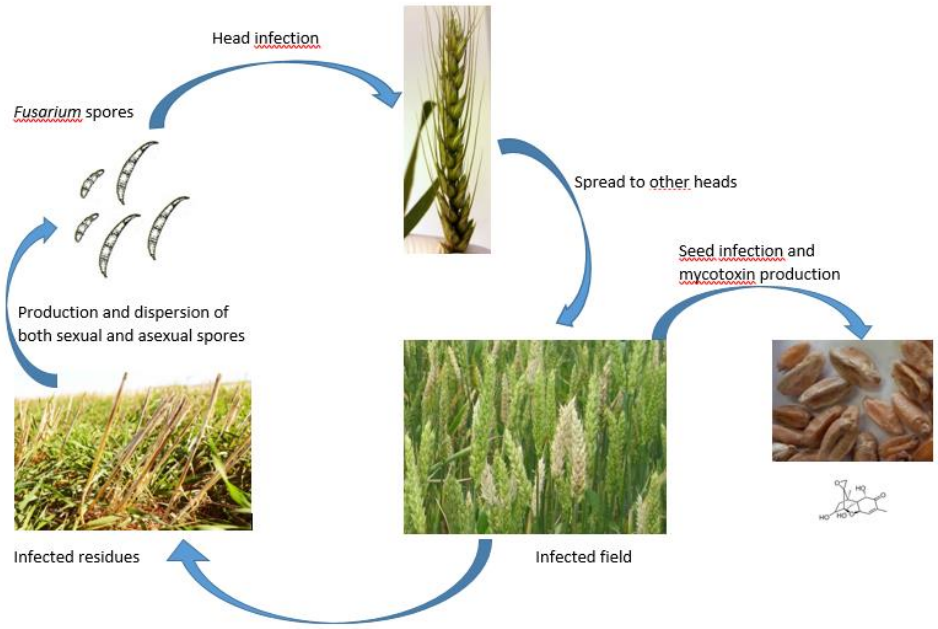


Fig. **6.** Fusarium head blight cycle.

*F. graminearum* inoculum, able to maintain the disease through seasons, could derive from crop debris, infected seeds, and other infected species or fields. FHB occurs in coincidence with favourable weather conditions, particularly warm and wet conditions during anthesis. Under these circumstances, spores on the head surface germinate. Entrance into the host floret was reported both through natural openings, like glume stomata (Pritsch et al. 2000), or *via* penetration of short infection-hyphae through the epidermal cell wall (Miller et al. 2004; Boenisch and Schäfer 2011). Inside the floret, the fungus grows on the inner surface, developing a hyphal network particularly evident in anthers and pollen, and then progressing toward the ovary, lemma and palea (Miller et al. 2004). Indeed, it was demonstrated that host anthers attract *Fusarium* spp. to the spikelets (Strange and Smith 1971). However, although anthers are heavily colonized, they do not stimulate the induction of trichothecene biosynthesis (Ilgen et al. 2009; Boenisch and Schäfer 2011). The pathway is instead induced in this early infection stage by developing kernels (Ilgen et al. 2009). After cuticle penetration, subcuticular growth and intracellular colonization of parenchyma tissues is observed, and this is considered the biotrophic growth phase that precedes necrosis of host tissue (Pritsch et al. 2000; Jansen et al. 2005).

During penetration and colonization, the fungus secretes CWDEs in order to invade the plant tissue and feed from the released nutrients (Wanjiru et al. 2002; Kikot et al. 2009). After complete infection of the inoculated floret, 4-7 days post-infection, the fungus starts node infiltration to move into the rachis, following in general a downwards movement, and through

the rachis it spreads across the spike (Miller et al. 2004). Nevertheless, the fungus was also observed to spread on the exterior portion of the inoculated spike. Typical disease symptoms, such as brownish necrosis and chlorosis, develop rapidly in the progressively infected tissues, reaching complete head infection in a fully compatible plant-pathogen interaction.

Importantly, the involvement of the rachis node between the rachilla and the rachis seems to have a central role in pathogenesis. Indeed, most of resistant wheat genotypes display their ability to arrest fungal spread in the rachis node, and in this spike region the fungus shows the most extensive increase in production of virulence factors. Miller et al. (2004) observed a brown deposit at the base in the node of the inoculated floret, both in susceptible Roblin and resistant Sumai 3 cultivars (cv). In some cases, these deposits were also able to occlude the vascular bundles, thus preventing movement of solutes and hyphae through the vascular tissues. The deposits appeared earlier and more pronounced during cv Sumai 3 infection, restricting the spread of the fungus in the spike, whereas the progression inside the rachis was more rapid and extensive in cv Roblin. On the other hand, both virulence factors DON (Ilgen et al. 2009; Boenisch and Schäfer 2011) and FGL1 (*F. graminearum* lipase-1; Voigt et al. 2005) are induced early after infection. In particular, the first one is highly induced once the fungus reaches the rachis node. Both *F. graminearum* trichothecene-deficient mutant *Δtri5* (*FgΔTri5;* Bai et al. 2001) and lipase-deficient mutant *Δfgl1* (*FgΔfgl1*; Voigt et al. 2005) failed the overcome the rachis node; consequently, the disease spread throughout the spike after infection of the inoculated floret. Moreover, *FgΔfgl1* mutant overproduces DON since, remaining trapped in the transition zone of the rachis, *Tri5* expression is constantly induced (Voigt et al. 2007). Despite DON increased production, *FgΔfgl1* mutant virulence is not 'restored'. This confirmed that, although DON is a virulence factor, it is not enough alone for pathogenicity (Voigt et al. 2007).

### 1.3.2 Fusarium crown rot (FCR)

Foot and root rot, or Fusarium crown rot (FCR), is an important wheat disease, which, depending on the time of infection, causes seedling death or tillers abortion (Fig. **7**). The disease is a serious problem for wheat production in many parts of the world, in particular in the presence of dry climatic conditions and conservation agricultural practices. It causes extensive damage to growing seedlings and leads to a reduction in plant establishment, number of heads, grain yield and mycotoxin contamination of wheat stubble and heads. For

example, 35% of wheat yield reduction was reported in the Pacific Northwest of the USA under FCR epidemics (Smiley et al. 2005). Moreover, in five bread wheat varieties and one durum wheat cultivar, concomitantly grown in different sites of west Australia, an average 25% and 58% yield loss, respectively, was detected (Daniel et al. 2008).

Main causal agents of FCR are *F. culmorum*, *F. pseudograminearum* and, less frequently, *F. graminearum*. All pathogens are also able to cause FHB disease, depending on host stage and environmental conditions. Dyer et al. (2009) compared FCR effects caused by the three *Fusarium* species in inoculated field trials. Their results suggested that *F. culmorum* is the most consistent seedling pathogen causing significant stand losses, whereas *F. graminearum* and *pseudograminearum* caused the highest crown rot severity in adult plants. In general, *F. pseudograminearum* is the most prevalent *Fusarium* species isolated during crown rot infections in warmer and drier regions, like Australia and Pacific Northwest area of the USA (Chakraborty et al. 2006; Poole et al. 2013; Kazan and Gardiner 2017).

Notably, *F. culmorum* is capable of surviving between subsequent seasons in the form of durable chlamydospores, present in the soil as well as in plant residues, and chlamydospore survival was higher than that of *F. graminearum* after different treatments, like rapid air drying, high temperature exposure or residual burial (Sitton and Cook 1981). Not requiring residues for survival, *F. culmorum* may result a more aggressive seedling pathogen. Indeed, *F. graminearum* (*G. zeae*) can survive and produce ascospores on wheat residues in the field for at least two years after harvest. However, *F. graminearum* colonizes wheat residues as senescing plant tissue, prior to the arrival of saprophytes, which are more effective colonizers of partially decomposed wheat residues (Pereyra et al. 2004)

*F. culmorum* is an ubiquitous soil-borne fungus with a highly competitive saprophytic capability, causing cereal diseases both in living plants and in post-harvest phases, especially on freshly harvested grain that has not been dried or stored properly (Scherm et al. 2013). *F. culmorum* does not produce ascospores and its perfect stage (teleomorph) is unknown. Previous crops, residue management, nitrogen fertilization, plant density and the environmental conditions, all contribute as inoculum source and survival for FCR establishment. Drought conditions increase the susceptibility of the plant and therefore FCR is more severe when wheat grows in warm areas, where the host plant is more subject to water stress (Scherm et al. 2013).

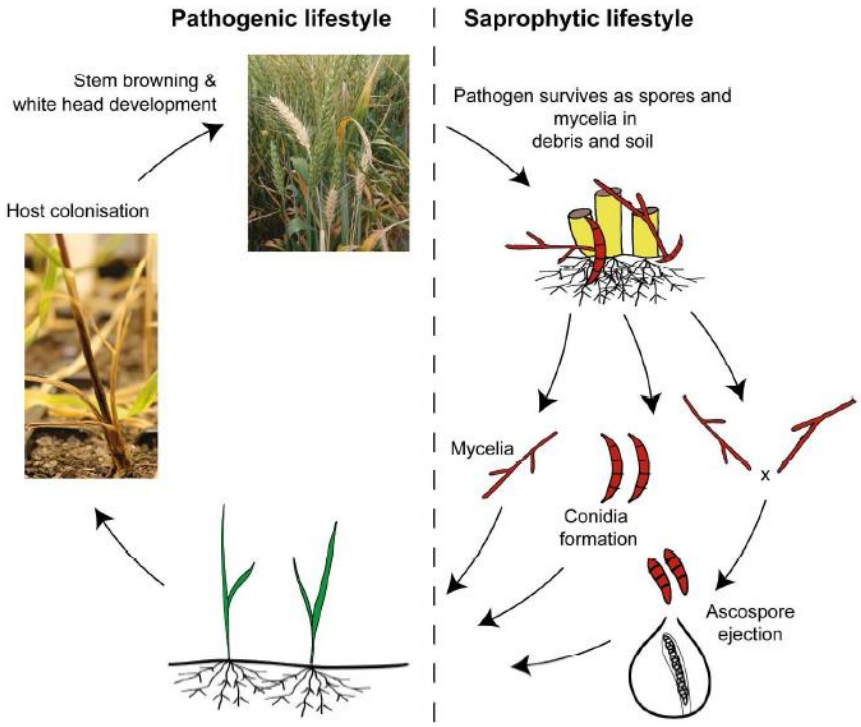


Fig. **7.** General Fusarium crown rot cycle in cereal crops. From Kazan and Gardiner (2017).

The pathogen enters the stem *via* the point of attachment of the leaf sheath to the stem base, without direct penetration (Covarelli et al. 2012). Alternatively, when the seed germinates, the fungus penetrates through the lesions formed during primary root emergence, and then progresses towards the culm (Scherm et al. 2013). Once inside the parenchyma tissue of the stem, the fungus colonizes the tissues both intercellularily and intracellularily. *F. culmorum* may have an initial brief biotrophic phase within plant tissues, but then shifts to a necrotrophic stage through the production of trichothecenes and, possibly, CWDEs (Bushnell et al. 2003).

Stephens et al. (2008) studied the infection progress of *F. graminearum* during FCR infection combining biomass estimations and histological analyses. They identified three distinct phases during colonization. In phase 1, in the first two days after inoculation, a significant increase in fungal biomass was observed, due to spore germination and hyphal growth on the leaf-sheath surface. Leaf-sheath surface is poor in nutrients and, in fact, genes encoding enzymes involved in remobilization of stored nutrients as well as nutrient acquisition were frequently induced. During phase 2, a significant decrease in fungal biomass was observed for at least two weeks. Indeed, during this period the fungus penetrated the outer leaf sheath and migrated to the leaf-sheath base, colonizing the leaf epidermis with both intracellular and intercellular hyphae. The decreased biomass can be explained by the fact

that only a small number of germ tubes successfully penetrated the leaf-sheath tissue and survived. Finally, in phase 3, fungal biomass again increased, since the fungus colonized the wheat crown parenchyma. Interestingly, the authors reported that stem elongation started during phase 3, and the elongating tissue provides continuity throughout the shoot, which may permit more rapid colonization of stem parenchyma. Moreover, coinciding with phase 3 was also DON accumulation: necrotic symptoms appeared and a significant increase in fungal biomass was observed.

If the fungus attacks at early stages, just after sowing, seedling death may occur, as indicated by brown discoloration on coleoptile, roots and pseudostem. If the infection occurs later during plant growth, brown lesions appear on the first two or three internodes of the main stem and tiller abortion frequently occurs (Scherm et al. 2013). However, the fungus does not reach the head (Covarelli et al. 2012). This observation could be linked to the host response. Although the fungus is blocked from progression beyond half of the stem, DON is detected even in the last internode and in the head (Covarelli et al. 2012). In accordance to this, the presence of typical FCR brown discoloration of stem tillers are observed ahead the tissues colonized by the fungus, indicating a host response. Indeed, DON induces typical host reactions, such as production of reactive oxygen species and programmed cell death in wheat (Desmond et al. 2008b). Moreover, DON is water-soluble and it could be distributed through plant vessels and even enter the kernel *via* the phloem from glume and lemma.

## 1.4 Deoxynivalenol (DON)

Trichothecenes are mycotoxins produced by phytopathogenic fungi. These secondary metabolites are low sesquiterpenoids, all capable of producing a wide range of toxic effects. The general structure presents a cyclohexene ring with a C-9, C-10 double bond, a tetrahydropyranyl ring, a cyclopentyl ring, and an epoxide at C-12, C-13 epoxide group (Fig. **8**). Depending on the functional groups present in the R1-R5 positions, trichothecenes are classified into A, B, C and D types. Type A and B trichothecenes (Fig. **8**) are considered more important, due to their natural occurrence in food and their high toxicity. In general, type A trichothecenes tend to be more toxic than type B, but the latter ones occur more frequently and at higher concentrations (Foroud and Eudes 2009).

| Toxin | R1 | R2 | R3 | R4 | R5 |
|---|---|---|---|---|---|
| **DON** | –OH | –H | –OH | –OH | =O |
| **3-ADON** | –OAc | –H | –OH | –OH | =O |
| **15-ADON** | –OH | –H | –OAc | –OH | =O |
| **NIV** | –OH | –OH | –OH | –OH | =O |
| **T-2** | –OH | –OAc | –OAc | –H | –OIsoval |
| **HT-2** | –OH | –OH | –OAc | –H | –OIsoval |
| **4,15-DAS** | –OH | –OAc | –OAc | –H | –H |

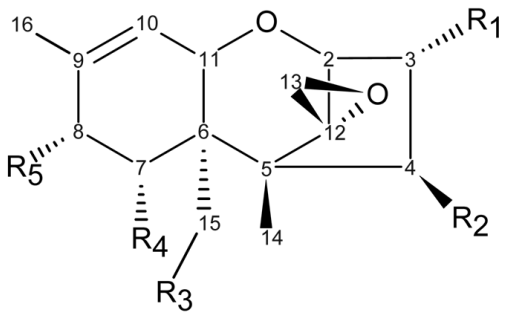


Fig. **8.** Type A and B trichothecene structures.
Examples of type A (T-2 toxin (T-2), HT-2 toxin (HT-2), 4,15-diacetoxyscirpenol (4,15-DAS)) and type B trichothecenes (nivalenol (NIV), deoxynivalenol (DON), 3-O-acetyl DON (3-ADON), 15-O-acetyl DON (15-ADON)). OAc= acetyl function; OIsoval= isovalerate function.
From: Foroud and Eudes (2009).

Trichothecenes bind to the 60S subunit of eukaryotic ribosomes and interfere with the activity of peptidyltransferase (Ueno et al. 1973; Wei et al. 1974; Payros et al. 2017; Dellafiore et al 2018). The presence of an intact double bond at C-9,10 and the C-12,13 epoxide is necessary for the inhibition activity (Ehrlich and Daigle 1987).

Due to food safety problems caused by trichothecenes to animals and humans, the US Food and Drug Administration has set advisory levels for their presence in grains and finished products for human consumption and in animal feed (U.S. Food and Drug Administration 2010). The EU has set maximum levels for trichothecenes in cereals and their derived products, distinguish maximal concentration between animal feed and human/infant food (European Commission 2006).

Among trichothecenes, deoxynivalenol (DON) is the one detected most widely and at the highest concentrations in cereals and cereal-derived products (Canady et al. 2001; Streit et al. 2012). DON has been classified by the International Agency from Research on Cancer (IARC) in group 3, as “not classifiable as to its carcinogenicity to humans”. Moreover, fungal and plant DON-derivatives occur in cereal products, although at lower doses than DON. The main fungal derivatives are 3- and 15-acetyl deoxynivalenol (3ADON, 15ADON), while the plant derivative is deoxynivalenol-3-β-D-glucoside (D3G). These derivatives are called ‘masked mycotoxins’, since these substances escape routine detection methods, but can release their toxic precursors after hydrolysis (Berthiller et al. 2005).

In wheat, high concentrations of DON induced the production of ROS, apoptosis-like processes, with chlorotic and necrotic lesions, and root growth inhibition (Masuda et al. 2007;

Desmond et al. 2008b). The role of DON during pathogenesis will be discussed in the paragraph below.

Feed and food matrices contaminated with DON cause acute and chronic effects, depending on DON doses. Acute DON exposure causes emesis, whereas chronic low-dose exposure induces mainly anorexia, growth retardation, immune function alteration, immunotoxicity and reproduction impairing (Rotter 1996; Pestka 2010; Maresca 2013). The sensitivity of animals to oral DON relies on the localization of the intestinal bacteria in their gut, which can massively decrease the amount of DON that reach the small intestine. Indeed, intestinal bacteria are able to convert DON into its non-toxic de-epoxide metabolite DOM-1, and the high bacterial contents in rumen and in bird crop makes ruminants and poultry almost insensitive to DON oral intoxication (Rotter 1996; Maresca 2013).

Among DON-derivatives, 3ADON and 15ADON present similar or lower toxicity compared to DON, respectively (Broekaert et al. 2015, 2016) and are directly or indirectly absorbed, as DON, by intestinal cells, whereas absence of adverse intestinal effects are observed for D3G (Pierron et al. 2016). Although the toxicity relevance of DON-derivatives, intestinal bacteria can de-acetylate and hydrolyse the glucoside, releasing the native mycotoxin DON that can be absorbed by intestinal cells. However, the toxicological relevance of D3G is different from the acetylated forms, which are themselves toxic. In particular, Berthiller et al. (2011) conducted different assays *in vitro* to hypothesize the fate of D3G along the digestion trait. They found that: i) D3G is resistant to acidic conditions, thus it cannot be hydrolysed into DON in the stomach of mammals; ii) enzymes expressed in human gut, liver, kidney, spleen and plasma do not modify the mycotoxin; iii) intestinal bacteria convert D3G into DON. Therefore, the hazard of D3G differs between monogastric and ruminant/poultry animals. Indeed, the absorption in monogastric of the D3G-derived DON is limited, since the release of DON takes place in the colon and most of the toxin remains in the faeces. However, other factors should be considered, such as the consumption of fermented milk products or probiotic bacteria together with D3G contaminated cereal products. In ruminants and poultry, instead, the transformation of D3G in DON takes place before the small intestine, potentially allowing the absorption of the released toxin (Maresca 2013).

Another important issue of DON in food is its high stability during food processing. As reviewed by Kushiro (2008), DON is continuously reduced step by step during processing, but not completely eliminated from final products. During milling process, DON is stable and not

decomposed from naturally contaminated wheat. For example, if the outer skin of kernels is discarded at the stage of milling, a reduction of DON content can be achieved. DON is very stable during thermal cooking such as baking, frying and extrusion cooking (i.e. stable during baking at temperatures between 170˚C - 350˚C, with no reduction of DON concentration after 30 min at 170˚C), but, due to its water-solubility, boiling in large amount of water reduces DON content in cooked pasta and noodles. Moreover, in some cooking styles, such as heating under alkaline conditions, DON can be degraded to DON-related chemicals, such as the norDON series, whose toxicological effects remain unknown.

### 1.4.1 Role in phyto-pathogenesis

Although DON is of particular concern for human and animal health, the fungus produces DON to overcome plant defence and potentially "win" the plant-pathogen "battle". Whether DON might have a role during the saprophytic stage of *Fusarium* spp. on crop debris, it is not clear, since information is scarce. Tunali et al. (2012) correlated DON production of *Fusarium* spp. during survival on wheat stubble with their aggressiveness during pathogenesis. Indeed, DON could give the pathogen an advantage in the competition for a niche on crop residues. For example, Lutz et al. (2003) found that DON produced by *Fusarium* spp. modulates chitinase gene expression in the competitor fungus *Trichoderma*. This gene is part of the biocontrol activity of *Trichoderma* spp. and is thus important for competitiveness. On the other hand, confirming the continuous battle during biotic interactions, Tian et al. (2016) reported the occurrence of the modified mycotoxin D3G in a dual culture of *Fusarium* and *Trichoderma*, providing evidence that *Trichoderma* strains possess a self-protection mechanism, as plants, to detoxify DON into D3G when in competition with *F. graminearum*.

Even though *Fusarium* species produce DON during both FHB and FCR, the role of DON during pathogenesis could be different for the two diseases. For this reason, it will be discussed below separately.

During early stages of FHB infection, the fungus germinates and grows biotrophically into the intercellular spaces. The role of DON seems not to be important during these stages. However, DON pathway is already active and low *Tri5* expression can be detected (Mudge et al. 2006; Ilgen et al. 2009). Very low concentration of DON (10 ppm) were described to inhibit plant cell death (PCD) in *Arabidopsis* cells (Diamond et al. 2013). Possibly, DON could inhibit host PCD, facilitating the initial spread of the fungus during the biotrophic stage.

Afterward, the necrotrophic switching begins and, as already mentioned in the § 1.3.1, the fungus produces large amount of DON, particularly at the rachis node. It was demonstrated that high doses of DON (100 - 200 ppm) infiltrated in wheat leaves cause $H_2O_2$ production within six hours, and then cell death (Desmond et al. 2008b). $H_2O_2$ production, in addition to trigger plant defence mechanism and HR, not effective against necrotrophs, induces also DON production in the fungus (Ponts et al. 2007, 2006), leading to a positive feedback to increased DON and again $H_2O_2$.

During FHB, DON is considered a virulence factor, essential for fungal spread along the spike from the inoculated floret, though not essential for the initial establishment of the infection. Indeed, Bai et al. (2001) demonstrated that a *F. graminearum* a DON-nonproducing mutant (*FgΔTri5*) caused initial infection but did not determine spread of disease symptoms in inoculated spikes of both susceptible and resistant genotypes. A further confirmation was given by Jansen et al. (2005). Their work allowed the observation of fungal growth of wild type (wt*Fg*) and *FgΔTri5* mutant by transforming the fungi with the constitutively expressed green fluorescent protein (*GFP*) reporter gene. After injection of the two strains in the wheat spikelet, *FgΔTri5* infection was stopped at the rachis node, where heavy cell wall thickening was formed by the plant defence mechanisms. This fortification was not built up during wt*Fg* colonization, where hyphal movement was observed through the rachis. Finally, Ilgen et al. (2009) monitored the trichothecene pathway during plant infection by developing a *F. graminearum* strain expressing the *GFP* gene under the control of the endogenous promoter of *TRI5*, and in the meantime localizing hyphal growth with the constitutive expression of the *dsRed* gene. They found that the most extensive GFP fluorescence was observed at the rachis node, confirming the high induction of the *Tri* pathway and mycotoxin production at this point.

Concerning FCR, less evidence is available about the role of DON during infection establishment and progress. Mudge et al. (2006) described that *Tri5* expression was maintained throughout FCR development. Moreover, they also compared the infection by wt*Fg* and *FgΔTri5* strains during stem base colonization in FCR. Similarly to FHB, they found that DON is not essential for initial infection, since no differences were observed in the first phases after inoculation. However, at the higher nodes, DON-mutant strain colonization was reduced in *FgΔTri5* as compared to wt*Fg*; therefore, they concluded that DON might have a role in fungal progression through the plant stem. In accordance to this, Scherm et al. (2011)

developed *F. culmorum* strains transformed with an RNA interfering construct targeted at the endogenous regulatory gene *TRI6* (*Fc*iRNA*Tri6*). They obtained several *Fc*iRNA*Tri6* strains with a reduced *TRI5* expression and, consequently, reduced DON production. These strains were significantly less virulent compared to wild type strain (wt*Fc*) in FCR assays on durum wheat seedlings. Moreover, they unexpectedly obtained also some *Fc*iRNA*Tri6* strains with increased *TRI5* expression and higher DON production. These strains were significantly more virulent than wt*Fc* in the FCR assay. Altogether, they demonstrated the role as virulence factors of type B trichothecenes in the FCR disease of durum wheat caused by *F. culmorum*. In contrast, Powell et al. (2017) recently developed a *F. pseudograminearum* DON-nonproducing mutant (*FpΔTri5*) starting from two wild type strains (wt*Fp*) differing in aggressiveness. After a FCR assay on wheat seedlings, only the *FpΔTri5* with a less aggressive background was found to be significantly less virulent than the wt*Fp*. They suggested that DON is also a virulence factor for *F. pseudograminearum* during FCR but not when the aggressiveness of the pathogen is very high, suggesting that other virulence factors probably contribute to virulence.

As a whole, we can conclude that, although it is sure and clear a role of DON in both FHB and FCR disease, its role varies in different pathogenesis stages. In fact, DON is not essential during first infection stages, but it is crucial for the spread of the pathogen in FHB. In FCR, some incongruities among results using different strategies and *Fusarium* species make complicate to assess a clear role of DON after first infection. However, all reports indicate a reduction in virulence of the DON-mutant *Fusarium* strains, clearly suggesting that DON takes part in fungal progression through the stem.

### 1.4.2 DON-detoxification *in planta*

The active groups that explain DON toxicity are the epoxide on C12/C13 and the hydroxyl on C3. Modifications at these sites can lead to reduction in toxicity of the molecule (Fig. **9**). Although some microorganisms can reduce or hydrolyse the epoxide group (Karlovsky 2011), no evidence of plant modification of this group was reported yet. The hydroxyl on C3 can be modified by acetylation, oxidation, epimerisation or glycosylation reactions, the latter being the only reaction naturally performed by plants (Karlovsky 2011). The transgenic expression of a trichothecene 3-O-acetyltransferase was not effective in field experiments (Okubara et al. 2002; for further details, see § 1.5.1) since DON and 3ADON have similar effect on wheat tissues; therefore, DON C3 acetylation could not be considered as a detoxification strategy for

plant. Detoxification *via* conjugation to glutathione (GSH) is also a possible mechanism; indeed, the formation of DON-GSH conjugates was reported *in planta* (Kluger et al. 2013). However, conjugation of DON with glucose was identified as the main strategy that takes place in wheat (Berthiller et al. 2005; Kluger et al. 2015). The resulting bio-transformed products are subsequently transported to and stored in the vacuole (Coleman et al. 1997; Bowles et al. 2006).

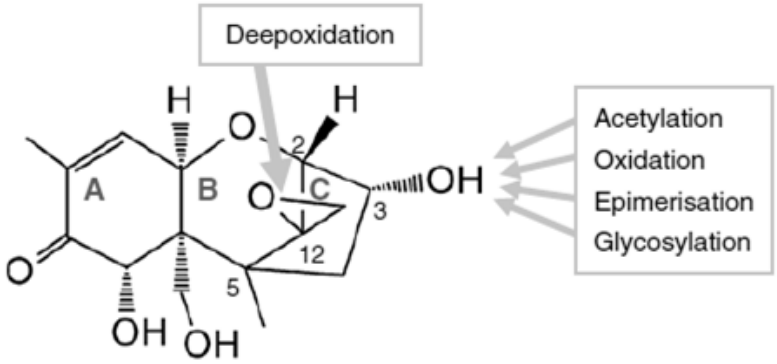


Fig. **9.** Targets for detoxification in DON structure with the designation of the ring system A-C. From: Karlovsky (2011).

In wheat, DON detoxification was correlated with *Fhb1*, a major QTL for FHB resistance (Lemmens et al. 2005). Kluger et al. (2015) investigated the presence of the glycosylation and the glutathione pathway for the detoxification of DON in six wheat lines, which carried different combinations of two major FHB resistance QTLs (*Fhb1* and *Fhb5*). They found that all wheat lines have both pathways, but the treatment with pure DON at the beginning of flowering revealed a faster D3G formation in *Fhb1*-carrying lines, in contrast to a more efficient production of DON-GSH conjugates in *Fhb1*-lacking lines, less resistant to FHB. This result suggested a clear involvement of D3G formation in the resistance to DON, and the speed of DON detoxification seems to be a decisive factor for resistance.

#### 1.4.2.1 UDP-glucosyltransferases

Glycosylation is an important modification performed by glycosyltransferases (GTs), usually on hormones, secondary metabolites, biotic and abiotic stress-related chemicals, as well as xenobiotics present in the environment. In plants, the largest family of GTs is GT1. It consists of UDP-dependent glucosyltransferases (UGTs), characterized by a 44-amino acid PSPG (plant secondary product glycosyltransferase) box near the C-terminus of the proteins. The activated sugar donor of plant GTs is typically UDP-glucose, although UDP-rhamnose, -galactose,

-xylose, and -glucuronic acid have also been identified. Single or multiple glycosylations can occur at –OH, –COOH, –NH2, –SH, and C–C groups of the acceptors. Moreover, different GTs can glycosylate the same substrate and a single GT could glycosylate multiple substrates (Bowles et al. 2006).

The first identified UGT involved in detoxification of trichothecenes was UGT73C5 (also called DOGT1) in *A. thaliana* (Poppenberger et al. 2003). The ability of UGT73C5 to convert DON to D3G was demonstrated expressing the *AtUGT73C5* gene in a DON-sensitive yeast, which acquired resistance to DON. The same *UGT*, overexpressed in transgenic *Arabidopsis*, conferred also enhanced tolerance to DON. However, it was found that the UGT73C5 is also involved in endogenous glycosylations, particularly of brassinosteroids (BRs) (Poppenberger et al. 2005). For this reason, the transgenic *Arabidopsis* showed a dwarf phenotype, since BRs play a major role in regulating plant growth and development.

Afterward, a barley UGT named HvUGT13248 was validated for conferring resistance against DON, both by heterologous expression in DON-sensitive yeast (Schweiger et al. 2010) and by overexpression in transgenic *A. thaliana* (Shin et al. 2012), and also for conferring FHB resistance by constitutive overexpression in transgenic bread wheat (Li et al. 2015c). Recently, the same UGT was also validated as able to provide resistance against NIV by converting it to NIV3G (Li et al. 2017). Transgenic wheat constitutively overexpressing *HvUGT13248* showed also high levels of resistance to disease spread after inoculation with a NIV-producing *F. graminearum* strain (Li et al. 2017).

Other UGTs able to efficiently convert DON to D3G were identified in other cereals, namely the Os79 in rice (Schweiger et al. 2013a; Michlmayr et al. 2015; Wetterhorn et al. 2016), the Sb06g002180 in sorghum (Schweiger et al. 2013a) and the Bradi5g03300.1 in *Brachypodium distachyon* (Schweiger et al. 2013a).

In *B. distachyon*, Pasquet et al. (2016) produced both overexpressing transgenic lines and knockout mutant lines for the endogenous gene *Bradi5g03300.1*. They demonstrated that early conjugation of DON into D3G is linked to root tolerance to the mycotoxin as well as to spike resistance against FHB. Interestingly, the mutant line showed increased FHB susceptibility compared to wild type *B. distachyon* after spray inoculation assay with the fungus, but not after point inoculations. Since no other known *UGTs* seemed differentially expressed to compensate the mutation, the authors hypothesized a possible involvement of DON in primary infection (type I resistance).

Concerning wheat, only two *UGTs* were identified as associated to DON or FHB, though lacking the ability to efficiently convert DON to D3G. One is the *TaUGT3* gene, identified by expression analysis of DON-induced samples using Gene-Chip Wheat Genome Array, which was cloned from the wheat variety Wangshuibai (Lulin et al. 2010). Overexpression of the *TaUGT3* gene in *A. thaliana* enhanced tolerance against DON (Lulin et al. 2010), but in a less pronounced manner than the *AtUGT73C5* and the barley *HvUGT13248* discussed above. Indeed, the heterologous expression of *TaUGT3* in DON-sensitive yeast did not confer resistance against DON (Schweiger et al. 2013a). The other wheat *UGT* gene is *TaUGT12887* (Schweiger et al. 2013b). The gene was identified using NILs differing in the two QTLs *Fhb1* and *Fhb5*. *TaUGT12887* was induced in response to *F. graminearum* in lines harbouring both QTLs, compared to lines carrying only the *Fhb5* resistance allele, suggesting an *Fhb1* dependence. As a functional test to assess the capacity to detoxify DON, heterologous expression in yeast was performed, but much weaker resistance to DON than that conferred by other UGTs, like HvUGT13248, was observed (Schweiger et al. 2013b).

## 1.5 Resistance to FHB

Different strategies for managing FHB and DON accumulation can be applied. They include the use of fungicides, biological control, crop management practices and the use of resistant genotypes. FHB and DON contamination prediction tools are available in the USA and Europe; they are based on weather conditions, and aim to help growers in evaluating the risk and in adopting the best management practices (i.e. Fusarium Risk Assessment Tool, DONcast Europe, Fusaprog, SortInfo).

Fungicides containing triazole, imidazole or triazolinthione as active ingredients, which inhibit the biosynthesis of ergosterol, are the most active against FHB. Chemical control using effective substances and proper timing and application methods can reduce *Fusarium* severity (Willyerd et al. 2012). However, crop management and agrochemicals alone are only partly effective in controlling the disease, and integrated strategies for *Fusarium* control and prevention of mycotoxin contaminations are preferable (Blandino et al. 2012; Willyerd et al. 2012). Indeed, among the different strategies, the use of resistant genotypes is the most sustainable and stable one.

Genotype resistance to FHB can be classified into five typologies. Type I involves resistance of the plant to the initial fungal infection. Type II concerns the prevention of the infection

spread within the spike. Type III involves resistance to the infection of the kernel and type IV corresponds to tolerance to the infection, which, albeit present, does not cause substantial yield and quality losses. Finally, Type V is the ability of the host plant to degrade the mycotoxin that is responsible for virulence. Combination of different resistance mechanisms in wheat cultivars and, in particular, cultivars which possess Type I and II resistance mechanisms are preferable, as the resistance is expected to be of a higher degree and durable (Dweba et al. 2017). Morphological and developmental characteristics, such as plant height, ear compactness, flower opening and heading date, also influence the response to pathogen inoculation under field conditions (Buerstmayr et al. 2009). However, it should be considered that architectural traits unfavourable for infection, such as taller stature, awnless heads and low floret density, are generally associated with reduced yields (Yuen and Schoneweis 2007).

Improvement of resistance to FHB is a major target in both durum and bread wheat breeding. The former species is especially vulnerable, as effective sources of resistance are particularly limited (Stack et al. 2002; Buerstmayr et al. 2009). This contrasts with the fact that mycotoxin risk in food chain is particularly high, since durum wheat is almost exclusively used for human consumption. Durum wheat cultivated germplasm has been described to range from moderately to highly susceptible to FHB disease (Stack et al. 2002; Elias et al. 2005; Ban et al. 2005; Oliver et al. 2008; Buerstmayr et al. 2009). Among materials that exhibit moderate resistance, there are Tunisian genotypes (Elias et al. 2005) as well as some *T. turgidum* subsp. *carthlicum* and subsp. *dicoccum* accessions (Oliver et al. 2008). The lack of effective resistance sources is also accompanied by few breeding efforts in this species targeting FHB resistance, and/or by presence of FHB susceptibility factors (Ban and Watanabe 2001; Ban et al. 2005). Among bread wheats, the highest level of FHB resistance is present in the germplasm from China and Japan, for example in the Chinese cultivar Sumai 3 and landrace Wangshuibai, or in the Japanese accessions Nyu Bai, Nobeokabouzu and Shinchunaga (Bai and Shaner 2004). Not last, wild relatives, such as *T. dicoccoides* and *Ae. squarrosa*, and related species, like from *Thinopyrum* and *Elymus* genera, can be an effective source of FHB resistance (Bai and Shaner 2004; Ceoloni and Jauhar 2006; Buerstmayr et al. 2009).

FHB resistance is considered a typical quantitative trait. A review from Buerstmayr et al. (2009) reported the presence of at least 22 quantitative trait loci (QTL) or regions located on all wheat chromosomes, except for 7D. The most consistently observed and stable QTLs are those on chromosomes 3BS (*Fhb1*), 5AS (*Fhb5* or *Qfhs.ifa-5A*) and 6BS (*Fhb2*) (Buerstmayr et

al. 2009). Among them, the latter one is the less documented. The QTL *Fhb2* is correlated with significant type II resistance to FHB (Waldron et al. 1999; Cuthbert et al. 2007; Buerstmayr et al. 2009) explaining approximately 21% of the phenotypic variation in two doubled haploid (DH) populations (Yang et al. 2003).

The *Fhb1* QTL was identified in the cv Sumai 3 and initially designated as *Qfhs.ndsu-3BS* (Waldron et al. 1999; Anderson et al. 2001). The locus was mapped as a single Mendelian gene and it was placed in 1.2 cM marker interval flanked by sequence-tagged site (STS) markers (Liu et al. 2006). Moreover, in different populations, the largest effect on type II resistance appeared regularly at *Fhb1* (Buerstmayr et al. 2009). In accordance to this, Buerstmayr et al. (2003) demonstrated in a fully homozygous DH population that *Fhb1* showed a much larger effect than *Fhb5* after single floret inoculation. On the other hand, the effect of the two QTLs was comparable after spray inoculation experiments. Thus, the locus *Fhb5* on chromosome 5AS (Xue et al. 2011), initially designated as *Qfhs.ifa-5A*, may contribute more to type I resistance. Schweiger et al. (2013) investigated transcriptional differences of near-isogenic lines (NILs) segregating for *Fhb1* and *Fhb5*. They identified a constitutively expressed lipid transfer protein (*LTP*) gene, with more abundant transcript level in NILs carrying *Fhb5*, as well as an *UGT* gene, named *TaUGT12887*, expressed in NILs carrying both *Fhb1* and *Fhb5*, but, compared to NILs carrying a single QTL, more associated to *Fhb1*. *TaUGT12887* confers weak DON resistance when heterologously expressed in a DON-sensitive yeast (see § 1.4.2.1).

To date, many works have investigated various aspects of the resistance associated to the major *Fhb1* QTL. Lemmens et al. (2005) found that wheat DH lines carrying *Fhb1* derived from Sumai 3 were able to convert DON into D3G; on this basis, they hypothesized that the locus could encode a *UGT* gene or modulate the expression or the activity of an UGT enzyme. However, no such a gene has been reported until now. On the other hand, Gunnaiah et al. (2012) reported that in NILs segregating for *Fhb1* derived from the Nyubai genotype, the resistance was mainly associated with cell wall thickening and not to DON conversion. They also observed higher abundance of the jasmonic acid (JA) hormone related to *Fhb1*. Zhuang et al. (2013) have instead associated the downregulation of a *pmei* gene with absence of the *Fhb1* QTL. Notably, the overexpression in durum wheat of a *pmei* gene from *Actinidia chinensis* led to a reduction in FHB symptoms (Volpi et al. 2011). Yi et al. (2009) identified in the DON-resistant landrace Wangshuibai, carrying the *Fhb1* locus, an ATP-binding cassette (ABC) transporter gene, named *TaPDR1*, belonging to pleiotropic drug resistance (PDR) sub-family.

They showed that *TaPDR1* is upregulated by induction of both DON and *F. graminearum*, and the upregulation is significantly faster in the wild type genotype, compared to the *fhb1* mutant, which highly accumulates DON. Walter et al. (2008) showed that, in wheat, the regulation of the ABC transporter gene expression was positively correlated with DON resistance conferred by *Fhb1.* By means of virus-induced gene silencing (VIGS), the same group demonstrated that *TaABCC3* genes contributed to DON tolerance (Walter et al. 2015). Recently, Rawat et al. (2016) claimed to have identified the major genetic determinant of *Fhb1*-based FHB resistance in a pore-forming toxin-like (*PFT*) gene, located at the *Fhb1* QTL. They hypothesized that PFT could arrest fungal growth by interacting with the fungal wall. This is in line with the durable and broad-spectrum nature of *Fhb1* resistance, since it is not a classical gene-for-gene component, neither an *R* gene, which would have been easily overcome during evolution.

Breeding programs for the introgression of QTLs and hence resistance phenotypes in elite varieties from non-adapted genetic sources, frequently lead to undesired side effects on yield and quality, due to 'linkage drug'. Finely tuned chromosome engineering strategies of the alien donor and of the wheat recipient chromosome can allow to target the desired genes or QTLs and to minimize linkage drag (Ceoloni et al. 2005; Ceoloni and Jauhar 2006). For instance, the FHB resistance QTL *Fhb-7el$_2$L* from *Thinopyrum ponticum* was successfully transferred into durum and bread wheat genomes, and provides high reduction in FHB symptoms in both species (Forte et al. 2014). More recently, the *Fhb-7EL* resistance QTL from *Th. elongatum* was also transferred into the bread wheat genome, to which it was shown to provide an extremely effective and broad-spectrum of resistance against *Fusarium* diseases, including both FHB and FCR (Ceoloni et al. 2017).

### 1.5.1 Resistance through a transgenic approach

The modern tools of genetic engineering may provide an alternative approach to increase the level of FHB resistance in wheat by incorporating specific genes. However, due to the quantitative nature of resistance to some pathogens and diseases, as for FHB, the expression of single genes is unlikely to provide complete resistance. On the other hand, the transgenic approach remains crucial for providing evidence of the involvement of certain components in resistance. Furthermore, the introduction of genes from completely unrelated sources is impossible by conventional breeding and also by chromosome engineering (Bhalla 2006).

In 2016, global hectarage of biotech crops increased from 179.7 million hectares of 2015 to 185.1 million hectares in 26 countries (ISAAA 2016). The main biotech cultivated crops are soybean, maize, cotton and canola. However, public and consumer perception of genetic modified (GM) crops strongly influences their utilization. In particular, the perceived absence of consumer benefits, the prospect of multinational companies controlling the main crops, and the presence of selectable markers and plasmid backbones, are the main motivations against GM crops. Aside from the last two points, that can be overcome with several techniques, the environmental benefits, food security, human health and nutrition are the main motivations *pro* GM, implying, in particular, reduction of pesticide use and limitation of mycotoxin contamination. Moreover, it was estimated that the world will require 50% to 70% increase in food production for feeding the world population, which is continuously increasing and predicted to be 9.9 billion in 2050 and 12.3 billion in 2100 (ISAAA 2016).

Efficient protocols are available for genetic transformation of a few wheat cultivars, which are suitable for tissue culture regimes, in particular *via* biolistic gene transfer (also called particle bombardment) of bread (Vasil et al. 1993; Weeks et al. 1993) and durum (Bommineni et al. 1997) wheat and *via Agrobacterium*-mediated transformation (Cheng et al. 1997; Ishida et al. 2015). Moreover, new breeding techniques such as cisgenesis, intragenesis, site direct mutagenesis, genome editing using zinc finger nucleases or TALENs, CRISPRs/Cas9, RNA dependent DNA methylation and other epigenetic methods were developed to improve and finely modify genomes (Barabaschi et al. 2016; Dunwell 2014).

The transgenic engineering to achieve FHB resistance in wheat can be grouped based on the types of candidate genes used for: interfering with fungal growth, like using pathogenesis-related (PR) and anti-fungal proteins; antagonizing fungal virulence factors, such as trichothecenes; manipulating natural resistance mechanisms, like counteracting CWDEs or modifying host defence response pathways.

PR proteins are involved in plant defence and can effectively interfere with fungal growth. Based on similarities, they are grouped in 11 types. Chen et al. (1999) tried to introduce into spring wheat cv Bobwhite a rice thaumatin-like protein (TLP) gene (*tlp*) and a rice chitinase gene (*chi11*) under the control of constitutive promoters. Due to silencing phenomena, only the transgene *tlp* was expressed and conferred a slight reduction of FHB symptoms. Anand et al. (2003) obtained four transgenic wheat lines co-expressing genes for a chitinase and a β-1-3-glucanase cloned from Sumai 3. Only one line with high expression of both PR-proteins

showed a significant increase in FHB resistance in greenhouse trials. However, both this line and the rice-*tlp* line did not confirmed their resistance in field tests (Anand et al. 2003). Contrary to these results, Mackintosh et al. (2007) demonstrated that enhanced resistance to FHB can be obtained through overexpression of defence response genes. Indeed, the overexpression of wheat α- *1-purothionin*, a barley *tlp-1*, or a barley β-*1,3-glucanase* in wheat, resulted in enhanced resistance to FHB compared to untransformed Bobwhite plants, under both greenhouse and field conditions (Mackintosh et al. 2007). Also the overexpression of a lipid transfer protein (*PR-14*) from wheat, the *TaLTP5*, conferred significantly enhanced resistance in transgenic wheat to both common root rot caused by *Cochliobolus sativus* and FHB, providing therefore a broad spectrum antifungal activity (Zhu et al. 2012).

Effective expression in transgenic wheat of antifungal peptides toward FHB was also achieved, by overexpressing a wheat puroindoline (Gerhardt et al. 2002), a *Fusarium*-specific recombinant antibody fused with an antifungal peptide from *Aspergillus* (Li et al. 2008), the radish defensin RsAFP2 (Li et al. 2011) or a bovine lactoferricin peptide (Han et al. 2012).

To confer resistance to the mycotoxin DON is also an effective and promising strategy against FHB. In addition to the already discussed use of *UGT* genes (Li et al. 2015c, 2017) against DON (see § 1.4.2.1), transgenic expression of an acetyltransferase (Okubara et al. 2002) and of ribosomal protein L3 (RL3) (Di et al. 2010) were performed. The trichothecene 3-O-acetyltransferase *Tri101* is a key gene in fungal self-protection, since it converts DON into the less toxic 3ADON. The constitutive expression of the *Tri101* gene from *F. sporotrichioides* (*FsTri101*) in transgenic bread wheat was demonstrated to be effective in conferring only partial protection to FHB symptom spread in greenhouse conditions (Okubara et al. 2002). The low efficacy of the gene was later attributed to the kinetic proprieties of the *Fs*TRI101; indeed the orthologue in *F. graminearum* (*Fg*TRI101) has a 70-fold greater *in vitro kcat/Km* with DON (Garvey et al. 2007). Another issue of using this approach is that 3ADON is a masked mycotoxin still toxic for human and animal cells, and it can be de-acetylated in the digestive tract of mammals, releasing the native DON.

The ribosomal protein L3 at the peptidyltransferase centre is a target for translation inhibition by trichothecene mycotoxins. Transgenic wheat plants expressing a N-terminal yeast L3 fragment (L3Δ), non-functional as ribosomal protein, under the control of the maize *Ubi1* promoter (constitutive) and the barley *Lem1* one (floral tissue-specific), showed reductions in FHB disease severity and kernel DON levels, compared to non-transformed

plants, under greenhouse conditions (Di et al. 2010). In field tests, under high disease pressure, the line constitutively expressing L3Δ confirmed the significant reductions compared to the untransformed control (Di et al. 2010).

Another innovative approach is the host-induced gene silencing utilizing small-RNAs against fungal virulence factors. Indeed, the RNA interference (RNAi) of the virulence factor *Chs3b*, a chitin synthase gene of *F. graminearum*, enhanced wheat resistance to FHB and FCR on seedlings in two independent elite cultivar transgenic lines (Cheng et al. 2015).

Strengthening of plant cell wall by inhibitors of CWDEs was proved effective in reducing FHB disease symptoms in wheat, for example overexpressing the PvPGIP2 (Ferrari et al. 2012), AcPMEI (Volpi et al. 2011) or TAXI-III (Moscetti et al. 2013), as described in § 1.2.1.2.

Modification by a transgenic approach of plant defence pathways to better respond to *Fusarium* attack is also an efficient mechanism, probably the one with better results to date. Some examples are reported below.

The premature senescence of wheat heads infected by *F. graminearum* implicated ethylene (ET) signalling in disease development. Transgenic cv Bobwhite wheat, silenced for ET-pathway by RNAi of the *EIN2* gene, showed reduction in FHB symptoms and DON contents in infected heads (Chen et al. 2009). Interfering with the necrotrophic phase of infection is therefore relevant to symptom development, since clearly the fungus exploits an ET signalling to colonize the wheat head.

Faster activation of defence responses in the presence of the fungus also increases plant resistance. Indeed, the *A. thaliana NPR1* gene (*AtNPR1*), which regulates the activation of systemic acquired resistance (SAR), confers type II resistance to FHB when constitutively expressed in transgenic cv Bobwhite wheat, in greenhouse conditions (Makandar et al. 2006). In fact, SAR is associated with the accumulation of the hormone salicylic acid (SA) and the expression of the *PR* genes. The transgenic *AtNPR1* lines activate in a faster and stronger way *PR1* expression in response to *F. graminearum*. However, although the overexpression of *AtNPR1* in an elite wheat cultivar increased resistance to FHB, it increased also FCR susceptibility, associated with the expression the two defence genes *PR3* and *PR5* (Gao et al. 2013).

On the other hand, also the activation of JA-pathway contributes to FHB resistance. Indeed, the suppressor of the G2 allele of *skp1* (SGT1) is involved in HR and JA signalling and positively regulates R protein-mediated and PAMPs-triggered resistance. SGT1 from *Haynaldia villosa*

(HvSGT1) activates resistance mechanisms through the JA-dependent defence pathway, while suppresses the SA-dependent pathway but does not affect the activities of the ET-dependent pathway (Xing et al. 2013). The overexpression in wheat of the *HvSGT1* showed enhanced resistance to both powdery mildew and FHB, caused by a biotroph and an hemibiotroph pathogen, respectively (Xing et al. 2013).

Another class of DNA-binding transcription regulators connected to pathogen defence mechanisms is the WRKY family. The constitutive overexpression of the *TaWRKY45* conferred an enhanced type II resistance against FHB to transgenic wheat plants, under greenhouse conditions (Bahrini et al. 2011). Recently, the wheat *TaWRKY70* gene, located at the *QTL-2DL* was identified (Kage et al. 2017). Its silencing by VIGS in wheat, decreased expressions of resistance genes and resistance related induced (RRI) metabolites and increased fungal biomass after *F. graminearum* infection (Kage et al. 2017).

## 1.6 Resistance to FCR

Crop management, fungicides, biocontrol practice and cultivar resistance are the main strategies for disease control of FCR. *Fusarium* spores in infested stubbles from previous season represent the primary source of FCR infection. Therefore, burning stubble after harvest could significantly reduce FCR infection but this practice is linked to many disadvantage related to the soil composition and environment. Moreover, an increased adoption of conservation tillage practices resulted in an increased survival of the pathogen and in increasing in FCR severity (Wagacha and Muthomi 2007). Effective cultural practices include crop rotation with a non-cereal crop, appropriate use of fertilizers, irrigation, proper land preparation and timely harvesting (Pereyra et al. 2004; Wagacha and Muthomi 2007). Biological control using seed treatment with bacteria, including *Pseudomonas*, *Pantoea* and *Bacillus* spp., and the fungus *Trichoderma* has shown promise for control of FCR on seedlings (Dal Bello et al. 2002; Johansson et al. 2003; Khan et al. 2006). Although pesticide use in seed treatment has been shown to be effective in reducing the seedborne inocula (Reddy et al. 1999; Balmas et al. 2006), the use of fungicides is problematic both for the environment and for the legislation. Moreover, if sublethal or not effective doses are employed, the mycotoxin production, and therefore contamination, could also improve (D'Mello et al. 1998; Ramirez et al. 2004).

Among all strategies, the use of resistant varieties has long been recognized as the most effective way to minimize FCR damage. However, wheat genotype that shows complete resistance to this pathogen are unknown, only partial resistance or tolerance are reported (Powell et al. 2017), *i.e.* the bread wheat varieties EGA Wylie, Kukri and Sunco from Australia, and variety Ernie from USA.

Among the QTLs associated to FCR resistance, only three QTLs showed significant effects in more than two populations (Ma et al. 2010; Zheng et al. 2014): the QTLs *Qcrs.cpi-3B*, *Qcrs.cpi-5D* and *Qcrs.cpi-2D*. They are located on the chromosome 3BL, 5DS and 2DL, respectively, and explain up to 49%, 31% and 20% of phenotypic variance, respectively (Ma et al. 2010; Zheng et al. 2014). However, different QTLs seem to be associated with partial crown rot resistance at the different developmental stages of seedling or adult plant resistance (Martin et al. 2015).

Importantly, although FCR and FHB can be caused by the same pathogens, loci conferring resistance to the two diseases are located on different chromosomes (Li et al. 2010). This is not very surprising since the different time of infection and the different target organs, which characterize the diseases. However, the different location of resistance loci in the genome does not exclude the presence of common genes or components involved in *Fusarium* defense. Indeed, Stephens et al. (2008) show that *F. graminearum* gene expression in the very early stages of FHB infection is significantly similar to those of FCR, speculating that developing a control for FCR disease may also be effective in arresting early stages of infection of FHB and *vice versa*.

# 2. Objectives

The objectives of this doctoral thesis can be summarized as in the following:

I. To verify whether the expression of the HvUGT13248, able to detoxify the mycotoxin DON, could enhance *Fusarium* resistance in durum wheat, as already demonstrated in transgenic bread wheat constitutively expressing the *HvUGT13248* gene.

*Rationale*: Durum wheat is more susceptible than bread wheat and effective sources of resistance are particularly limited. Moreover, the mycotoxin risk in food chain is looked as particularly threatening, since durum wheat is almost exclusively used for human consumption.

*Actions*:

1. To assess the effectiveness of DON-detoxification strategy as a means of reducing the effects of *Fusarium* diseases, transgenic durum wheat plants constitutively expressing the barley *HvUGT13248* were produced by biolistic bombardment and then tested for their reaction to FHB and FCR diseases compared to wild type plants, by infection experiments with *F. graminearum* and *F. culmorum*, respectively.
2. To verify if the tissue-specific expression of the *HvUGT13248* transgene in the tissues site of FHB pathogenesis could be sufficient to enhance FHB resistance, while minimizing possible undesirable effects due to a constitutive expression, transgenic durum and bread wheat plants were produced by biolistic bombardment to express *HvUGT13248* under the control of the *Lem1* promoter. The latter regulates expression in lemma, palea, rachis and anthers. FHB symptom progression in transgenic wheat lines was compared to wild type plants, following infection with *F. graminearum*.

II. To assess if pyramiding of UGT and CWDE inhibitors genes, controlling different resistance mechanisms, could further improve *Fusarium* disease resistance.

*Rationale*: CWDE inhibitors counteract fungal infection by contrasting CWDEs, hence reinforcing the plant cell wall. This mechanism confers enhanced type II FHB resistance, as well as resistance against other diseases caused by necrotrophic fungi. However, the involvement of CWDE inhibitors in FCR disease was not previously evaluated, nor their effect in combination with other potential resistance factors.

*Actions*: Transgenic lines produced and evaluated for resistance as described for the previous objective, were crossed with transgenic wheat lines expressing inhibitors of CWDEs.

1. In durum wheat, the combined presence of HvUGT13248 and AcPMEI proteins was assessed, in comparison to that of individual proteins present in parental transgenic lines, for possible additive effects toward FHB and FCR diseases.
2. In bread wheat, pyramiding of HvUGT13248 and PvPGIP2 proteins was similarly assayed for its effect on resistance against FHB in comparison to the parental transgenic lines.

# 3. Materials and methods

## 3.1 Preparation of constructs

### 3.1.1 pAHC17_Ubi1::HvUGT13248

The pAHC17_Ubi1::HvUGT13248 construct (Fig. **10**) was prepared by inserting the complete coding region of *HvUGT13248* into the *Bam*HI site of pAHC17 (Christensen and Quail 1996) under control of the maize *Ubiquitin1* and *NOS* terminator. The coding sequence of *HvUGT13248* (Accession number GU170355) was synthetized and inserted in pUC57 vector by GenScript Biotech (New Jersey, USA), with amino acidic sequence optimized for *T. turgidum* subsp. *durum* codon usage. A FLAG®-tag region was added at the 3' end of the *HvUGT13248*. Moreover, two *Bam*HI restriction sites were added at the 5' and 3' ends of the sequence, respectively. Nucleotide and amino acidic sequences alignments between optimized and original *HvUGT13248* are provided in Fig. **SM-1** and Fig. **SM-2** (in Supplementary materials).

The *HvUGT13248* sequence, as well as the pAHC17, were digested with *Bam*HI (Promega; Milano, Italy) following the producer's protocol, and then ligated using the T4 Ligase (Promega) generating the pAHC17_Ubi1::HvUGT13248 construct (6,104 bp). The correct sequence and the insertion sites were confirmed by nucleic acid sequencing. The construct was amplified by transforming *Escherichia coli* DH5α competent cells and was isolated using the plasmid Miniprep kit or Maxiprep purification kit (Qiagen; Milano, Italy) depending on the desired yields, according to the protocols described by the producer.

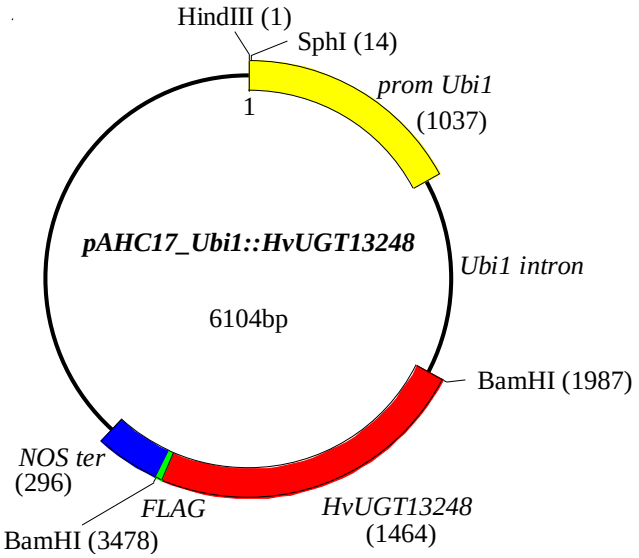


Fig. **10.** Schematic representation of pAHC17_Ubi1::HvUGT13248 with main restriction sites.

### 3.1.2 pAHC17_Lem1::HvUGT13248

The pAHC17_Lem1::HvUGT13248 construct (Fig. **11**) was prepared by inserting the complete coding region of *HvUGT13248* into the *Bam*HI site of pAHC17 (Christensen and Quail 1996) under control of the barley *Lem1* promoter and *NOS* terminator. The pAHC17_Lem1 construct was obtained from the pAHC17_Lem1::PvPGIP2 (Tundo et al. 2016a) exciding the *PvPGIP2* sequence by *Bam*HI restriction digestion. The pAHC17_Lem1, as well as the *HvUGT13248* (see § 3.1.1) were digested with *Bam*HI (Promega) following the producer's protocol, and then ligated using the T4 Ligase (Promega) generating the pAHC17_Lem1::*HvUGT13248* construct (5,409 bp). The correct sequence and the insertion sites were confirmed by nucleic acid sequencing.

The pAHC17_Lem1::HvUGT13248 construct was used to transform *E. coli* DH5α competent cells. The isolation of plasmid DNA was performed using Plasmid Mini or Maxi kit (Qiagen) depending on the desired yields, according to manufacturer's protocols.

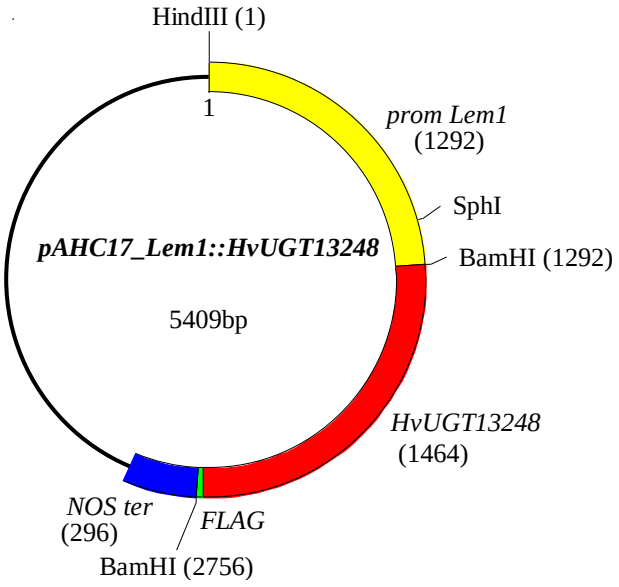


Fig. **11.** Schematic representation of pAHC17_Lem1::HvUGT13248 with main restriction sites.

## 3.2 Transgenic plants production

*Media*

Modified Murashige and Skoog (MS) media for wheat cellular cultures were used (Sears and Deckard 1982) with MS Salt (Duchefa Biochemie; Haarlem, Netherlands), Maltose, Thiamine-HCl, L-asparagine at pH 5.85 and Phytagel as gelling agent. Media composition varied in the different phases of plant production (Dissection, Bomb, Regeneration and Rooting) as indicated in Weeks et al. (1993) and are reported in Table **3**. After autoclaving at

121°C for 20 min, 2,4-dichlorophenoxyacetic acid (2,4-D) was added and the medium poured in 100 mm x 15 mm Petri dishes for Dissection and Regeneration media, in 60 mm x 15 mm Petri dishes for Bomb medium, and in Pyrex tubes for Rooting medium. Selection marker phosphinotricin (PPT; Duchefa Biochemie) is present only in regeneration and rooting media.

Table **3.** Culture media and compositions.

| Medium | Composition |
|---|---|
| **Dissection** | • Murashige & Skoog Salt mixture 4.3 g/l<br>• Maltose 40 g/l<br>• Thiamine-HCl (25 mg/500 ml) 10 ml/l;<br>• L-asparagine 0.15 g/l<br>• 0.25% v/v phytagel<br>• 2,4 D (0.5 mg/ml) 2 ml/500 ml |
| **Recovery** | • Murashige & Skoog Salt mixture 4.3 g/l<br>• Maltose 40 g/l<br>• Thiamine-HCl (25 mg/500 ml) 10 ml/l;<br>• L-asparagine 0.15 g/l<br>• 0.25% v/v phytagel<br>• 2,4 D (0.5 mg/ml) 2 ml/500 ml |
| **Bombardment (Bomb sucrose)** | • Murashige & Skoog Salt mixture 4.3 g/l<br>• Maltose 40 g/l<br>• Thiamine-HCl (25 mg/500 ml) 10 ml/l<br>• L-asparagine 0.15 g/l<br>• 0.25% v/v phytagel<br>• Sucrose 171.5 g/l<br>• 2,4 D (0.5 mg/l) 2 ml/500 ml |
| **Regeneration** | • Murashige & Skoog Salt mixture 4.3 g/l<br>• Maltose 40 g/l<br>• Thiamine-HCl (25 mg/500 ml) 10 ml/l<br>• L-asparagine 0.15 g/l<br>• 0.25% v/v phytagel<br>• 2,4 D (0.5 mg/ml) 0.2 ml/500 ml<br>• PPT (5 mg/l) |
| **Rooting** | • Murashige & Skoog Salt mixture 2.15 g/l<br>• Maltose 20 g/l<br>• Thiamine-HCl (25 mg/500 ml) 5 ml/l<br>• L-asparagine 0.075 g/l<br>• 0.25% v/v phytagel<br>• PPT (5 mg/l) |

*Embryo isolation*

Caryopses at 10 to 18 days post-anthesis (Zadoks stage 72) from *T. durum* cv Svevo plants or *T. aestivum* cv Bobwhite, grown in the field, were collected and surface-sterilized

using sodium hypochlorite 1% (10 min), 70% ethanol (15 min) followed by three times washing (5 min) with distilled sterile water. Immature embryos of 0.5 to 1 mm long were aseptically removed under the stereo microscope and placed with the scutella exposed on the Dissection medium (Fig. **13**A). Collected embryos were stored in the dark at 23° C for 5 days to induce callus formation.

*DNA-coating of gold particles*

Thirty mg of gold particles (0.6 µm) (Bio-Rad Laboratories; Segrate, Italy) were resuspended in 500 µl of 100% ethanol. Thirty-five µl of the suspension were aliquoted into 1.5 ml tubes, quickly centrifuged and the ethanol removed. The microprojectiles were then washed with cold sterile water (200 µl), spun and the supernatant discarded. Afterwards, the gold particles were coated with the pUbi::Bar construct (5,505 bp; Fig. **12**), carrying the *Bar* gene (accession number X17220.1) that confers resistance to phosphinotricin (PPT) and the construct of interest in a 1:3 molar ratio. The following formulas were used to calculate the µl of plasmid DNA needed for coating the gold particles, using 15 µg of pUbi::Bar:

Gene plasmid (pAHC17_Lem1::HvUGT13248 or pAHC17_Ubi::HvUGT13248) (µl):

bp gene/bp marker x 15 µg x (1/ plasmid concentration) x 3.

Marker plasmid (µl): 15 µg x (1/plasmid concentration).

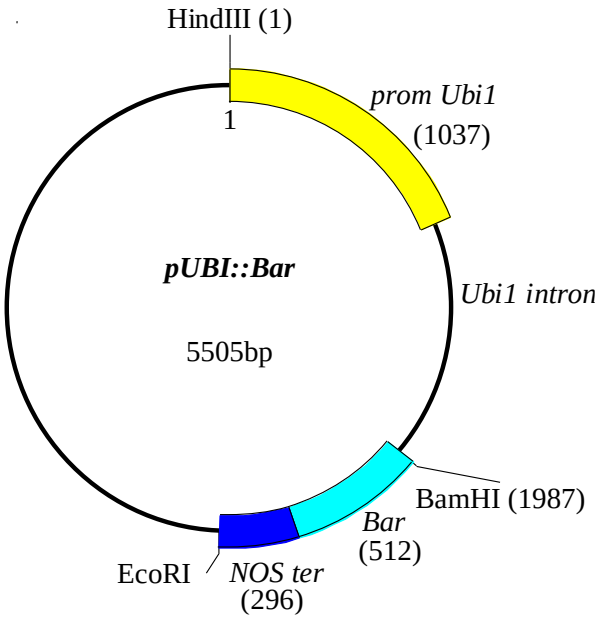


Fig. **12.** Schematic representation of pUbi::Bar construct with main restriction sites.

The microprojectiles pellet was resuspended in a solution containing 2.5 M CaCl2 (250 µl), spermidine (50 µl), plasmid DNA and water (250 µl - µl of plasmid). The tubes were shaken with a vortex mixer at 4° C for 20 min and briefly centrifuged. The supernatant was removed and the pellet was washed with 600 µl of 100% ethanol. The DNA-coated gold pellets were resuspended in 36 µl of 100% ethanol and stored on ice until they were used.

*Bombardment*

Constructs were introduced into immature embryos-derived calli by biolistic bombardment (details of performed bombardment experiments are provided in Table **7**, in § 4.1.1). About 100 embryos-derived calli were transferred in each of the Bomb medium plate (characterized by a high osmolarity) 4 h before the bombardment (Fig. **13**B). For each bombardment, 10 µl of the DNA-gold suspension was placed in the center of a macrocarrier and bombarded using a Model PDS-1000/He Biolistic particle delivery system (Bio-Rad Laboratoires) (Fig. **13**B) as described in Weeks et al. (1993). The distance from the stopping plate to the target was 13 cm, and the rupture disc strength was 1100 psi. Immediately after the bombardment, calli were kept in the bombardment medium and stored in the dark at 23°C for 24 h; then they were maintained in the Recovery medium for 4 weeks transferring them to a fresh medium at two week intervals.

*Plant regeneration*

Calli were transferred to the regeneration medium containing the selective marker PPT for 6 weeks at 23°C with 16 h light period (43 µE/m2) transferring them to a fresh medium at 2 week intervals. Usually starting from the third week, new shoots come from the calli resistant to the herbicide (Fig. **13**C). Shoots were individually transferred to Pyrex tubes containing the rooting medium, under herbicide selection, for additional 2-3 weeks. At this stage, plants capable to form long, highly branched roots in the selective medium were considered resistant (Fig. **13**C). Sensitive plantlets exhibited yellow necrosis, and reduced vigor within 1 week and did not produce roots, whereas resistant plantlets thrived in the rooting media. Resistant plantlets were transferred into pots and kept in a growth chamber, completely covered with plastic bags to increase the humidity, at 23°C, 16 h day light for 5-10 days to allow them to acclimate to *in vivo* conditions (Fig. **13**D). Then, plants were transferred to bigger pots; these primary regenerants are called $T_0$ plants (Fig. **13**D). Some of the lines

showed normal levels of fertility and seed set, whereas others showed reduced seed set or sterility compared with non-transformed Svevo/Bobwhite plants.

*PCR-screening of transgenic plants*

The presence of the *HvUGT13248* transgene and the selective *Bar* gene in the $T_0$ plants was checked as described in § 3.6.1 by PCR analysis using the primer pairs in Table **5**.

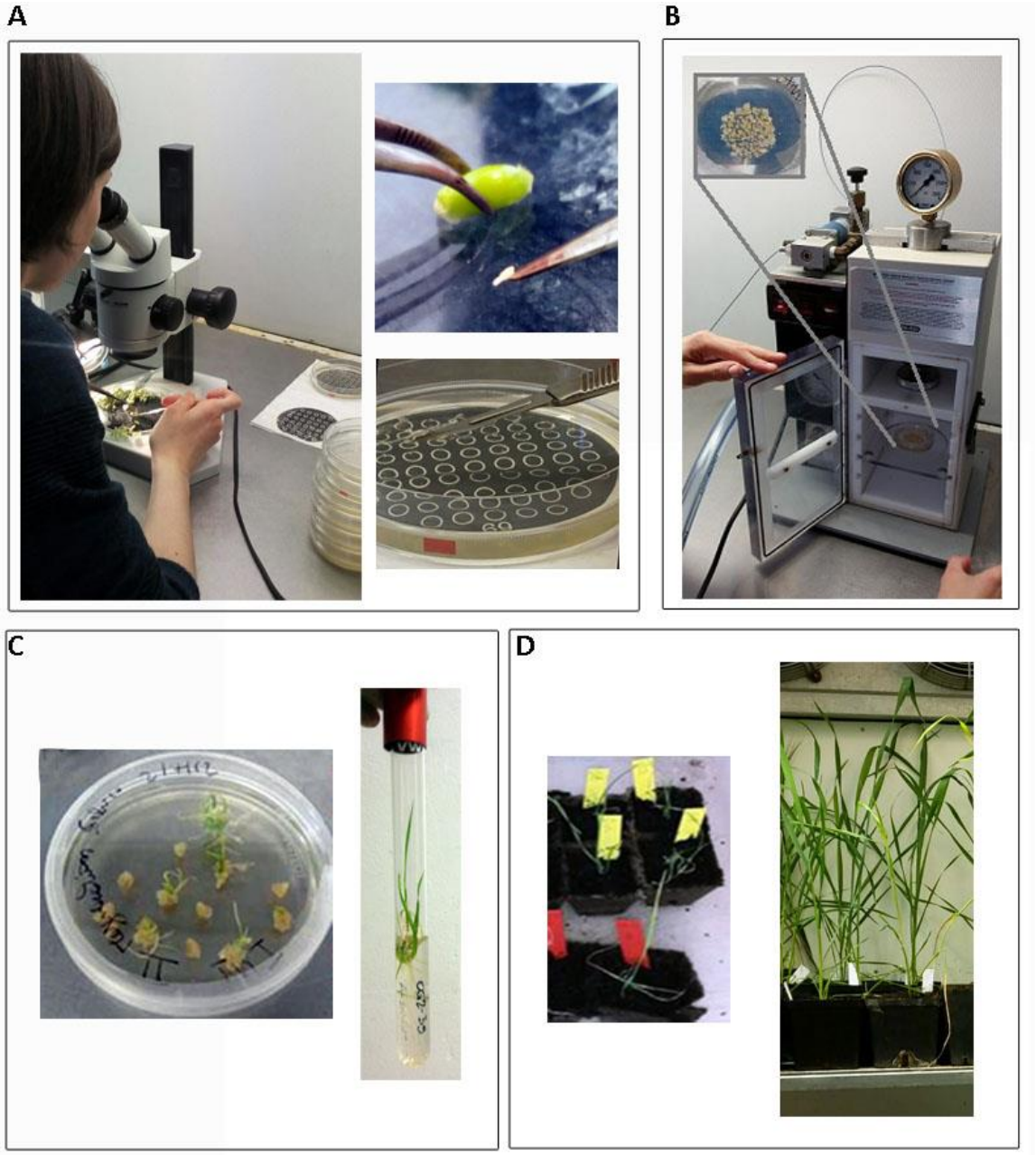


Fig. **13.** Production of transgenic wheat plants. **A)** Dissection of embryos from caryopsis (left), placed in dissection media for callus induction. **B)** Model PDS-1000/He Biolistic particle delivery system (Bio-Rad Laboratoires) used for bombardment, with bombarded embryos in Bomb sucrose medium. **C)** Plant regeneration: calli in regeneration medium (left) and plantlet in tube with rooting medium (right). **D)** Plantlets in soil for acclimatation (left) and regenerated plants (right).

## 3.3 Pyramiding of different transgenes

Crosses were performed between transgenic wheat lines expressing different resistance genes. Briefly, in the plant chosen as female parent, the upper and lower spikelets were eliminated, as well as the central flowers of the remained spikelets. The remaining flowers were carefully emasculated, removing the three bilobed anthers, after complete head emergence but when anthers were still green and the stigmas not feathery yet. When the stigmas became feathery, mature anthers from the male parent were used for pollination. The crossed spikes were covered with a small paper bag.

In particular, durum wheat $T_3$ plants of the lines ST7 (Ubi-UGT), containing *HvUGT13248* transgene, were crossed with $T_7$ plants of the line MJ15-69 (named PMEI-plants; Volpi et al. 2011), containing *AcPMEI* (*Actinidia chinensis* pectin methylesterase inhibitor; accession number P83326), to obtain 16A $F_1$ plants (UGT+PMEI), which express simultaneously both *HvUGT13248* and *AcPMEI*. Bread wheat $T_3$ plants of the ST8 lines (Lem-UGT), containing *HvUGT13248* transgene, were crossed with $T_6$ plants of the line J82-23a (named PGIP-plants; Janni et al. 2008), containing *PvPGIP2* (*Phaesolus vulgaris* polygalacturonase-inhibiting protein-2; accession number DQ105561), to obtain 16B $F_1$ plants (UGT+PGIP), which express simultaneously both *HvUGT13248* and *PvPGIP2*. Details of crossing are provided in Table **12** and Table **15** (in § 4.2.1.1 and § 4.2.2.1).

The co-presence of transgenes in $F_1$ plants was confirmed by PCR screening, carried out as described in § 3.6.1.

## 3.4 Plant materials and growth conditions

Wheat seeds were surface sterilized with sodium hypochlorite (0.5%, v/v) for 10 min and then rinsed thoroughly in sterile water. Seed germination was performed on 3 mm paper. When seminal roots and the hypocotyls emerged (Zadok stage 10), around 5 days post-germination, seedlings were transferred in jiffy pots with soil, and vernalized at 4°C for 2 weeks. Afterwards, plants were grown in a climatic chamber at 18 to 23°C with a 14-h photoperiod (300 µE $m^{-2}$ $s^{-1}$). When plants presented the second/third leaf (Zadok stage 12-13), they were two by two transferred in 14x14 cm pots. The growth stages were assessed using the Zadoks method (Zadoks, 1974). A summary of wild type and transgenic plant materials is provided in Table **4**.

Table **4.** Summary of plant materials used in this work.

| **Name** (other synonyms used) | **Genotype** | **Additional information** |
|---|---|---|
| **Svevo** (SV, untransformed/non-transgenic control of Ubi-UGT, ST1/4, MJ15-69 and 16A lines) | Wild-type *T. durum* cv Svevo | Italian early-flowering elite variety, highly susceptible to FHB |
| **ST7-47I** (Ubi-UGT) | Transgenic *T. durum* cv Svevo constitutively (*Ubi1* promoter) expressing the *HvUGT13248* | |
| **ST7-56II** (Ubi-UGT) | Transgenic *T. durum* cv Svevo constitutively (*Ubi1* promoter) expressing the *HvUGT13248* | |
| **ST1-22; ST1-10a** | Transgenic *T. durum* cv Svevo expressing the *HvUGT13248* in floral tissues (*Lem1* promoter) | Occurrence of silencing phenomena |
| **ST4-2; ST4-3a** | Transgenic *T. durum* cv Svevo expressing the *HvUGT13248* in floral tissues (*Lem1* promoter) | Occurrence of silencing phenomena |
| **Bobwhite** (BW, untransformed/non-transgenic control of Lem-UGT, J82-23a and 16B lines) | Wild-type *T. aestivum* cv Bobwhite | CIMMYT-derived spring wheat variety, moderate susceptible to FHB |
| **ST8-74I** (Lem-UGT; higher-expressing line) | Transgenic *T. aestivum* cv Bobwhite expressing the *HvUGT13248* in floral tissues (*Lem1* promoter) | |
| **ST8-49I** (Lem-UGT; lower-expressing line) | Transgenic *T. aestivum* cv Bobwhite expressing the *HvUGT13248* in floral tissues (*Lem1* promoter) | Weak expression of the *HvUGT13248* transgene. |
| **MJ15-69** (PMEI-plants, PMEI parental line) | Transgenic *T. durum* cv Svevo constitutively (*Ubi1* promoter) expressing the *AcPMEI* | Provide resistance against FHB (30% symptom reduction at early stages of infection) and Spot Blotch caused by *B. sorokiniana* (50% symptom reduction) (Volpi et al. 2011). |
| **16A** (UGT+PMEI-plants, double transgenic line) | Transgenic *T. durum* cv Svevo constitutively (*Ubi1* promoter) expressing the *HvUGT13248* and the *AcPMEI* | Progeny of ST7-47I x MJ15-69 |
| **J82-23a** (PGIP-plants, PGIP parental line) | Transgenic *T. aestivum* cv Bobwhite constitutively (*Ubi1* promoter) expressing the *PvPGIP2* | Provide resistance against FHB (30% symptom reduction) and Spot Blotch caused by *B. sorokiniana* (50% symptom reduction) (Janni et al. 2008; Ferrari et al. 2012) |
| **16B** (UGT+PGIP-plants, double transgenic line) | Transgenic *T. aestivum* cv Bobwhite expressing in floral tissues (*Lem1* promoter) the *HvUGT13248* and constitutively (*Ubi1* promoter) the *PvPGIP2* | Progeny of ST8-49I x J82-23a |

## 3.5 Root Assay

Sterilized wheat seeds of Ubi-UGT durum wheat lines and untransformed cv Svevo were sown in glass tubes containing MS Rooting medium (without PPT, see Table **3**) supplemented with DON (Romer Labs, Getzersdorf, Austria) 10 µM, diluted in 70% ethanol. Mock controls were prepared adding the same amount of 70% ethanol into the same medium without DON. Glass tubes were kept in dark until germination (approx. 3 days after seeding) and then moved in a climatic chamber at 22°C with a 16-h photoperiod (300 µE $m^{-2}s^{-1}$). For each line, the experiment was performed in five replicates.

Root growth was determined by measuring (cm) the longest root of each seedling once a week for one month. Percentage of root inhibition was calculated as the difference between mock and DON-treated samples for each line.

## 3.6 Nucleic acid analyses

### 3.6.1 PCR

Polymerase chain reaction (PCR) was performed to discriminate the presence of transgenes in transgenic plants. Genomic DNA was extracted from plants leaves using the method described by D'Ovidio and Porceddu (1996), obtaining a DNA solution of about 15 ng/µl. Briefly, up to 0.1 g of leaf tissue was ground with pestle in Eppendorf 1.5 ml tubes in the presence of liquid nitrogen. Eighty µl of DNA-extraction solutions (Tris 100 mM pH 8, EDTA 50 mM pH 8, NaCl 500 mM) and 36 µl of SDS 10% were added, and the samples were incubated for 10 min at 65° C in water bath. Potassium acetate 5 M (27 µl) was added and samples were kept in ice for 20 min. After centrifugation, the surnatant was supplemented with the same volume of cold isopropanol. The pellet, with DNA, was washed once in cold ethanol. After eliminating the ethanol, DNA was resuspended in 20 µL of RNase-free sterile water and stored at 4°C for up to one month.

PCR reactions were prepared in 10 µl composed as follow: 5 µl of GoTaq® Green Master Mix (Promega), 0.5 µM of each primers (Table **5**), 1 µl of extracted DNA, remain volume of nuclease-free sterile water. Amplification conditions were: 1 cycle at 95°C for 3 min; 35 cycles of denaturation at 95°C for 45 s, annealing at suitable temperature for each primer pairs (Table **5**) for 45 s, extension at 72°C for 1 min/1Kb; final extension step at 72°C for 5 min. *Actin*

(Accession number AB181991.1) amplification was used as housekeeping control. Amplicons were then confirmed by electrophoresis in 1% agarose gel.

Table **5.** List of oligonucleotides used in PCR amplifications.

| Primer name | Sequence 5'-3' | Annealing temp. | Amplicon size (bp) | Utilization |
|---|---|---|---|---|
| TaAct77F | TCCTGTGTTGCTGACTGAGG | 60° | 335 (gDNA) | Reference housekeeping gene |
| TaAct321R | GGTCCAAACGAAGGATAGC | | | |
| Ubi-49F | TCGATGCTCACCCTGTTGTTT | 60° | 568 | Screening of selection marker *Bar* gene in $T_0$ plants |
| Bar2R | GAAACCCACGTCATGCCAGT | | | |
| Ubi-49F | TCGATGCTCACCCTGTTGTTT | 60° | 522 | Screening of *HvUGT13248* in Ubi-UGT and UGT+PMEI plants |
| UGT472R | CTGCATGGTTGGGAGAAGAA | | | |
| Lem789 F | ACCTTAACCTGGCGCCTTAG | 60° | 788 | Screening of *HvUGT13248* in Lem-UGT and in UGT+PGIP plants |
| UGT472R | CTGCATGGTTGGGAGAAGAA | | | |
| Ubi-49F | TCGATGCTCACCCTGTTGTTT | 60° | 456 | Screening of *AcPMEI* in UGT+PMEI plants |
| AcPMEIR4 | TGAGTTGGAATATTTGGTGGAC | | | |
| Ubi-49F | TCGATGCTCACCCTGTTGTTT | 60° | 902 | Screening of *PvPGIP2* in UGT+PGIP plants |
| PvPGIP2-853R | TTAGCTGCGTCAGTCCCTGC | | | |
| Tri6-10F | TCTTTGTGAGCGGACGGGACTTTA | 60° | 245 | Detection of fungal biomass in infected spikelets |
| Tri6-4R | ATCTCGCATGTTATCCACCCTGCT | | | |
| UGT759F | AACCCTGCCATCGTACTACC | 60° | 697 | Preparation of *HvUGT13248* hybridization probe for southern blotting of UGT plants |
| FlagR | CTTGTCGTCGTCGTCCTTGTAGTC | | | |
| PvPGIP2-40F | TCTTTGAGCACTGCACA | 60° | 813 | Preparation of *PvPGIP2* hybridization probe for southern blotting of UGT+PGIP plants |
| PvPGIP2-853R | TTAGCTGCGTCAGTCCCTGC | | | |
| AcPMEIF4 | CTTGTATCTTTGAGAACTGCAC | 60° | 407 | Preparation of *AcPMEI* hybridization probe for southern blotting of UGT+PMEI plants |
| AcPMEIR4 | TGAGTTGGAATATTTGGTGGAC | | | |

### 3.6.2 RT-PCR

Total RNA was extracted from leaf or spike (discarding ovaries) tissues using Spectrum™ Plant Total RNA Kit (Sigma-Aldrich; Milano, Italy) according to the manufacturer's instructions. Total RNA was qualitatively evaluated by electrophoresis in 1% agarose gel and quantified by µDrop™ Plate (Thermo Scientific; Monza, Italy) in Multiskan™ GO Microplate

Spectrophotometer (Thermo Scientific). One µg of total RNA was subjected to genomic DNA elimination, and first-strand cDNA synthesis using QuantiTect® Reverse Transcription Kit (Qiagen) according to the manufacturer's protocols.

Reverse Transcriptase-PCR (RT-PCR) reactions were prepared as described in § 3.6.1 with primer pairs and annealing temperatures reported in Table **6**, and 0.5 µl of cDNA. *Actin* amplification was used as housekeeping control. Amplicons were then confirmed by electrophoresis in 1% agarose gel.

Table **6.** List of oligonucleotides used in RT-PCR amplifications.

| Primer name | Sequence 5'-3' | Annealing temp. | Amplicon size (bp) | Utilization |
|---|---|---|---|---|
| TaAct77F | TCCTGTGTTGCTGACTGAGG | 60° | 235 (cDNA) | Reference housekeeping gene |
| TaAct321R | GGTCCAAACGAAGGATAGC | | | |
| UGT759F | AACCCTGCCATCGTACTACC | 60° | 697 | Confirmation of *HvUGT13248* expression in transgenic plants |
| FlagR | CTTGTCGTCGTCGTCCTTGTAGTC | | | |
| UGT35F | GCACCACCTCATCGTCAGTC | 60° | 1430 | Confirmation of *HvUGT13248* complete coding region expression in transgenic plants |
| UGT1430R | GGATCCTCACTTGTCGTCGTC | | | |

### 3.6.3 Southern blotting

Southern hybridization was carried out on green leaf material. Genomic DNA was extracted from 3 to 5 g of green leaf material following Tai and Tanksley (1990) or D'Ovidio et al. (1992). DNA was qualitatively evaluated as 1:20 dilution on a 1% agarose gel and was quantified by µDrop™ Plate (Thermo Scientific) in Multiskan™ GO Microplate Spectrophotometer (Thermo Scientific).

Genomic DNA (10 µg) was restrict-digested with *Bam*HI or *Sph*I enzyme and were separated on 1.2% agarose gel. The *Bam*HI digestion excide the coding regions inserted in the pAHC17 plasmid (Fig. **10**, **Fig**. **11**), whereas the *Sph*I digestion cause a single cut in the plasmid (Fig. **10**, **Fig**. **11**). Transfer of digested DNA from agarose gel to positively charged nylon membranes (Roche Diagnostics) was performed as described by Sambrook et al. (1989). Briefly, the gel was incubated for 45 min in denaturation buffer (0.5 M NaOH and 1.5 M NaCl) and 1 h in neutralization buffer (1.5 M NaCl; 1 M Tris-HCl pH 8.0). The DNA fragments were transferred by capillarity onto the nylon membranes using 10x SSC buffer (150 mM NaCl; 15

mM sodium citrate) and, after about 18 h, the DNA was fixed in the membranes with UV light at 150 Joules.

Nylon membranes were hybridized with probe representing the coding region for each transgene labelled with digoxigenin (digoxigenin-11-uridine-50-triphosphate; Roche Diagnostics), following the procedure of D'Ovidio and Anderson (1994). Hybridization probes were prepared by PCR performed in 100 µL final volume, composed as follow: dATP 0.05 mM, dGTP 0.05 mM, dCTP 0.05 mM, dTTp 0.045 mM, dUTP 1:10 labelled with digoxigenin (Roche Diagnostics), 5x Green GoTaq® Flexi Buffer (Promega), $MgCl_2$ 25 mM, GoTaq® Flexi G2 DNA Pol (5U/µL) (Promega), 0.5 µM of each primers (Table **5**), 200 ng of the corresponding construct as template. Amplification conditions were used as explained in § 3.6.1. The hybridization probe was run on 1% agarose gel and purified by using the Gel/PCR DNA Fragments Extraction Kit (Geneaid). The membranes were pre-hybridized for 3 h at 65°C with hybridization buffer (5x SSC buffer, 0,1% N-Laurilsarcosine, 0,2% SDS, 0,5% Blocking Reagent -Boehringer Mannheim) without probe. Afterwards, the membranes were hybridized overnight with the same hybridization buffer supplemented with the denatured probe (5 min at 95°C, 1 min in ice before hybridization).

The probe in the probe-hybridized membranes was detected by immunological detection with a chemiluminescence assay. Anti-digoxigenin-AP' antibody (Roche Diagnostics) conjugated to an alkaline phosphatase were incubated in 1:10,000 ratio with the probe-hybridized membranes for 30 min. Then, CSPD (Roche Diagnostics) was used to allow the alkaline phosphatase reaction and therefore to detect the anti-digoxigenin-AP' associated with the probe. Dephosphorylated CSPD leads to a distinct luminescent signal that was detected by an autoradiography film, after 3 h or overnight expositions.

## 3.7 Protein analyses

### 3.7.1 Protein extraction and quantification

The fresh or frozen (-80°C) leaves or spike of transgenic and wild type plants were crushed in a mortar and pestle using liquid nitrogen. Plant tissues were then homogenized with Laemmli buffer (2% SDS, 60 mM Tris-HCl pH 6.8, 14.4 mM β-mercaptoethanol, 10% glycerol; Laemmli 1970) (2 ml/g) or 20mM sodium acetate 1M NaCl pH 4.6 buffer (2ml/g) for Western blot and enzymatic assays, respectively. For Western blot protocol, homogenized material was kept 15 min in ice, whereas for enzymatic assay protocol it was kept for 1 h

vortexing at 4°C. Afterwards, homogenized material was centrifuged at 12,000 rpm for 20 min at 4°C and the supernatant was recovered. Last steps were repeated again centrifuging for 5 min.

Protein concentration of the total protein extracts was determined with the 'Bio-Rad Protein assay' kit (Bio-Rad Laboratories; Bradford 1976) using Bovine Serum Albumin (BSA) as standard.

### 3.7.2 Western blotting

Ten µg of total proteins extracted with Laemmli buffer, supplemented with 0.1% Bromophenol Blue, were separated by SDS-PAGE. Briefly, SDS-PAGE was made according to Sambrook et al. (1989), using resolving gels containing 15% polyacrylamide and stacking gels with 5%. Precision Plus Protein™ Dual Colour Standard (Bio-Rad Laboratories) was used as molecular weight marker. The composition of the running buffer was 0.2 M Glycine, 0.02 M Tris pH 8.8, 0.1% SDS. Gel was run at a constant voltage of 200 V, stopping the run 10 min after the bromophenol blue dye front disappeared. Two identical gels were prepared. One gel was stained with 0.25% Coomassie Brillant Blue G250 in 45% ethanol, 10% acetic acid and destained with water in order to visualize the total protein extracts. On the second gel, protein blotting to PVDF transfer membrane (Immuno-Blot 0.2 µm PVDF Membrane for protein Blotting 10x15 cm, Bio-Rad Laboratories) was performed for 1 h at 100 V (maximum 400 mA), using Mini Trans-Blot® Electrophoretic Transfer Cell apparatus (Bio-Rad Laboratories). The PVDF membrane was saturated by incubation with blocking buffer (Tris 10 mM, NaCl 150 mM, Tween20 0.2 %, Not-fat dry milk 5%) for 2 h with gentle shaking. The blocked membrane was then incubated with gentle shaking overnight at 4°C with polyclonal rabbit primary OctA-Probe antibody (1:2,000; Santa Cruz Biotechnology), recognizing the FLAG®-tag sequence added at the N-terminus of the HvUGT13248. The membrane was then incubate for 1 h at room temperature with HRP-conjugated secondary antibody produced in rabbit (1:25,000; Sigma-Aldrich). Signals were detected using Luminata Crescendo Western HRP Substrate (Millipore) as peroxidase HRP substrate, by an autoradiography film, after 1 and 3 h expositions.

### 3.7.3 Enzymatic assays

#### 3.7.3.1 PGIP inhibition assay

PGs enzymatic activity of was evaluated using a modified radial diffusion assay (Taylor and Secor 1988), also called 'Cup-plate'. Briefly, a solution (30 µl) containing *Fusarium phyllophilum* PG (*Fp*PG) and total protein extracts of transgenic or wild-type plants was added to 0.5 cm wells on plates containing 100mM sodium acetate, pH 4.6, 0.5% polygalacturonic acid (Honeywell Fluka, Monza, Italy) and 0.8% agarose. *Fp*PG was used since its activity is not inhibited by wheat endogenous PGIPs but not by PvPGIP2. Plates were incubated for 19 hours at 30°C. The halo caused by enzyme activity was visualized after 15 min of treatment with 6 N HCl. PG-activity was expressed as agarose diffusion units, with 1 agarose diffusion unit defined as the amount of enzyme that produced a halo of 0.5 cm radius (external to the inoculation well) after 19 hours at 30°C. Inhibitory activity was expressed as inhibitory units, with 1 inhibitory unit defined as the amount of PGIP that reduced by 50% 1 agarose diffusion unit of PG. *Fp*PG used in the assays were kindly provided by Pr. Felice Cervone (Department of Plant Biology, Università degli Studi di Roma La Sapienza, Rome, Italy).

#### 3.7.3.2 PMEI inhibition assay

PME enzymatic activity was quantified by the agarose diffusion assay as described by Downie et al. (1998) with some modifications. Agar plates (15 ml per plate) were prepared with 0.1% (w/v) of pectin from apple 70-75% esterified (Honeywell Fluka), 1% agarose (w/v), 25 mM citric acid and 115 mM $Na_2HPO_4$, pH 6.3. Wells with a diameter of 0.5 cm were made and the protein samples (30 µl) containing 5 µg of total protein extract were loaded in each well. Plates were incubated for 18 h at 30°C. The gels were stained with 0.02% (w/v) ruthenium red (Sigma-Aldrich) for 45 min, de-stained with water and the diameter of the red-stained zones, resulting from the hydrolysis of esterified pectin in the gel, was measured. The inhibition activity of PMEI was calculated as percentage of the difference between halo cm of wild type and transgenic protein extracts.

## 3.8 Fungal materials and growth conditions

*F. graminearum* (strains 3827, PH1 and 8/1) and *F. culmorum* (strain UK99) were cultured on potato dextrose agar (PDA) medium (AppliChem GmbH; Darmstadt, Germany). In order to produce macroconidia, fungi were cultured in synthetic nutrient agar (SNA) medium

(Urban et al. 2002) containing 0.1% $KH_2PO_4$, 0.1% $KNO_3$, 0.1% $MgSO_4*7H_2O$, 0.05% KCl, 0,02% glucose, 0.02% sucrose, 2% bactoagar (Becton Dickinson; New Jersey, USA) with 200 ppm biotin and 200 ppm thiamine. Macroconidia were harvested by gently scraping the culture surface with 1ml of sterile water, and conidia concentration was estimated by Thoma chamber, adjusting the concentration to the proper concentration for the infection assays. Tween 20 was added to a final concentration of 0.05% to aid inoculum adhesion to the plant tissue.

## 3.9 *Fusarium graminearum* infection assay

Plant inoculation was performed with *F. graminearum* conidia adjusted at $2.5x10^4$ conidia/ml, using a final concentration of 500 conidia in 20 µl. Infection experiments of wheat plants were performed by single-spikelet inoculation. The conidia suspension (20 µl) was pipetted directly through the glumes of two opposite central florets of a wheat head during anthesis (Zadok stage 64). Infected spikes were covered with plastic bags for two days in order to maintain high humidity conditions. Fusarium Head Blight (FHB) disease symptoms were assessed by counting the number of visually diseased spikelets at different days post-infection (dpi) and by rapporting them to the total number of spikelets of the respective head, resulting in a percentage of symptomatic spikelets. For each experiment, at least 15 plants for each genotype were used.

### 3.9.1 PCR for fungal biomass presence in spikelets

Total DNA from different spikelets from infected spikes was extracted with DNeasy Plant Mini kit (Qiagen) according to manufacturer's instructions. RT-PCR was performed as described in § 3.6.1 with Tri6-10F/Tri6-4R primers pairs (Horevaj et al. 2011). The *Actin* gene was used as housekeeping.

### 3.9.2 DON and D3G content measurement

Metabolites were extracted from 100 mg of wheat semolina/flour in 400 µl of $C_2H_3N$-$H_2O$ 86:14 on a horizontal shaker for 24 h at 180 rpm at 4° C. The supernatant was recovered after centrifugation at 10,000× g for 10 min. DON and D3G levels were ascertained by UHPLC system coupled with Q Exactive™ hybrid quadrupole Orbitrap™ Mass Spectrometer (Thermo Scientific). Data were analyzed with MAVEN.52 software (Melamud et al. 2010). Standard

curves were obtained with serial dilutions of analytical standards of DON (Romer Labs, resuspended in 96% ethanol) and D3G (Romer Labs, 50 µg/ml in acetonitrile).

The level of DON and D3G were determined in two *F. graminearum* infection experiments, using three technical replicates.

## 3.10 *Fusarium culmorum* infection assay

Seedlings were individually grown jiffy pots, arranged in plastic trays, at 22°C, with a 16 h light period. Inoculation was performed with *F. culmorum* strain UK99 suspension adjusted at $1.5 \times 10^6$ conidia/ml, using a final concentration of $3 \times 10^4$ conidia in 20 µl. For inoculation, the method described by Mitter et al. (2006) was used with some modifications. The seedling stem base leaf sheath at the first-leaf stage (Zadoks stage 11), was inoculated with 20 µL of conidia suspension, evenly spread with the help of a small paintbrush. Plastic trays with infected seedlings were covered with a plastic film for 2 days to maintain high relative humidity.

Fusarium crown rot (FCR) disease symptoms were assessed each 3 days from days 5 to 21 post-inoculation (dpi), using two parameters: symptom extension (SE; cm) and browning index (BI) of the infected tissues (visual rating of the degree of extension of necrosis, as indicated by brown discoloration). BI is based on a five-point scale (0: symptomless; 1: slightly necrotic; 2: moderately necrotic; 3: severely necrotic; 4: completely necrotic. See Fig. **14**). Disease index (DI) was subsequently determined as SE × BI (Beccari et al. 2011). For each experiment, at least 12 plants for each genotype were used.


Fig. **14.** Visual aspect of the Browning Index (BI) scale.

## 3.11 Statistical analyses

All data were subjected to analysis of variance (ANOVA) by using SYSTAT12 software (Systat Software Incorporated, San Jose, CA, USA). The variable data (i.e. percentage of symptomatic spikelets for FHB, Disease index for FCR, metabolite quantification for DON/D3G content in flour) was considered as dependent factor against independent factors, represented by genotype and replica. Two levels of significance ($P<0.05$, $P<0.01$) were considered to assess significance of the F values. When significant F values were observed, a pairwise analysis was carried out by the Tukey Honestly Significant Difference test (Tukey test) at 0.95 or 0.99 confidence level.

# 4. Results

## 4.1 Objective I: Enhancing resistance in durum and bread wheat against *Fusarium* diseases by ectopic expression of an UDP-glucosyltransferase.

### 4.1.1 Production and selection of transgenic plants

Biolistic transformations of embryogenic calli of durum wheat cv Svevo and bread wheat cv Bobwhite were performed with co-bombardment of the pAHC17_Ubi1::HvUGT13248 or the pAHC17_Lem1::HvUGT13248, respectively, and the pBI_Ubi1::Bar as selectable marker. Both pAHC17 plasmids contain the coding region of the barley *HvUGT13248* gene, optimized for the codon usage of wheat and followed by a FLAG®-tag sequence before the stop codon. The promoters of maize *Ubiquitin1* and of barley *Lem1* were used for constitutive and floral-specific expression, respectively. The transformation experiments were carried out following the procedure reported by Janni et al. (2008). For the constitutive expression, two different bombardments, named ST7 and ST9, were performed on durum wheat calli (Table **7**). In ST7, 1,104 embryogenic calli were bombarded, obtaining 13 $T_0$ lines containing the *HvUGT13248* transgene, which corresponded to an efficiency of 1.18%. In ST9, 1,407 embryogenic calli were bombarded, obtaining 10 $T_0$ lines with *HvUGT13248*, hence with an efficiency of 0.7%. For the specific expression in floral tissues, two different bombardments, named ST1 and ST4, were performed on 1,104 and 1,008 durum wheat calli, respectively (Table **7**). A total of four $T_0$ lines carrying *HvUGT13248* were obtained, with an efficiency of 0.2%. In bread wheat, 1,272 embryogenic calli were bombarded. The experiment, named ST8 (Table **7**), resulted in four $T_0$ lines showing the presence of *HvUGT13248* (0.3% efficiency). The particularly low transformation efficiency of pAHC17_Lem1-driven constructs was also observed in previous studies (Tundo 2015).

In all $T_0$ lines, the presence of the gene of interest, i.e. *HvUGT13248*, and of the *Bar* marker were confirmed by PCR analysis using the primer pairs Ubi-49F/UGT472R or Lem789F/UGT472R and Ubi-49F/Bar2R, respectively.

Table **7**. Outline of the bombardment experiments.

| Bomb name | Genotype | Construct | Bombarded calli | No. of regenerants | No. of $T_0$ lines | Efficiency |
|---|---|---|---|---|---|---|
| ST7 | Svevo | pAHC17 Ubi1::HvUGT13248 | 1104 | 43 | 13 | 1.18 |
| ST9 | Svevo | pAHC17 Ubi1::HvUGT13248 | 1407 | 28 | 10 | 0.7 |
| ST1 | Svevo | pAHC17 Lem1::HvUGT13248 | 1104 | 8 | 2 | 0.2 |
| ST4 | Svevo | pAHC17 Lem1::HvUGT13248 | 1008 | 5 | 2 | 0.2 |
| ST8 | Bobwhite | pAHC17 Lem1::HvUGT13248 | 1272 | 14 | 4 | 0.3 |

Ten lines from the ST7 and ST9 experiments were subjected to RT-PCR (see, e.g., Fig. **15**) and Western blot (see, e.g., Fig. **16**) analyses in the $T_1$ generations to confirm the expression of the *HvUGT13248* gene and to compare the levels of expression among the different lines. Silencing phenomena were observed, which impaired transcript and protein production of some lines (see lanes 4 in Figs. **15**, **16**). Importantly, none of the analysed lines showed obvious phenotypic alterations vs wild type plants in $T_1$ generation. Transgenic lines ST7-47I and ST7-56II (from here on referred to as Ubi-UGT) were selected for further characterization in subsequent generations (Fig. **17**).

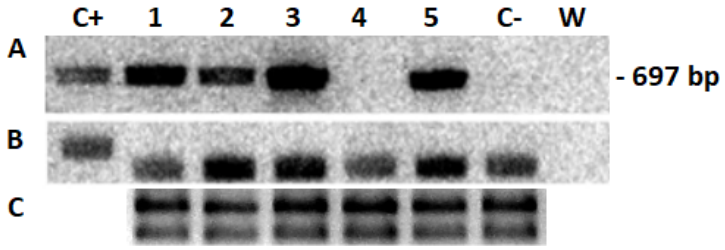


Fig. **15**. RT-PCR amplification products of cDNA of $T_1$ Ubi-UGT durum wheat plants. **A)** *HvUGT13248* transgene amplification; **B)** Amplification of housekeeping *Actin* gene; **C)** Total RNA.
(C+) positive Ubi-UGT gDNA used as positive control; (1-5) $T_1$ Ubi-UGT plants (leaf); (C-) *T. durum* cv Svevo used as negative control (leaf); (W) water.

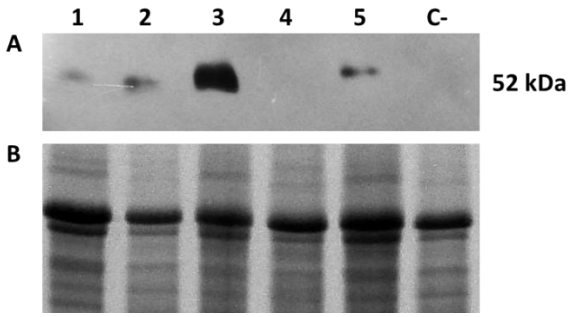


Fig. **16**. Western blot analysis on leaf extracts of durum wheat $T_1$ Ubi-UGT plants. **A)** Western blot detection. **B)** SDS-PAGE of 10 µg of total protein extracts.
(1-5) Leaf extracts of various $T_1$ Ubi-UGT plants. (C-) *T. durum* cv Svevo leaf extract used as negative control.


Fig. **17** Phenotypic appearance of (1) *T. durum* cv Svevo untransformed plant and of the (2) ST7-47 and (3) ST7-56 transgenic plants.

The expression of the *HvUGT13248* gene in $T_1$ lines isolated from the ST1 and ST4 experiments was confirmed by RT-PCR, amplifying almost 700 bp of the entire coding sequence. All four lines showed the expected band (Fig. **18**). However, since it was not detected any signal corresponding to HvUGT13248 by Western blot, the same lines were again subjected to RT-PCR using the primer pairs UGT35F/UGT1432R, in order to verify the actual presence of the entire coding region. As shown in Fig. **19**, none of the lines expressed the *HvUGT13248* at the anthesis stage. Probably, silencing phenomena affected these

transformation events. The amplification of almost half of the transcript in the first RT-PCR (Fig. **18**) suggests a post-transcription silencing. The observed amplicon might correspond to the native ~700 bp portion, or to smaller overlapping fragments of it, resulting from the silencing phenomena. For this reason, no further experiments were performed with the Lem-UGT durum wheat lines.

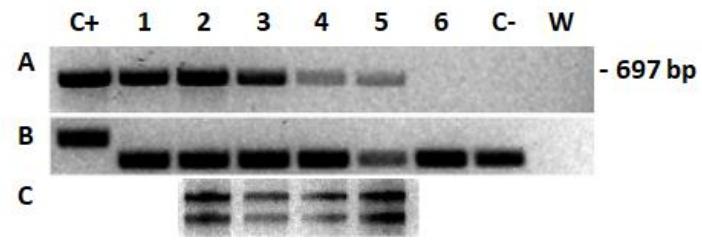


Fig. **18**. RT-PCR amplification products of cDNA of $T_1$ Lem-UGT durum wheat plants at the anthesis stage. **A)** Amplification of *HvUGT13248* transgene; **B)** Amplification of housekeeping *Actin* gene; **C)** Total RNA.
(C+) gDNA of a $T_0$ Lem-UGT plant, used as positive control; (1) $T_0$ Lem-UGT plant, used as positive control; (2-5) $T_1$ Lem-UGT durum wheat plants (spikelets), namely: ST1-22; ST1-10a; ST4-2; ST4-3a; (6) leaf cDNA of ST1-22; (C-) *T. durum* cv Svevo, used as negative control (spikelets); (W) water.

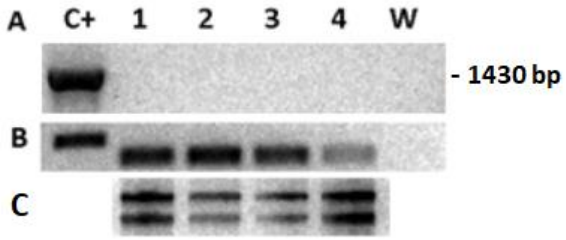


Fig. **19**. RT-PCR amplification products of cDNA of $T_1$ Lem-UGT durum wheat plants at the anthesis stage. **A)** Amplification of *HvUGT13248* complete coding region; **B)** Amplification of housekeeping *Actin* gene; **C)** Total RNA.
(C+) gDNA of a $T_0$ Lem-UGT plant, used as positive control; (1-4) $T_1$ Lem-UGT durum wheat plants (spikelets), namely: ST1-22; ST1-10a; ST4-2; ST4-3a; (W) water.

All four positive ST8 lines of the $T_1$ generation were subjected to RT-PCR of pre- and post-anthesis tissues (Fig. **20**), in order to confirm the expression of the *HvUGT13248* gene in the different lines. Western blot analysis was not performed in the $T_1$ generation in order to save seeds for the next generation. In all transgenic lines, a higher presence of the transcript was observed in the pre-anthesis stage (Fig. **20**A). This is in line with the observation by Tundo et al. (2016) of a higher expression induced by the *Lem1* promoter in this stage. Only the ST8-11 line showed evident lower expression compared to the other transgenic lines in the post-anthesis stage (Fig. **20**B). Notably, none of the analysed lines showed obvious phenotypic

alterations vs wild type plants in $T_1$ generation. ST8-49 and ST8-74 (from here on referred to as Lem-UGT) were selected for further characterization in subsequent generations (Fig. **21**).

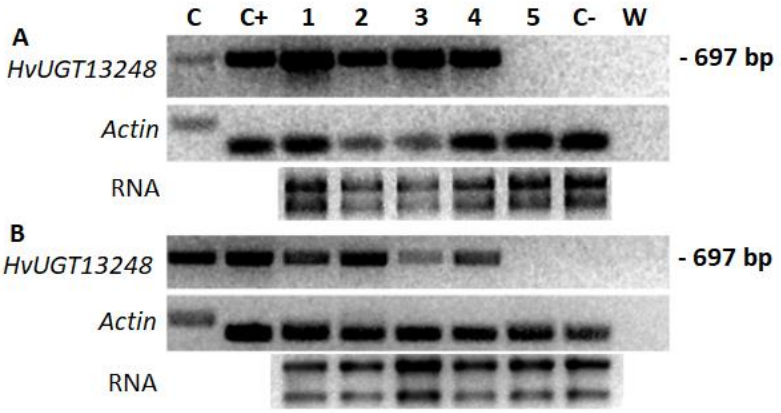


Fig. **20**. RT-PCR amplification products of spike tissues of $T_1$ Lem-UGT bread wheat plants. Amplifications of the *HvUGT13248* transgene and the housekeeping *Actin* gene were performed **A)** from pre-anthesis and **B)** from post-anthesis spikelets. Total RNA of the correspondent sample is provided.
(C) Lem-UGT gDNA, used as positive control; (C+) Ubi-UGT cDNA, used as positive control; (1-4) spikelet cDNA of $T_1$ Lem-UGT plants, namely: ST8-49I, ST8-74I, ST8-11, ST8-65I; (5) leaf cDNA of a $T_1$ Lem-UGT plant; (C-) spikelet cDNA of *T. aestivum* cv Bobwhite used as negative control; (W) water.


Fig. **21.** Phenotypic appearance of (1) *T. aestivum* cv Bobwhite untransformed plant and of (2) the ST8-74 and (3) ST8-49 transgenic plants.

### 4.1.2 Molecular characterization of selected transgenic lines

Molecular characterization of two transgenic events for each of the transformation experiments (namely ST7-47I and ST7-56II Ubi-UGT durum wheat lines and ST8-74I and ST8-49I Lem-UGT bread wheat lines) were carried out by Western blot, RT-PCR and Southern blot analyses.

Protein expression of the HvUGT13248 was confirmed by Western blot analysis, detecting the FLAG®-tag present at the N-terminus of the protein, with an anti-FLAG®antibody. Both the Ubi-UGT lines showed the signal corresponding to 52 kDa of the HvUGT13248 (Fig. **22**). Moreover, two signals of 25 and 20 kDa were also detected, suggesting a proteolytic cut, possibly due to protein turnover. Concerning the Lem-UGT lines, only ST8-74 showed the HvUGT13248 protein (Fig. **23**). No signal was detected in the untransformed controls.

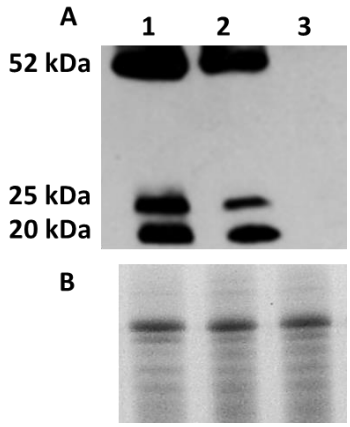


Fig. **22**. Western blot analysis on leaf extracts of Ubi-UGT durum wheat lines. **A)** Western blot detection. **B)** SDS-PAGE of 10 µg of total protein extracts.
(1) ST7-47I; (2) ST7-56II; (3) *T. durum* cv Svevo.

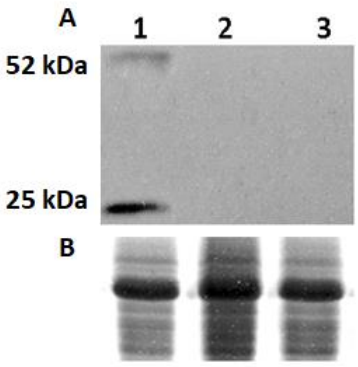


Fig. **23**. Western blot analysis on spike tissue extracts of ST8 Lem-UGT bread wheat lines. **A)** Western blot detection. **B)** SDS-PAGE of 10 µg of total protein extracts.
(1) ST8-74I; (2) ST8-49I; (3) *T. aestivum* cv Bobwhite.

To further validate transgene expression, an RT-PCR on the *HvUGT13248* complete coding region was performed. Among Ubi-UGT lines (Fig. **24**), ST7-47 showed a more intense band, indicating a higher transcript level. Concerning Lem-UGT lines (Fig. **25**), *HvUGT13248* expression was confirmed in both lines, although the ST8-49 line showed a very weak band, possibly reflecting a weak protein expression and accounting for the absence of protein detection by Western blot.

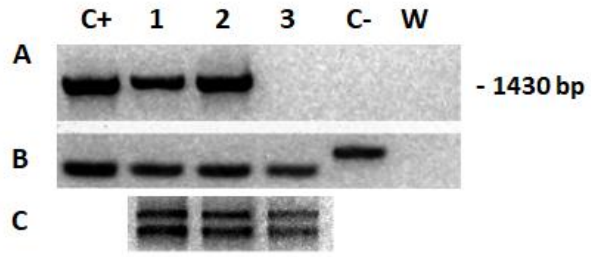


Fig. **24**. RT-PCR amplification products of cDNA from leaf of Ubi-UGT durum wheat plants. **A)** Amplification of *HvUGT13248* complete coding region; **B)** Amplification of housekeeping *Actin* gene; **C)** Total RNA.
(C+) Ubi-UGT $T_0$ plant, used as positive control; (1) ST7-56II; (2) ST7-47I; (3) *T. durum* cv Svevo; (C-) gDNA of *T. durum* cv Svevo, used as negative control; (W) water.

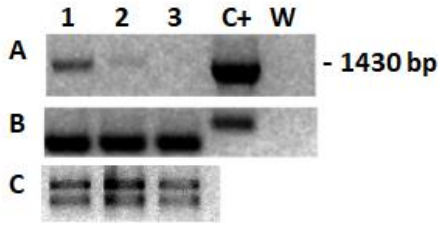


Fig. **25**. RT-PCR amplification products of cDNA from spikelets of Lem-UGT bread wheat plants at anthesis stage. **A)** Amplification of *HvUGT13248* complete coding region; **B)** Amplification of housekeeping *Actin* gene; **C)** Total RNA.
(1) ST8-74I; (2) ST8-49I; (3) *T. aestivum* cv Bobwhite, used as negative control; (C+) gDNA of a $T_0$ Lem-UGT plant, used as positive control; (W) water.

To confirm transgene integration, genomic DNAs of the selected transgenic lines were analyzed by Southern blot analysis using almost 800 bp of the *HvUGT13248* coding region as probe. The cleavage with *Bam*HI restriction enzyme, which causes the excision of the *HvUGT13248* coding region (Figs. **26**A, **27**A), confirmed the presence in all transgenic lines of the expected hybridization fragment of about 1400 bp (Figs. **26**B, **27**B). In particular, line ST7-47I showed a more intense signal than ST7-56II (Fig. **26**B), suggesting a higher copy number of integrated coding regions. Conversely, both ST8 transgenic lines displayed a similar band intensity, suggesting a similar copy number of integrated coding regions (Fig. **27**B).

Subsequently, digestion with *Sph*I enzyme, which has one restriction site within the constructs (Figs. **26**A, **27**A), produced in all transgenic lines the expected hybridization fragment, corresponding to entire constructs (Figs. **26**C, **27**C) of 6,104 and 5,409 bp for the pAHC17_Ubi1::HvUGT13248 and pAHC17_Lem1::HvUGT13248, respectively. In both ST7 lines, additional hybridizing fragments were also found (Fig. **26**C), suggesting the occurrence of transgene rearrangement events. On the other hand, hybridization bands in the ST8 lines were weakly visible, though present (Fig. **27**C), suggesting a low copy number of integrations. As expected, in all Southern blot experiments no hybridization signal was detected in genomic DNA of the non-transformed, wild type plants.

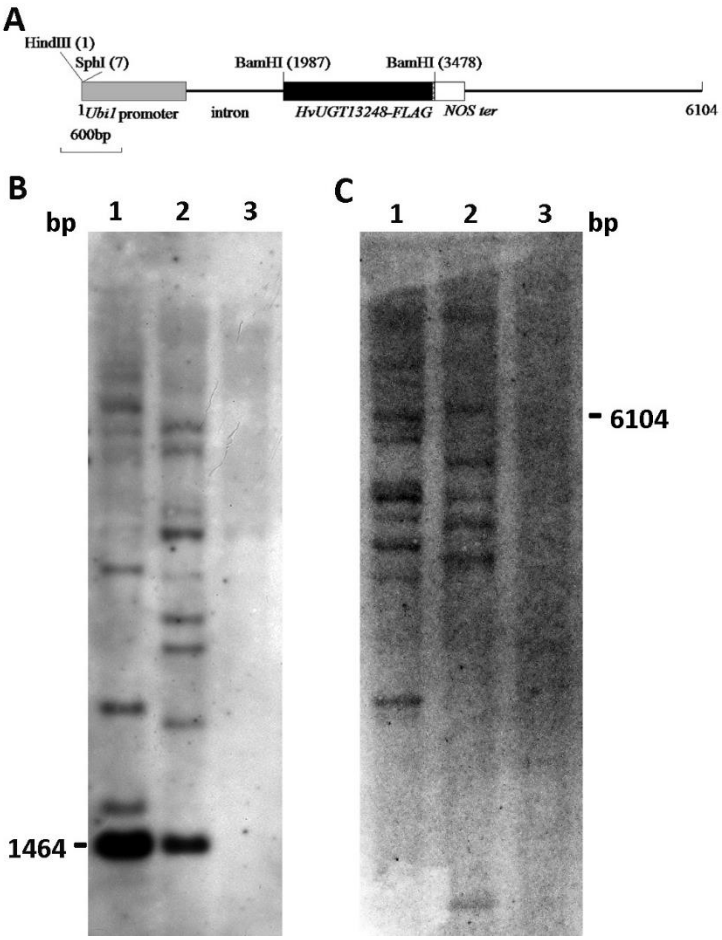


Fig. **26**. Southern blot analysis of the Ubi-UGT plants. **A)** The pAHC17 Ubi1::HvUGT13248 linearized construct, prepared by cloning the *HvUGT13248-FLAG* gene into the *Bam*HI site of pAHC17 under control of the maize *Ubiquitin1* promoter and *NOS* terminator.
Genomic DNA (10 µg) of $T_4$ transgenic lines was digested with **B)** *Bam*HI and **C)** *Sph*I and probed with a digoxigenin-labeled coding region of *HvUGT13248-FLAG*.
(1) ST7-47I; (2) ST7-56II; (3) *T. durum* cv Svevo (untransformed control).

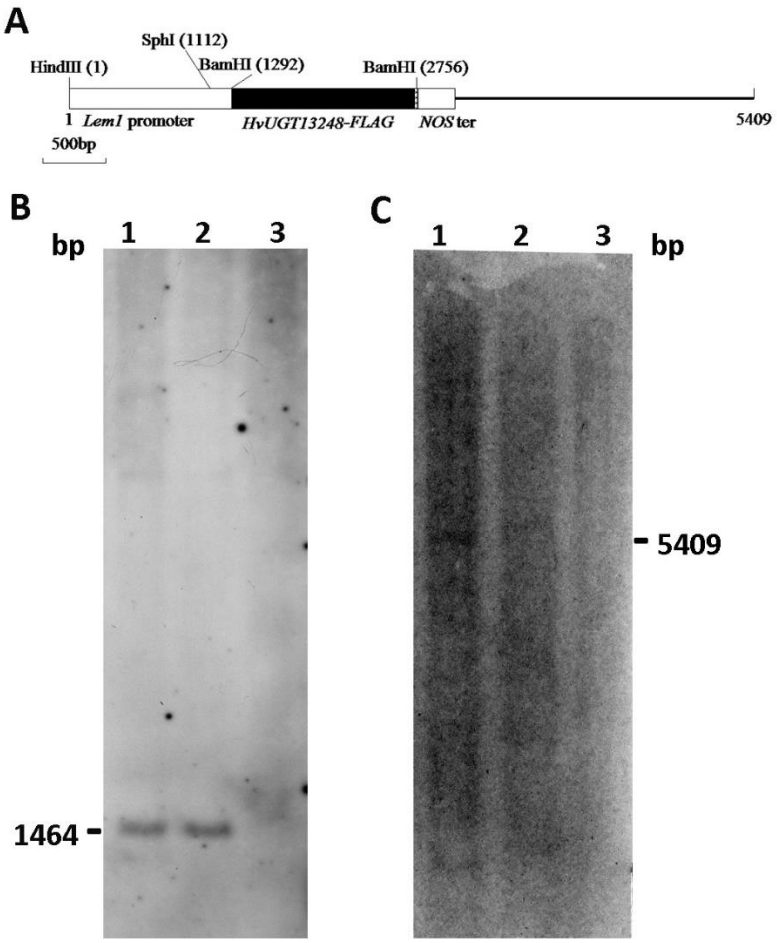


Fig. **27**. Southern blot analysis of the Lem-UGT plants. **A)** The pAHC17 Lem1::HvUGT13248 linearized construct, prepared by cloning the *HvUGT13248-FLAG* gene into the *Bam*HI site of pAHC17 under control of the barley *Lem1* promoter and *NOS* terminator.
Genomic DNA (10 µg) of $T_4$ transgenic lines was digested with **B)** *Bam*HI and **C)** *Sph*I and probed with a digoxigenin-labeled coding region of *HvUGT13248-FLAG*.
(1) ST8-74; (2) ST8-49; (3) *T. aestivum* cv Bobwhite (untransformed control).

### 4.1.3 Phenotypic characterization of selected transgenic lines

Due to the DON inhibiting effect on root elongation, an *in vitro* root growth assay was carried out to assess the response to DON of the durum wheat Ubi-UGT lines. In the presence of DON, expression of the barley UGT did not restore a normal root growth in the transgenic lines, as shown in Fig. **28**A. However, ST7-47I and ST7-56II lines showed significant less inhibition of root elongation (Fig. **28**B) compared to Svevo plants. In fact, roots of both transgenic lines were reduced of almost 50% and Svevo roots of almost 90%, compared to the respective mock treatments.

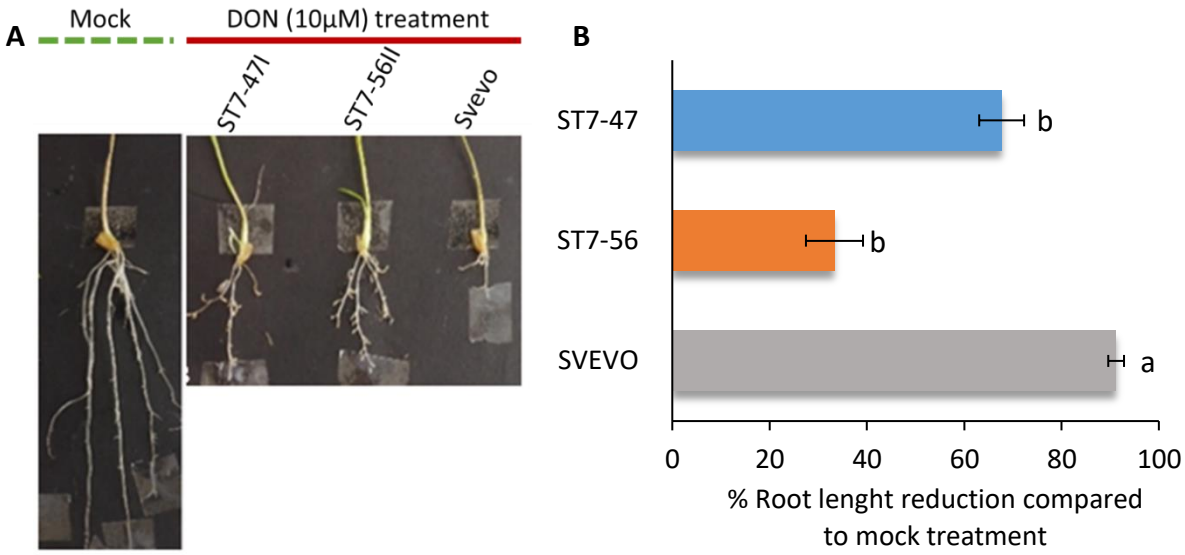


Fig. **28**. Root growth assay on Ubi-UGT and wild type plants. **A)** Example of roots after mock and 10 µM DON treatments. **B)** Inhibition of root elongation in Ubi-UGT and *T. durum* cv Svevo plants in presence of 10 µM DON, compared to mock treatment. Data represent means ± standard errors of at least three biological replicates.

### 4.1.4 Infection experiments for evaluation of FHB resistance

Independent infection experiments with *F. graminearum* were performed on both durum wheat plants constitutively expressing the *HvUGT13248* gene, and bread wheat plants expressing *HvUGT13248* in lemma, palea, anthers and rachis. The opposite central spikelets in the primary spikes (Zadoks stage 69) of the transgenic lines and the untransformed control plants were point inoculated and symptoms progression was visually scored for a period of 18 days.

Both Ubi-UGT lines showed a slower symptom progression compared to Svevo control (Fig. **29**). In particular, symptom severity was most evidently reduced between day 6 and 9 post infection ($P$<0.01) (Fig. **29**B), with a maximal level of 30% of symptom reduction. During those days, several transgenic plants showed a block of the infection in the inoculated spikelets (Fig. **30**). However, once the block was overcome, the fungus spread along the spike through the rachis, progressively reducing the difference with respect to the wild type until day 15 post-infection ($P$<0.05) (Fig. **29**B), and eventually reaching similar symptom level.

A

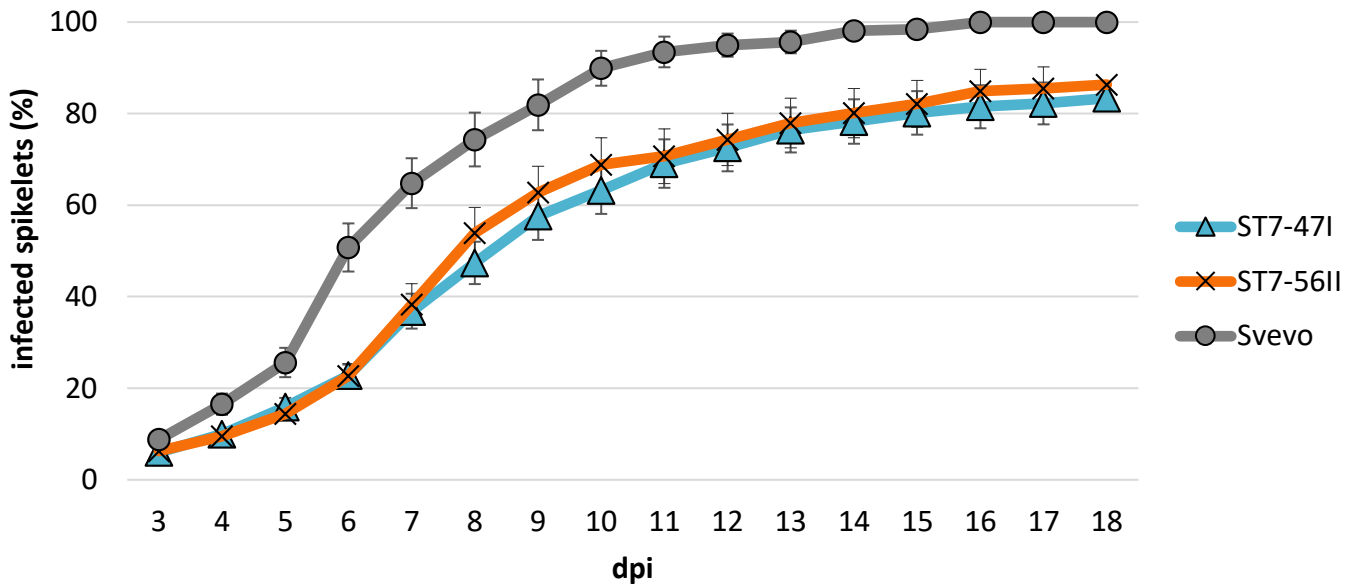


B

| | dpi | 3 | 4 | 5 | 6 | 7 | 8 | 9 | 10 | 11 | 12 | 13 | 14 | 15 | 16 | 17 | 18 |
|---|---|---|---|---|---|---|---|---|---|---|---|---|---|---|---|---|---|
| **Svevo** | M | 8.8 | 16.5 | 25.6 | 50.8 | 64.8 | 74.4 | 81.9 | 89.9 | 93.5 | 95.0 | 95.7 | 98.0 | 98.5 | 100.0 | 100.0 | 100.0 |
| | SE | 1.28 | 2.32 | 3.20 | 5.26 | 5.45 | 5.88 | 5.55 | 3.81 | 3.35 | 2.53 | 2.47 | 1.37 | 1.07 | 0.00 | 0.00 | 0.00 |
| | Tukey | ns | ns | ns | A | A | A | a | a | a | a | a | a | a | ns | ns | ns |
| **ST7-56II** | M | 6.3 | 9.5 | 14.5 | 22.7 | 38.3 | 54.0 | 62.8 | 68.8 | 70.7 | 74.4 | 78.0 | 80.1 | 82.2 | 84.9 | 85.5 | 86.4 |
| | SE | 0.48 | 0.78 | 1.58 | 2.68 | 4.55 | 5.56 | 5.72 | 5.93 | 5.97 | 5.72 | 5.44 | 5.39 | 5.11 | 4.75 | 4.69 | 4.55 |
| | Tukey | ns | ns | ns | B | B | B | b | b | b | b | b | b | b | ns | ns | ns |
| **ST7-47I** | M | 6.0 | 10.0 | 15.9 | 22.8 | 36.8 | 47.4 | 57.6 | 63.3 | 69.1 | 72.5 | 76.4 | 78.3 | 80.2 | 81.5 | 82.2 | 83.4 |
| | SE | 0.62 | 0.75 | 1.94 | 2.37 | 3.81 | 4.63 | 5.20 | 5.21 | 5.29 | 5.12 | 4.92 | 4.85 | 4.75 | 4.71 | 4.57 | 4.57 |
| | Tukey | ns | ns | ns | B | B | B | b | b | b | b | b | b | b | ns | ns | ns |

Fig. **29** Time-course development of Fusarium head blight (FHB) symptoms following *F. graminearum* infection of Ubi-UGT transgenic lines ST7-47I and ST7-56II and the untransformed *T. durum* cv Svevo (SV). Mean values (M) standard errors (SE) refer to two independent FHB assays performed with at least 15 plants per genotype in each experiment. M ± SE of the three genotypes are graphically represented in **A)**. In **B),** besides M ± SE values, results of Tukey test at $P<0.05$ (lower case) and $P<0.01$ (upper case) level are reported. ns: not significant.

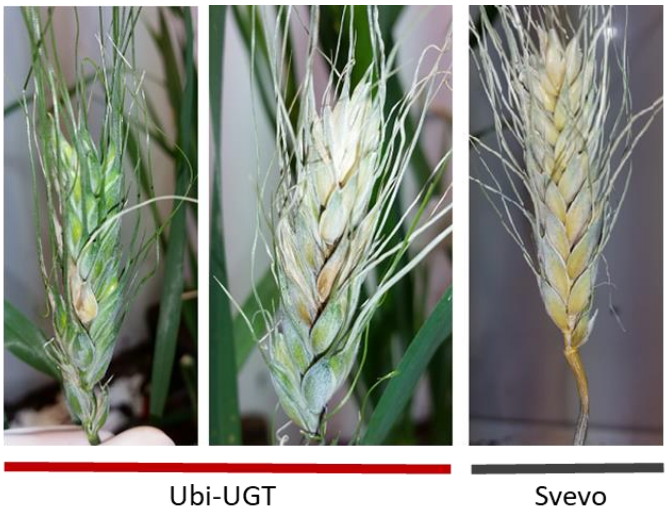


Fig. **30**. Example of symptoms of infected transgenic Ubi-UGT and Svevo heads, 9 days post infection.

At maturity stage, kernels from the infected spikes were collected. Kernels from the transgenic Ubi-UGT plants were more developed and filled, reflecting the longer period elapsed until the fungal spread as compared to the untransformed plants case. The phenotypic appearance and the 1000 kernel weight are shown in Fig. **31** and Table **8**, respectively.

UHPLC-MS/MS analyses were performed in order to quantify DON and D3G contents in flours from mature kernels of Ubi-UGT and control plants. Compared to untransformed Svevo, a significant reduction of DON content was detected in both transgenic lines, with ST7-56II exhibiting a lower content than ST7-47II (Table **9**). Irrespective of this latter difference, both ST7 lines showed similar D3G/DON ratios, averaging around 20-30% (Fig. **32**, Table **9**). By contrast, the same ratio amounted to 0.3% in Svevo untransformed control. DON+D3G content was not significantly different between the Ubi-UGT lines, but much lower than the control (Table **9**).


Fig. **31** Kernels deriving from spikes infected with *F. graminearum* of (1) untransformed *T. durum* cv Svevo, (2) transgenic line ST7-47I and (3) transgenic line ST7-56II.

Table **8**. Thousand kernel weight (TKW) and percentage of TKW increase of Ubi-UGT plants, compared to the untransformed *T. durum* cv Svevo kernels. Kernels were collected at maturity from the infected spikes of the first and second biological replicates of the FHB assay.

| Genotype | TKW (gr) | | % TKW increase | |
|---|---|---|---|---|
| | I replicate | II replicate | I replicate | II replicate |
| **Svevo** | 2.05 | 6.25 | | |
| **ST7-47** | 6.75 | 14.21 | 230.1 | 127.4 |
| **ST7-56** | 7.14 | 11.27 | 249.2 | 80.3 |

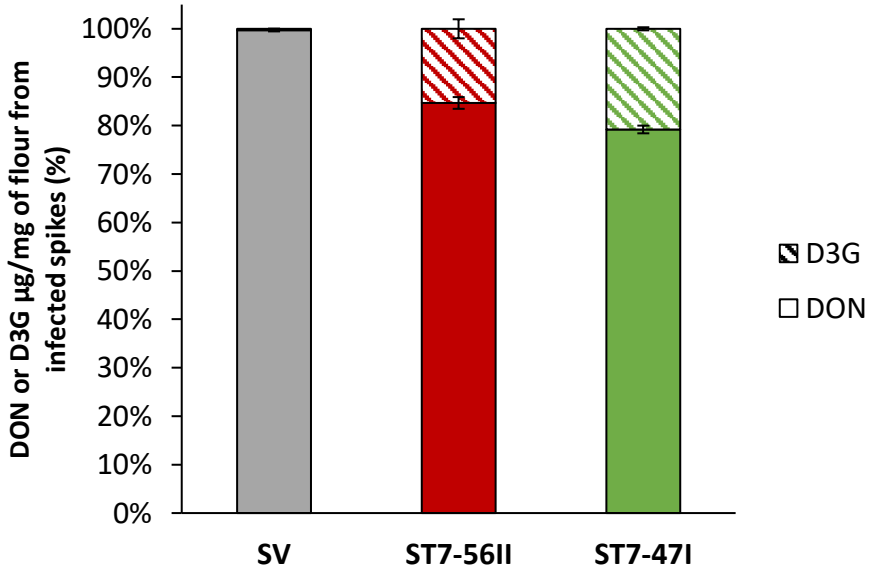


Fig. **32.** Deoxynivalenol (DON) to deoxynivalenol-3-glucoside (D3G) ratios in the flour of Ubi-UGT and untransformed cv Svevo (SV) plants, detected by UHPLC-MS/MS.

Table **9.** UHPLC-MS/MS results of deoxynivalenol (DON) and deoxynivalenol-3-glucoside (D3G) detection in flour from infected spikes of Ubi-UGT and untransformed cv Svevo plants.
Values represent means (M) ± standard errors (SE) of DON and D3G µg detected in 1 mg of flour, in independent replicates. Results of Tukey test at *P*<0.05 (lower case) and *P*<0.01 (upper case) level are reported.

| | | DON | D3G | DON+D3G | D3G/DON |
|---|---|---|---|---|---|
| **Svevo** | M | 0.45532 | 0.00132 | 0.45665 | 0.00291 |
| | SE | 0.00112 | 0.00002 | 0.00446 | 0.00020 |
| | Tukey | A | B | A | a |
| **ST7-56II** | M | 0.00068 | 0.00012 | 0.00080 | 0.16397 |
| | SE | 0.00001 | 0.00002 | 0.00010 | 0.02865 |
| | Tukey | B | B | B | b |
| **ST7-47I** | M | 0.00536 | 0.00141 | 0.00677 | 0.26407 |
| | SE | 0.00005 | 0.00002 | 0.00018 | 0.02474 |
| | Tukey | B | A | B | C |

Concerning the two bread wheat Lem-UGT lines, a different trend of symptom progression was observed (Fig. **33**). In particular, the ST8-74I line showed a slower symptom progression compared to untrasformed cv Bobwhite plants from 6 dpi until the end of the experiment, with a maximum reduction in symptom severity of 30-40% (*P*<0.05) between days 9 and 16 post infection (Figs. **33**A, **33**C, **34**). On the other hand, the ST8-49I line showed more variability between infected plants, and the symptom progression was significantly different from the Bobwhite control only at 6, 8, 10 and 11 dpi (Figs. **33**B, **33**C, **34**).

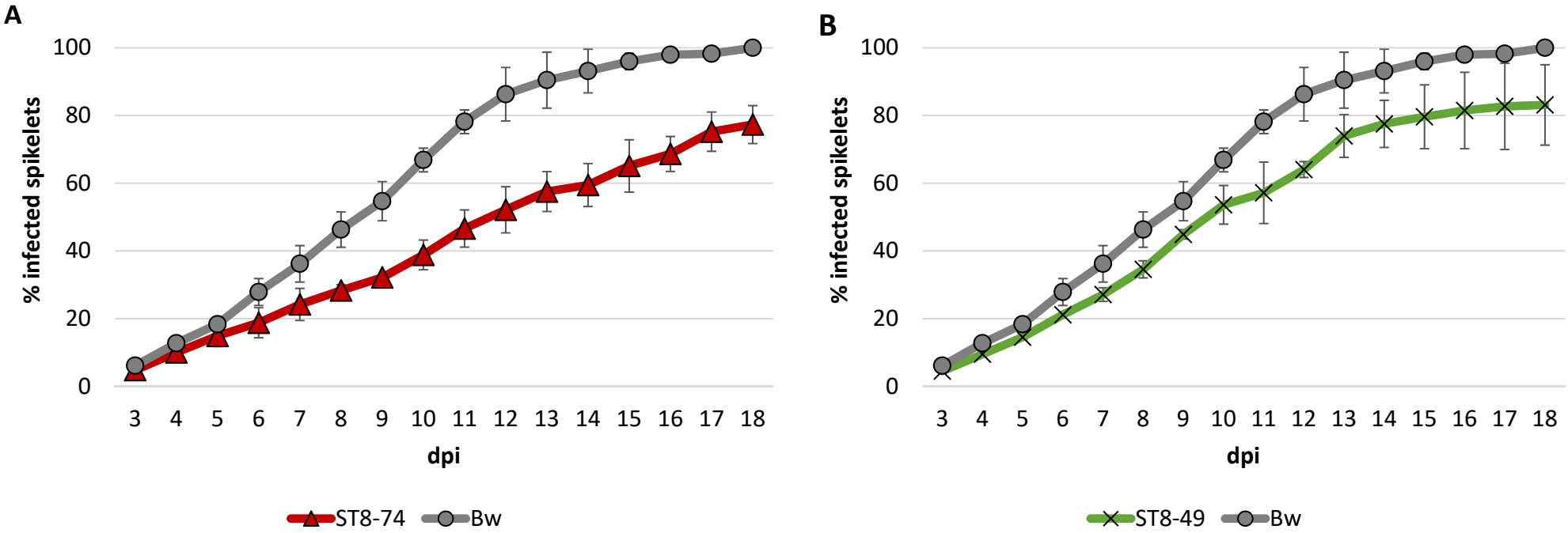


**C**

| | dpi | 3 | 4 | 5 | 6 | 7 | 8 | 9 | 10 | 11 | 12 | 13 | 14 | 15 | 16 | 17 | 18 |
|---|---|---|---|---|---|---|---|---|---|---|---|---|---|---|---|---|---|
| **Bobwhite** | M | 5.9 | 12.4 | 17.9 | 27.5 | 37.7 | 45.8 | 52.2 | 64.9 | 76.2 | 85.2 | 89.2 | 92.5 | 94.7 | 96.4 | 96.8 | 98.6 |
| | ES | 0.38 | 0.59 | 0.86 | 1.79 | 3.17 | 3.24 | 3.32 | 3.99 | 4.41 | 3.65 | 3.29 | 3.00 | 2.61 | 2.14 | 1.93 | 1.40 |
| | Tukey | ns | ns | ns | A | A | A | a | a | a | a | a | a | a | a | a | a |
| **ST8-74** | M | 4.8 | 10.0 | 14.9 | 18.8 | 24.2 | 28.3 | 32.2 | 38.8 | 46.6 | 52.1 | 55.8 | 59.5 | 65.1 | 68.6 | 71.0 | 73.1 |
| | ES | 0.46 | 0.73 | 1.58 | 1.89 | 2.66 | 3.01 | 3.50 | 4.47 | 5.56 | 6.02 | 6.16 | 6.21 | 6.48 | 6.64 | 6.70 | 6.71 |
| | Tukey | ns | ns | ns | B | B | B | B | B | B | B | B | B | B | B | B | B |
| **ST8-49** | M | 4.5 | 9.5 | 14.5 | 21.2 | 27.1 | 34.5 | 44.9 | 53.8 | 57.4 | 64.1 | 73.8 | 77.4 | 79.4 | 81.2 | 82.4 | 82.5 |
| | ES | 0.44 | 0.64 | 1.11 | 1.80 | 2.27 | 2.87 | 4.40 | 5.33 | 5.54 | 5.82 | 6.01 | 6.03 | 5.97 | 5.91 | 5.91 | 6.06 |
| | Tukey | ns | ns | ns | B | B | B | a | a | b | B | B | b | a | a | a | a |

Fig. **33**. Time-course development of Fusarium head blight (FHB) symptoms following *F. graminearum* infection of Lem-UGT transgenic lines ST8-74 and ST8-49 and the untransformed *T. aestivum* cv Bobwhite (BW). Mean values (M) standard errors (SE) refer to two independent FHB assays performed with at least 15 plants per genotype in each experiment. M ± SE of BW and **A)** ST8-74 and **B)** ST8-49, are graphically represented. In **C),** besides M ± SE values, results of Tukey test at $P<0.05$ (lower case) and $P<0.01$ (upper case) level are reported. ns: not significant.


Fig. **34**. Example of symptoms of infected transgenic Lem-UGT and Bobwhite heads, 9 days post infection.

Kernels were then collected at maturity stage from the infected spikes. Compared to the untransformed plants, kernels from the transgenic Lem-UGT lines, in particular from ST8-74I, were more developed and filled, reflecting the slower symptom progression. The phenotypic appearance and the 1000 kernel weight are shown in Fig. **35** and Table **9**, respectively.

DON and D3G contents were measured by UHPLC-MS/MS in the flours extracted from mature kernels of Lem-UGT and untransformed plants. As shown in Table **11**, the DON+D3G content was higher in both transgenic lines, compared to Bobwhite control, though significantly so in line ST8-49 only. However, the D3G/DON ratio was, on average, 10 times greater in Lem-UGT lines compared to the untransformed control (Fig. **36**). The D3G content followed the same relative trend (Table **11**).


Fig. **35**. Kernels deriving from spikes infected with *F. graminearum* of (1) untransformed *T. aestivum* cv Bobwhite, (2) transgenic line ST8-74 and (3) transgenic line ST8-49.

Table **10**. Thousand kernels weight (TKW) and percentage of TKW increase of Lem-UGT plants, compared to the untransformed *T. aestivum* cv Bobwhite kernels. Kernels were collected at maturity from the infected spikes of the first and second biological replicates of the FHB assay.

| Genotype | TKW (gr) | | % TKW increase | |
|---|---|---|---|---|
| | I replicate | II replicate | I replicate | II replicate |
| **Bobwhite** | 5.6 | 3.9 | | |
| **ST8-74** | 8.4 | 8.8 | 50.4 | 125.3 |
| **ST8-49** | 6.0 | 6.8 | 7.7 | 74.7 |

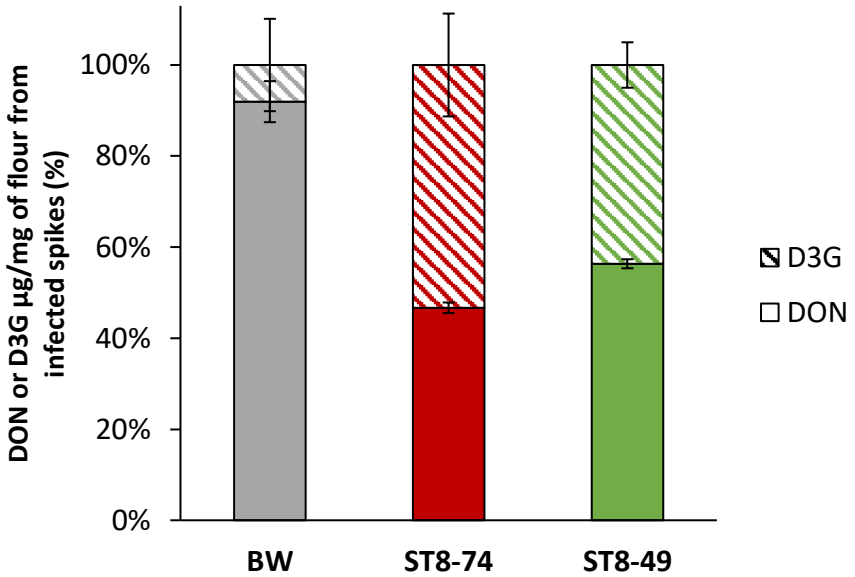


Fig. **36**. Deoxynivalenol (DON) to deoxynivalenol-3-glucoside (D3G) ratios in the flour of Lem-UGT and untransformed cv Bobwhite (BW) plants, detected by UHPLC-MS/MS.

Table **11.** UHPLC-MS/MS results of deoxynivalenol (DON) and deoxynivalenol-3-glucoside (D3G) detection in flour from infected spikes of Lem-UGT and untransformed cv Bobwhite (BW) plants. Values represent means (M) ± standard errors (SE) of DON and D3G µg detected in 1 mg of flour, in independent replicates. Results of Tukey test at *P*<0.05 (lower case) and *P*<0.01 (upper case) level are reported.

| | | DON | D3G | D3G/DON | DON+D3G |
|---|---|---|---|---|---|
| **BW** | M | 0.4116 | 0.0360 | 0.0909 | 0.4477 |
| | SE | 0.0202 | 0.0307 | 0.0780 | 0.0284 |
| | Tukey | a | b | b | b |
| **ST8-49** | M | 0.4151 | 0.3216 | 0.7778 | 0.7367 |
| | SE | 0.0068 | 0.0663 | 0.1725 | 0.0594 |
| | Tukey | a | a | a | a |
| **ST8-74** | M | 0.2738 | 0.3128 | 1.1470 | 0.5866 |
| | SE | 0.0073 | 0.0368 | 0.1649 | 0.0294 |
| | Tukey | b | a | a | ab |

#### 4.1.4.1 Comparison of FHB symptom development caused by three *F. graminearum* strains

Considering the very rapid development of fungal infections based on the use of *F. graminearum* strain 3827 (see Fig. **29**, Fig. **33**), we hypothesized a particularly high virulence of this strain, which might have made difficult to appreciate differences among genotypes (in terms of extent and speed of fungal progression, DON accumulation and detoxification), particularly in durum wheat. To verify this, three different strains of *F. graminearum* were compared in FHB infection experiments of durum wheat cv Svevo. Besides 3827, the *F. graminearum* strains used were PH1 and 8/1, the latter two being frequently used to test FHB resistance/susceptibility in wheat. The results (Fig. **37**) showed that strain 3827 leads more quickly than PH1 and 8/1 to a complete infection of the spike. In particular, strain 3827 exhibited 20% higher infection than strain PH1 between 5 and 7 dpi, and 10% higher in 8 and 9 dpi. Strain 8/1 showed a somewhat intermediate behavior between 3827 and PH1. As a whole, all strains of *F. graminearum* used exhibit in our conditions a rather strong virulence on durum wheat cv Svevo, leading to a complete infection of the spike between days 9 and 10 post-infection. Moreover, irrespective of the strain, Svevo plants showed an initial necrosis on the infected, central spikelet and in the adjacent ones, followed by a sudden bleaching of the upper part of the spike. This phenomenon, only occasionally observed in bread wheat cv Bobwhite, might be attributed to a typical vessel occlusion associated to the genotype (see Discussion).

A

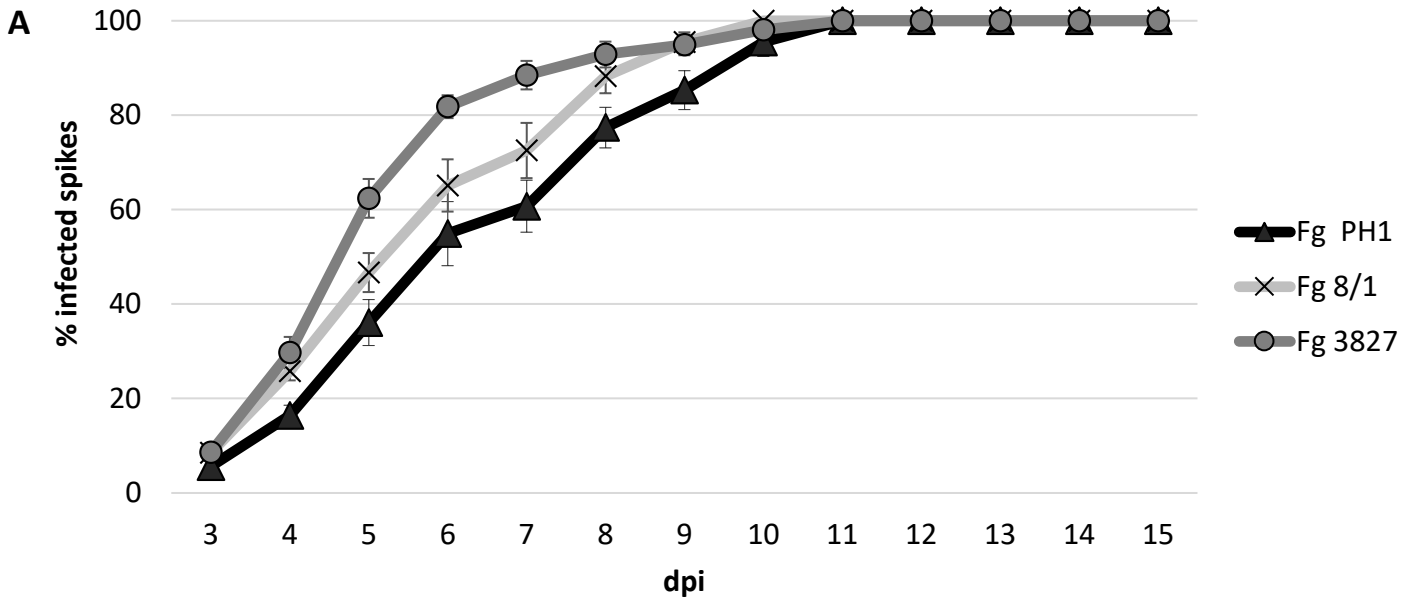


B

| | dpi | 3 | 4 | 5 | 6 | 7 | 8 | 9 | 10 | 11 | 12 | 13 | 14 | 15 | 16 | 17 | 18 |
|---|---|---|---|---|---|---|---|---|---|---|---|---|---|---|---|---|---|
| **Svevo - Fg 3827** | M | 8.6 | 29.7 | 62.4 | 81.8 | 88.5 | 92.9 | 94.9 | 98.1 | 100.0 | 100.0 | 100.0 | 100.0 | 100.0 | 100.0 | 100.0 | 100.0 |
| | SE | 0.84 | 3.35 | 4.11 | 2.42 | 3.02 | 2.73 | 2.18 | 1.45 | 0.00 | 0.00 | 0.00 | 0.00 | 0.00 | 0.00 | 0.00 | 0.00 |
| | Tukey | ns | ns | a | a | a | a | a | ns | ns | ns | ns | ns | ns | ns | ns | ns |
| **Svevo - Fg PH1** | M | 5.6 | 16.4 | 36.1 | 54.9 | 60.7 | 77.4 | 85.3 | 95.5 | 100.0 | 100.0 | 100.0 | 100.0 | 100.0 | 100.0 | 100.0 | 100.0 |
| | SE | 0.12 | 2.18 | 4.87 | 6.79 | 5.50 | 4.31 | 4.12 | 3.07 | 0.00 | 0.00 | 0.00 | 0.00 | 0.00 | 0.00 | 0.00 | 0.00 |
| | Tukey | ns | ns | b | b | b | b | b | ns | ns | ns | ns | ns | ns | ns | ns | ns |
| **Svevo - Fg 8/1** | M | 8.5 | 25.8 | 46.7 | 65.1 | 72.5 | 88.3 | 95.5 | 100.0 | 100.0 | 100.0 | 100.0 | 100.0 | 100.0 | 100.0 | 100.0 | 100.0 |
| | SE | 0.89 | 2.00 | 4.13 | 5.53 | 5.85 | 3.61 | 2.02 | 0.00 | 0.00 | 0.00 | 0.00 | 0.00 | 0.00 | 0.00 | 0.00 | 0.00 |
| | Tukey | ns | ns | b | b | b | ab | ab | ns | ns | ns | ns | ns | ns | ns | ns | ns |

Fig. **37**. Time-course development of Fusarium head blight (FHB) symptoms following infection of *T. durum* cv Svevo (SV) with different strains of *F. graminearum*. Fg PH1: *F. graminearum* strain PH1; Fg 8/1: *F. graminearum* strain 8/1; Fg 3827: *F. graminearum* strain 3827.
Mean values (M) standard errors (SE) refer to one FHB assay performed with at least 15 plants per infection. M ± SE of the three genotypes are graphically represented in **A)**. In **B),** besides M ± SE values, results of Tukey test at $P<0.05$ level is reported. ns: not significant.

### 4.1.5 Infection experiments for evaluation of FCR resistance

In order to evaluate the response to FCR disease, infection experiments with *F. culmorum* were performed on durum wheat seedlings (Zadoks stage 11) of Ubi-UGT transgenic and untransformed Svevo plants. The experiment was not conducted on Lem-UGT plants because of the tissue and developmental stage specificity of the transgene expression. Symptom progression was visually scored for a period of three weeks and evaluated by using a disease index (DI), which considers symptoms extension and the browning index (see § 3.10). Both transgenic lines showed less severe and extended symptoms compared to the untransformed control, significantly reducing the DI of almost 50% ($P$<0.01) (Fig. **38**, Fig. **39**). Importantly, symptom reduction was consistent throughout the time of infection for both transgenic lines.

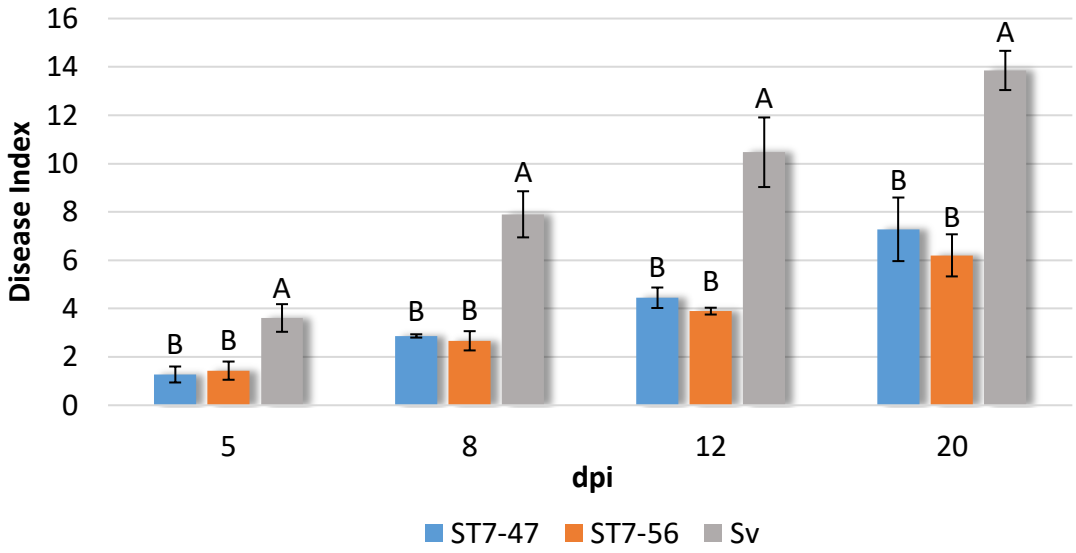


Fig. **38**. Fusarium crown rot (FCR) symptoms development following *F. culmorum* infection on seedlings of transgenic lines ST7-47I, ST7-56II and the untransformed *T. durum* cv Svevo.
Data represent mean values ± standard errors (SE) of three independent experiments performed with at least 12 plants per genotype. Letters above the bars represent the results of Tukey test at $P$<0.01 level.

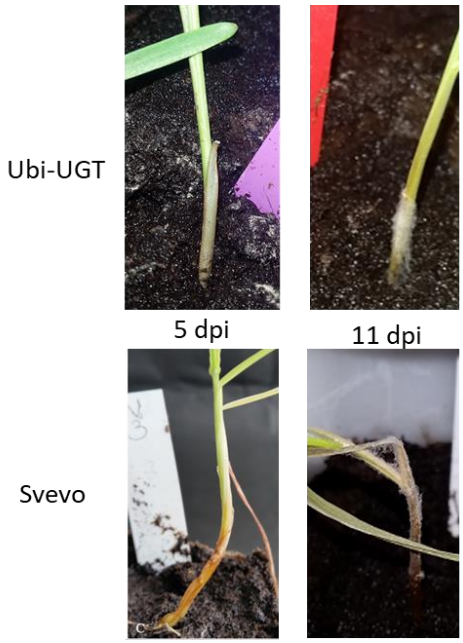


Fig. **39.** Example of FCR symptoms on Ubi-UGT (up) and Svevo (down) seedlings a 5 (left) and 11 (right) days post-infection.

## 4.2 Objective II: Pyramiding *UGT* and *CWDE inhibitor* genes to combine different resistance mechanisms against *Fusarium* diseases.

The evaluation of a possible synergistic effect of different resistance mechanisms against *Fusarium* diseases was investigated by pyramiding in the same genotype of different transgenes, obtained by crossing transgenic lines expressing single transgenes.

To this aim, we performed crosses in both durum and bread wheat between UGT-lines, described in § 4.1, and transgenic lines expressing glycosidase inhibitors previously produced (Janni et al. 2008; Volpi et al. 2011). In general, transgenic lines expressing glycosidase inhibitors contribute to limit fungal infection by inhibiting CWDE, thus strengthening the plant cell wall, the main site of fungal attack during the early infection stages (see § 1.2). On the other hand, transgenic lines expressing UGT contribute to resistance against *Fusarium* spp. by detoxification of the DON mycotoxin, produced throughout *Fusarium* infection and massively induced at the rachis node in FHB disease. The combination of these different mechanisms could potentially further reinforce plant defenses against pathogen attacks.

### 4.2.1 HvUGT13248 X AcPMEI pyramiding in durum wheat

#### 4.2.1.1 Production and selection of $F_1$ plants

Pyramiding of the *HvUGT13248* and *AcPMEI* genes in durum wheat cv Svevo was achieved by crossing transgenic durum wheat plants individually expressing these genes. Eleven crosses (Table **12**) were performed using the MJ15-69 transgenic line (from here on referred to as PMEI-plants), which express constitutively the *AcPMEI* gene (Volpi et al. 2011), and the ST7-47 or the ST7-56 transgenic lines (see § 4.1), which express constitutively the *HvUGT13248* gene. The crosses were named 16A and the PMEI- and UGT-plants were randomly chosen as female or male parents. As shown in Table **12**, 42 $F_1$ seeds were obtained from all crosses. Corresponding $F_1$ seedlings were screened by PCR in order to identify the genotypes possessing both transgenes. Out of 38 $F_1$ plants tested, 17 (44.7%) presented both the *HvUGT13248* and *AcPMEI* genes (from here on UGT+PMEI-plants). Eight and nine $F_1$ plants presented the *HvUGT13248* or the *AcPMEI* gene, respectively, while the remaining four plants did not present any transgene.

Table **12**. Crosses performed between UGT- (ST7-) and PMEI- (MJ15-) plants, and PCR screening results of derived $F_1$ plants.

| **Cross name** | **♀ plant** | **♂ plant** | **$F_1$ seeds** | **Not germ.** | ***PMEI*** | ***UGT*** | ***-/-*** | ***PMEI + UGT*** |
|---|---|---|---|---|---|---|---|---|
| 16A-1 | MJ15-69-3-7-15-4-2-17 | ST7-47-4-3-1 | 7 | | 3 | | | **4** |
| 16A-2 | MJ15-69-3-7-15-4-2-14 | ST7-47-4-3-1 | 7 | 1 | 3 | | | **3** |
| 16A-3 | MJ15-69-3-7-15-4-2-15 | ST7-47-4-3-1 | 4 | 2 | | | 1 | **1** |
| 16A-9 | ST7-56-8-5-1 | MJ15-69-3-7-15-4-2-6 | 3 | | | 3 | | **0** |
| 16A-10 | ST7-47-4-1-3 | MJ15-69-3-7-15-4-2-16 | 3 | | | 2 | | **1** |
| 16A-11 | ST7-47-4-3-1 | MJ15-69-3-7-15-4-2-6 | 1 | | | | 1 | **0** |
| 16A-12 | ST7-56-8-3-3 | MJ15-69-3-7-15-4-2-6 | 5 | 1 | | | | **4** |
| 16A-13 | ST7-47-4-5-2 | MJ15-69-3-7-15-4-2-16 | 3 | | | 1 | | **2** |
| 16A-14 | ST7-47-4-1-1 | MJ15-69-3-7-15-4-2-17 | 5 | | 2 | | 1 | **2** |
| 16A-17 | ST7-47-4-5-1 | MJ15-69-3-7-15-4-2-16II | 2 | | | 1 | 1 | **0** |
| 16A-19 | MJ15-69-3-7-15-4-2-10 | ST7-47-4-5-1 | 2 | | 1 | 1 | | **0** |
| | | | 42 | 4 | 9 | 8 | 4 | **17** |

The enzymatic activity of the AcPMEI and the expression HvUGT13248 were subsequently confirmed in the $F_1$ UGT+PMEI-plants by agarose diffusion assay and Western bot, respectively. The results (Table **13**) were positive for 11 $F_1$ plants.

Table **13**. $F_1$ plant screening for PMEI activity and UGT expression. Untransformed cv Svevo was used as negative control. Parental lines MJ15-69 and ST7-47 were used as positive control for PME inhibition activity and UGT expression, respectively.

| Genotype | % inhibition of PME activity | Western blot for UGT detection |
|---|---|---|
| Svevo | 0% | - |
| MJ15-69 (Ubi-PMEI) | 100% | - |
| ST7-47 (Ubi-UGT) | 0% | + |
| 16A1-1 | 100% | + |
| 16A1-3 | 100% | + |
| 16A1-5 | 100% | + |
| 16A1-6 | 100% | + |
| 16A2-1 | 100% | + |
| 16A2-2 | 0% | + |
| 16A2-3 | 100% | + |
| 16A3-4 | 100% | + |
| 16A10-2 | 100% | + |
| 16A12-1 | 100% | - |
| 16A12-2 | 100% | - |
| 16A12-3 | 100% | - |
| 16A12-5 | 100% | - |
| 16A13-2 | 100% | + |
| 16A13-3 | 100% | + |
| 16A14-1 | 40% | + |
| 16A14-2 | 100% | + |
| 16A19-1 | 100% | - |

#### 4.2.1.2 Characterization of the selected progeny

Different UGT+PMEI $F_2$ progenies, randomly selected, were subjected to PCR screening to identify individuals with *HvUGT13248* and *AcPMEI* co-presence. Table **14** summarizes the results and the corresponding segregation analysis. The tested hypothesis was of independent

segregation of the two transgenes, which was confirmed by the $\chi^2$ test, in all cases corresponding to >0.05 probability (*P*) values.

Table **14**. PCR genotyping of $F_2$ 16A (UGT+ PMEI) plants: results and segregation analysis.

| **$F_2$ plants** | **$F_1$ seeds** | ***PMEI*** | ***UGT*** | **-/-** | ***UGT* + *PMEI*** | **$\chi^2$** | ***P* value** |
|---|---|---|---|---|---|---|---|
| 16A13-2 | 52 | 7 | 6 | 2 | 37 | 4.75 | 0.191 |
| 16A12-5 | 23 | 6 | 0 | 0 | 17 | 7.69 | 0.053 |
| 16A2-1 | 22 | 2 | 3 | 0 | 17 | 4.35 | 0.225 |
| 16A14-2 | 20 | 3 | 1 | 3 | 13 | 4.89 | 0.180 |

Due to higher availability of $F_2$ seeds, the 16A13 progeny (from here on referred to as 16A-plants) was used for the further experiments. Importantly, no obvious phenotypic alternations were observed in the double transgenic progeny (Fig. **40**) in comparison to the untransformed cv Svevo control and the parental transgenic lines.


Fig. **40**. Phenotypic appearance of (1) the *T. durum* cv Svevo untransformed plant, (2) the 16A (UGT+PMEI-progeny), (3) the MJ15-69 (PMEI-parental line) and (4) the ST7-47 (UGT-parental line).

Genomic DNA of the 16A-plants, the untransformed control Svevo and the UGT- and PMEI-parental lines were subjected to Southern blot analysis in order to confirm the integration of the transgenes in the genome (Fig. **41**). The probes used represented almost 800 bp and 500 bp of the *HvUGT13248* and the *AcPMEI* coding region, respectively. The *Bam*HI cleavage, which causes the excision of the coding regions in both constructs used for the transformation (Fig. **41**A), results in a hybridization signal of about 1400 bp and 500 bp for *HvUGT13248* and *AcPMEI,* respectively (Fig. **41**B). The 16A-plants confirmed the presence of both hybridization signals. No signal was detected in the untransformed control Svevo.

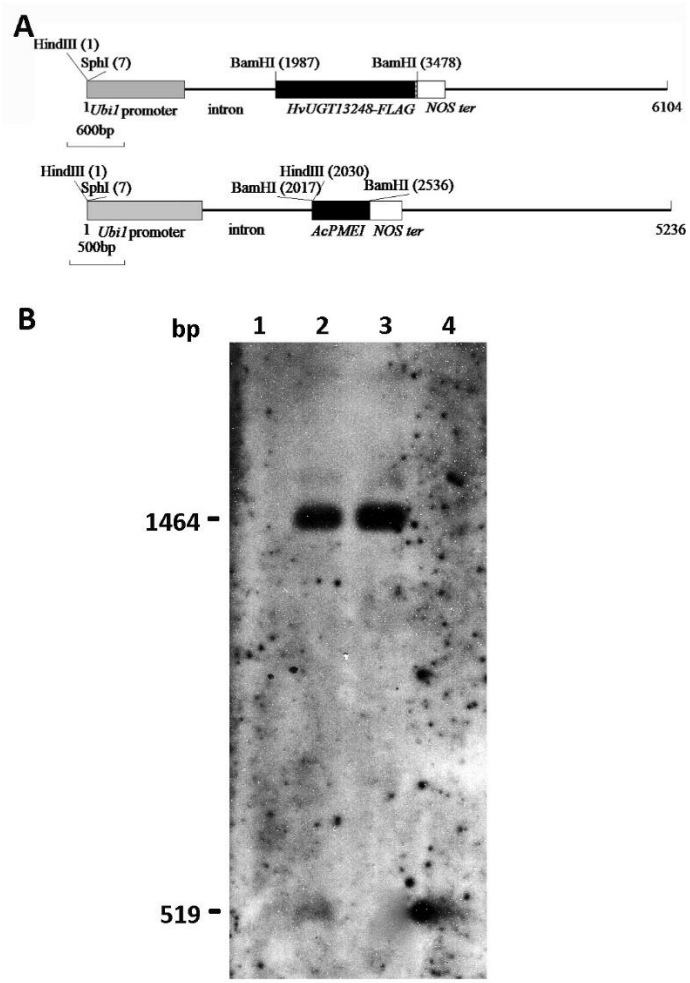


Fig. **41**. Southern blot analysis of the UGT+PMEI plants. **A)** The pAHC17_Ubi1::HvUGT13248-FLAG and the pAHC17_Ubi1::AcPMEI constructs, prepared by cloning the *HvUGT13248-FLAG* and the *AcPMEI* genes, respectively, into the *Bam*HI site of pAHC17 under control of the maize *Ubiquitin1* promoter and *NOS* terminator. **B)** Genomic DNA of transgenic lines digested with *Bam*HI and probed with the digoxigenin-labeled coding regions of *HvUGT13248-FLAG* and *AcPMEI*.
(1) *T. durum* cv Svevo (untransformed control); (2) 16A (UGT+PMEI) plants; (3) ST7-47 (Ubi-UGT parental line); (4) MJ15-69 (Ubi-PMEI parental line).

#### 4.2.1.3 Infection experiments for evaluation of FCR and FHB resistance

In order to verify a possible synergistic contribution of the *HvUGT13248* and *AcPMEI* genes to *Fusarium* resistance, infection experiments were performed with *F. culmorum* and *F. graminearum* to evaluate FCR and FHB resistance, respectively. In all experiments, untransformed *T. durum* cv Svevo was used as negative control, the ST7-47 and MJ15-69 transgenic lines were used as parental control lines, and the 16A-plants represented the double-positive UGT+PMEI $T_2$ progeny.

Infection experiments on seedlings were firstly performed to evaluate FCR symptoms in the UTG+PMEI selected progeny and control plants. The results (Fig. **42**) showed that the UGT-parental line confirmed the level of resistance compared to the untransformed control. In contrast, the PMEI- parental line did not show symptoms reduction compared to wild type (cv Svevo) plants. On the other hand, throughout the infection experiment, the UGT+PMEI-plants exhibited resistance to FCR of a similar level to that of the UGT parental line, with a DI reduction of almost 50% compared to the untransformed control.

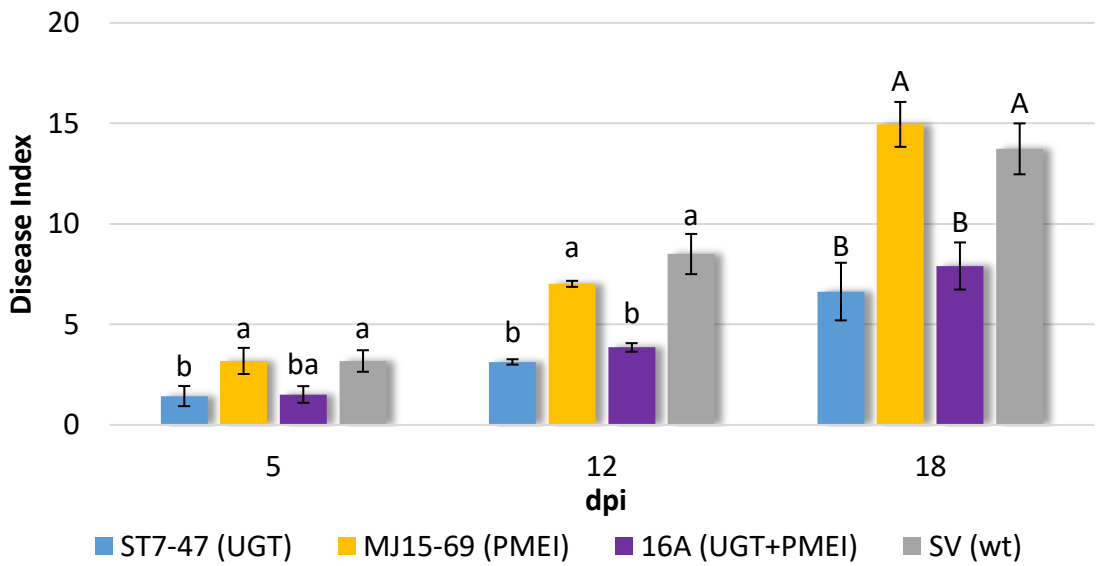


Fig. **42**. Fusarium crown rot (FCR) symptoms development following *F. culmorum* infection on seedlings of transgenic lines ST7-47I, MJ15-69, the 16A-plants and the untransformed *T. durum* cv Svevo.
Data represent mean values ± standard errors (SE) of two independent experiments performed with at least 10 plants per genotype. Letters above the bars represent the results of Tukey test at $P<0.05$ (lower case) and $P<0.01$ (upper case) level.

The results of the FHB infection experiments have to be considered as “preliminary” since, to date, they represent a single biological replicate. These results (Fig. **43**) confirmed the levels of resistance of both UGT- and PMEI-parental lines compared to the untransformed control. In this case, the combination of the two effective and distinct resistance mechanisms in the UGT+PMEI-plants seemed to have a synergic effect on resistance, significantly reducing FHB symptoms of almost 10-15 % between 7 and 9 dpi, compared to the parental lines (Fig. **43**B).

A

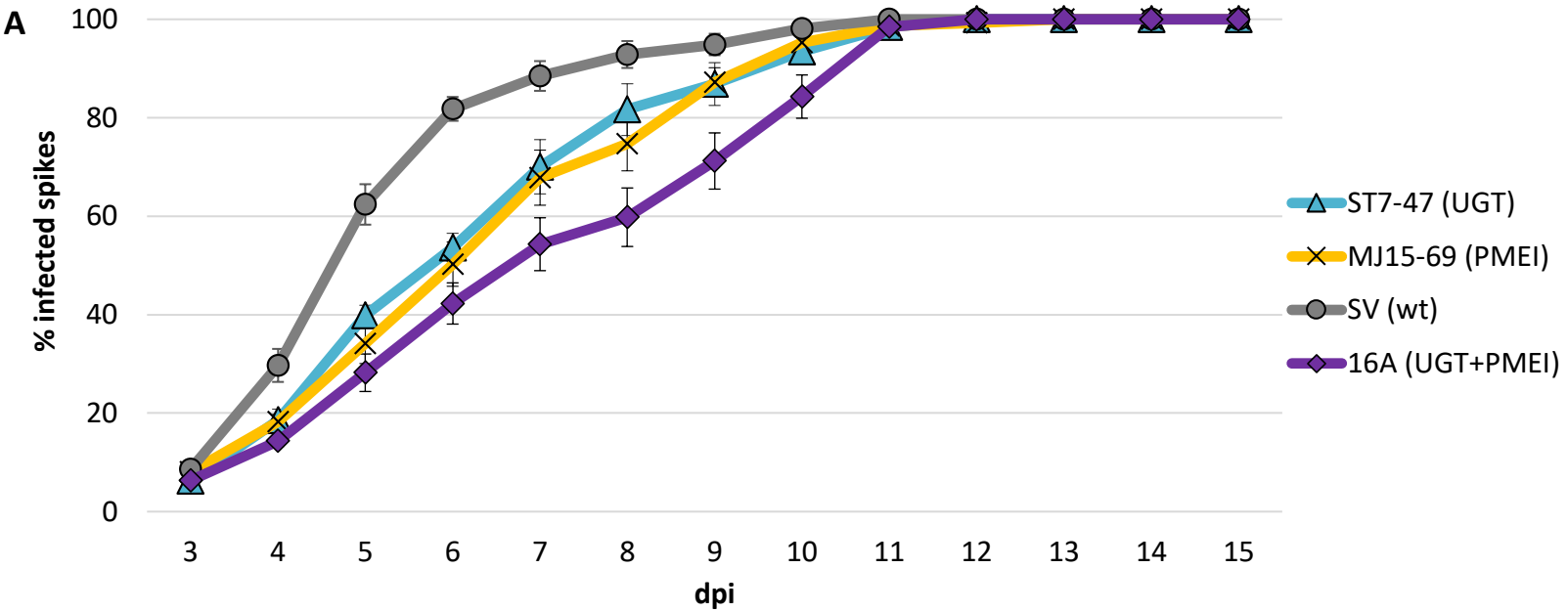


B

| | dpi | 3 | 4 | 5 | 6 | 7 | 8 | 9 | 10 | 11 | 12 | 13 | 14 | 15 | 16 | 17 | 18 |
|---|---|---|---|---|---|---|---|---|---|---|---|---|---|---|---|---|---|
| **Svevo** | M | 8.6 | 29.7 | 62.4 | 81.8 | 88.5 | 92.9 | 94.9 | 98.1 | 100.0 | 100.0 | 100.0 | 100.0 | 100.0 | 100.0 | 100.0 | 100.0 |
| | SE | 0.84 | 3.35 | 4.11 | 2.42 | 3.02 | 2.73 | 2.18 | 1.45 | 0.00 | 0.00 | 0.00 | 0.00 | 0.00 | 0.00 | 0.00 | 0.00 |
| | Tukey | ns | a | a | a | a | a | a | a | ns | ns | ns | ns | ns | ns | ns | ns |
| **ST7-47I** | M | 6.2 | 18.5 | 39.9 | 53.6 | 70.0 | 81.6 | 86.8 | 93.5 | 98.5 | 100.0 | 100.0 | 100.0 | 100.0 | 100.0 | 100.0 | 100.0 |
| | SE | 0.63 | 2.39 | 4.45 | 4.38 | 3.85 | 3.15 | 3.68 | 2.72 | 1.11 | 0.00 | 0.00 | 0.00 | 0.00 | 0.00 | 0.00 | 0.00 |
| | Tukey | ns | b | b | b | b | b | a | ab | ns | ns | ns | ns | ns | ns | ns | ns |
| **MJ15-69** | M | 8.1 | 18.2 | 34.1 | 50.3 | 67.8 | 74.7 | 87.2 | 95.3 | 98.7 | 100.0 | 100.0 | 100.0 | 100.0 | 100.0 | 100.0 | 100.0 |
| | SE | 0.73 | 1.51 | 4.07 | 4.52 | 5.60 | 5.45 | 2.96 | 2.18 | 1.33 | 0.00 | 0.00 | 0.00 | 0.00 | 0.00 | 0.00 | 0.00 |
| | Tukey | ns | b | b | b | b | b | a | ab | ns | ns | ns | ns | ns | ns | ns | ns |
| **16A** | M | 6.3 | 14.4 | 28.2 | 42.3 | 54.3 | 59.8 | 71.2 | 84.3 | 98.5 | 100.0 | 100.0 | 100.0 | 100.0 | 100.0 | 100.0 | 100.0 |
| | SE | 0.64 | 1.15 | 3.81 | 4.18 | 5.37 | 5.94 | 5.71 | 4.40 | 1.52 | 0.00 | 0.00 | 0.00 | 0.00 | 0.00 | 0.00 | 0.00 |
| | Tukey | ns | b | b | b | c | c | b | b | ns | ns | ns | ns | ns | ns | ns | ns |

Fig. **43**. Time-course development of Fusarium head blight (FHB) symptoms following *F. graminearum* infection of the transgenic lines ST7-47I, MJ15-69, the 16A-plants and the untransformed *T. durum* cv Svevo (SV). Mean values (M) standard errors (SE) refer to one FHB assays performed with at least 15 plants per genotype. M ± SE of the three genotypes are graphically represented in **A)**. In **B)**, besides M ± SE values, results of Tukey test at $P<0.05$ (lower case) and $P<0.01$ (upper case) level are reported. ns: not significant.

### 4.2.2 HvUGT13248 X PvPGIP2 pyramiding in bread wheat

#### 4.2.2.1 Production and selection of $F_1$

Pyramiding of the *HvUGT13248* and *PvPGIP2* genes in bread wheat cv Bobwhite was obtained by crossing transgenic bread wheat plants individually expressing the two genes. Eight crosses, named 16B, were performed (Table **15**), using the J82-23a transgenic line (from here on referred to as PGIP-plants), which expresses constitutively the *PvPGIP2* gene (Janni et al. 2008), and the ST8-74I or the ST8-49II transgenic line, both expressing in the floral tissue the *HvUGT13248* gene (see § 4.1.1). The PGIP- and UGT-plants were randomly chosen as female or male parents. Fifty-one $F_1$ seeds were obtained (Table **15**), and $F_1$ seedlings were screened by PCR to identify the genotypes possessing both transgenes. Twelve (27.3%) $F_1$ plants were identified with both transgenes (from here on referred to as UGT+PGIP-plants). Fifteen and eight $F_1$ plants presented the *HvUGT13248* or the *PvPGIP2* gene only, respectively, while nine plants did not present any transgene.

The enzymatic activity of the PvPGIP2 was subsequently confirmed in the $F_1$ UGT+PGIP-plants by agarose diffusion assay. The results (Table **16**) were positive for ten $F_1$ plants. In order to save seeds for further analyses, western blot on the floral tissue was not performed on $F_1$ UGT+PGIP-plants.

Table **15**. Crosses performed between UGT- (ST7-) and PGIP- (J82-23a) plants, and PCR screening results of derived $F_1$ plants.

| Cross name | ♀ plant | ♂ plant | $F_1$ seed | Not germ. | *PGIP* | *UGT* | *-/-* | *PGIP + UGT* |
|---|---|---|---|---|---|---|---|---|
| 16B-4 | J82-23a-7-2-5-1-61-24 | ST8-49-13-1-8 | 7 | | 1 | 3 | 1 | **2** |
| 16B-5 | J82-23a-7-2-5-1-61-23 | ST8-49-13-1-8 | 7 | 2 | | 2 | 3 | **1** |
| 16B-6 | J82-23a-7-2-5-1-61-25I | ST8-49-13-1-8 | 9 | 1 | 3 | 3 | 2 | **0** |
| 16B-7 | ST8-74-2-7-1 | J82-23a-7-2-5-1-61-23II | 4 | | | 1 | 1 | **2** |
| 16B-8 | ST8-49-13-1-3 | J82-23a-7-2-5-1-61-23II | 7 | 3 | | | | **4** |
| 16B-15 | ST8-49-13-1-1 | J82-23a-7-2-5-1-61-24 | 12 | 1 | 4 | 5 | 2 | **2** |
| 16B-16 | J82-23a-7-2-5-1-61-14 | ST8-49-13-1-11 | 0 | | | | | **0** |
| 16B-18 | J82-23a-7-2-5-1-61-25III | ST8-74-2-7-3 | 5 | 3 | | 1 | | **1** |
| | | | 51 | 10 | 8 | 15 | 9 | **12** |

Table **16**. $F_1$ plant screening for PGIP activity. Untransformed cv Bobwhite and ST8-49I parental line were used as negative control. Parental lines J82-23a was used as positive control for *Fp*PG inhibition activity.

| Genotype | % inhibition of *Fp*PG activity |
|---|---|
| Bobwhite | 0% |
| ST8-49I (Lem-UGT) | 0% |
| J82-23a (Ubi-PGIP) | 100% |
| 16B4-2 | 100% |
| 16B4-4 | 100% |
| 16B5-1 | 100% |
| 16B7-3 | 6.7% |
| 16B7-4 | 100% |
| 16B8-1 | 100% |
| 16B8-2 | 100% |
| 16B8-3 | 100% |
| 16B8-5 | 100% |
| 16B15-5 | 100% |
| 16B15-7 | 100% |
| 16B18-2 | 37.5% |

#### 4.2.2.2 Characterization of the selected progeny

Two randomly selected UGT+PGIP progenies, named 16B4 and the 16B8, were subjected to PCR screening in the $F_2$ generation to identify possible segregates exhibiting the co-presence of the *HvUGT13248* and the *PvPGIP2* transgenes. The results are presented in the Table **17**, together with a segregation analysis. In both progenies, the different transgenes show independent segregation (Table **17**).

Table **17**. PCR genotyping of $F_2$ 16B (UGT+PGIP) plants: results and segregation analysis.

| $F_1$ plants | $F_2$ seeds | *UGT* | *PGIP* | -/- | *UGT* + *PGIP* | $\chi^2$ | *P* value |
|---|---|---|---|---|---|---|---|
| **16B4-4** | 42 | 8 | 9 | 5 | 20 | 2.87 | 0.41 |
| **16B8-2** | 10 | 2 | 1 | 0 | 7 | 1.38 | 0.71 |

Due to a higher availability of $F_2$ seeds, the double-positive 16B4 progeny (from here on referred to as 16B-plants) was used for further experiments. Notably, no obvious phenotypic alterations were observed in the double transgenic plants (Fig. **44**) as compared to the untransformed control Bobwhite and the parental, single transgenic lines.


Fig. **44**. Phenotypic appearance of the (1) *T. aestivum* cv Bobwhite untransformed plant, (2) the 16B -plants, (3) the ST8-49 (UGT-parental line) and (4) the J82-23a (PGIP-parental line).

Genomic DNA of the 16B-plants, the untransformed control Bobwhite and the Lem-UGT and Ubi-PGIP parental lines were analyzed by Southern blot analysis to confirm the integration of the transgene in the genome, using almost 800 bp of both the *HvUGT13248* and the *PvPGIP2* coding regions as probe (Fig. **45**). The cleavage with *Bam*HI restriction enzyme, which causes the excision of the coding regions in both constructs used for the transformation (Fig. **45**A), results in hybridization signals of about 1400 bp and 1000 bp for *HvUGT13248* and *PvPGIP2,* respectively (Fig. **45**B). The 16B-plants confirmed the presence of both specific hybridization signals, separately present in the parental lines. No signal was detected in the untransformed control Bobwhite.

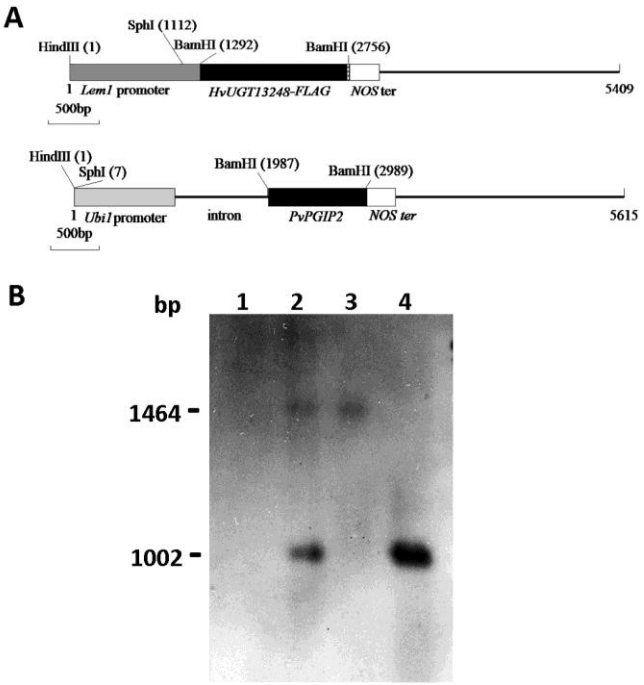


Fig. **45**. Southern blot analysis of the UGT-PGIP plants. **A)** The pAHC17_Lem1::HvUGT13248 and the pAHC17_Ubi1::PvPGIP2 constructs, prepared by cloning the *HvUGT13248-FLAG* and the *PvPGIP2* genes, respectively, into the *Bam*HI site of pAHC17 under control of the barley *Lem1* and the maize *Ubiquitin1* promoter, respectively, and *NOS* terminator. **B)** Genomic DNA (10 µg) of transgenic lines digested with *Bam*HI and probed with the digoxigenin-labeled coding regions of *HvUGT13248-FLAG* and *PvPGIP2*.
(1) *T. aestivum* cv Bobwhite (untransformed control); (2) 16B-plants, (3) ST8-49 (UGT-parental line); (4) J82-23a (PGIP-parental line).

### 4.2.2.3 Infection experiments for evaluation of FHB resistance

In order to verify whether a synergic effect could result from the combination of the *HvUGT13248* and *PvPGIP2* genes for FHB resistance of bread wheat, infection experiments were performed with *F. graminearum* on $F_2$ 16B-plants, the parental lines ST8-49 and J82-23a, UGT- and PGIP-plants respectively, and the untransformed *T. aestivum* cv Bobwhite. The choice of the progeny was done before knowing that the Lem-UGT lines do not exhibit the same level of FHB resistance (see § 4.1.4), being only based on the number of available $F_2$ seeds.

As for the durum wheat UGT+PMEI plants (see § 4.2.1.3), the results of the FHB infection experiments (Fig. **46**) are of a preliminary nature, representing a single biological replicate. The UGT- and PGIP-parental lines confirmed their levels of resistance compared to the untransformed control. On the other hand, the UGT+PGIP progeny showed an increased resistance, from 10 to 30%, compared to both parental lines from 9 to 11 dpi, and an increased resistance compared to the untransformed control throughout the experiment time points.

A

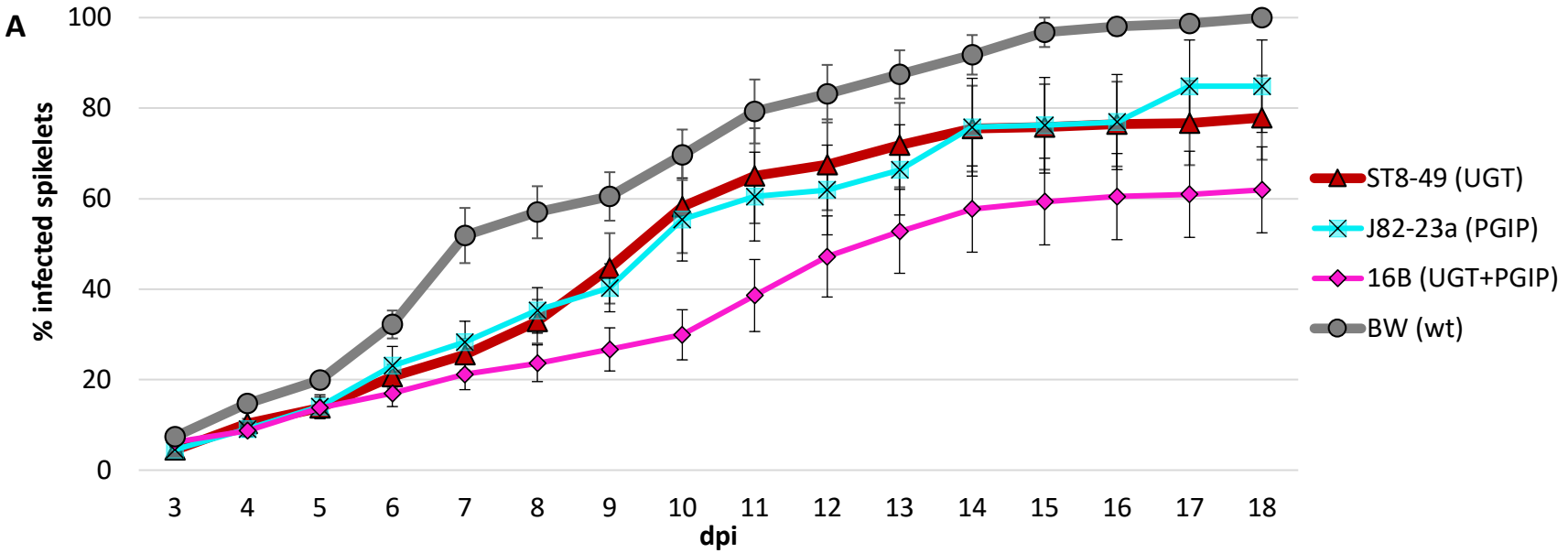


B

| | dpi | 3 | 4 | 5 | 6 | 7 | 8 | 9 | 10 | 11 | 12 | 13 | 14 | 15 | 16 | 17 | 18 |
|---|---|---|---|---|---|---|---|---|---|---|---|---|---|---|---|---|---|
| **Bobwhite** | M | 7.4 | 14.5 | 19.4 | 32.7 | 49.1 | 53.8 | 57.0 | 66.3 | 77.4 | 81.0 | 84.9 | 88.9 | 93.5 | 94.6 | 95.2 | 96.4 |
| | SE | 0.66 | 1.10 | 1.74 | 3.36 | 6.20 | 6.13 | 5.98 | 6.13 | 6.71 | 6.20 | 5.49 | 4.92 | 4.44 | 3.85 | 3.66 | 3.57 |
| | Tukey | ns | ns | ns | a | a | a | a | a | a | a | a | a | a | a | a | a |
| **J82-23a** | M | 4.6 | 9.0 | 13.8 | 23.7 | 30.6 | 38.4 | 44.3 | 59.1 | 63.8 | 65.1 | 69.2 | 77.8 | 78.2 | 78.8 | 86.1 | 86.1 |
| | SE | 0.55 | 1.53 | 2.35 | 3.97 | 4.78 | 5.53 | 6.31 | 9.16 | 9.54 | 9.59 | 9.53 | 10.06 | 9.84 | 9.78 | 9.41 | 9.41 |
| | Tukey | ns | ns | ns | b | b | b | a | a | a | ab | ab | ab | ab | ab | ab | ab |
| **ST8-49** | M | 4.5 | 10.2 | 14.0 | 22.2 | 27.7 | 35.9 | 48.6 | 61.2 | 67.5 | 69.8 | 73.8 | 77.2 | 77.6 | 78.2 | 78.4 | 79.5 |
| | SE | 0.69 | 0.96 | 1.19 | 2.85 | 3.87 | 5.40 | 8.22 | 9.92 | 10.04 | 9.58 | 8.86 | 8.97 | 8.92 | 8.83 | 8.78 | 8.76 |
| | Tukey | ns | ns | ns | b | b | b | a | a | a | ab | ab | ab | ab | ab | ab | ab |
| **16B** | M | 6.0 | 8.5 | 14.0 | 17.3 | 21.4 | 23.7 | 27.6 | 31.3 | 41.9 | 50.5 | 55.7 | 60.3 | 61.9 | 62.9 | 63.4 | 64.3 |
| | SE | 0.95 | 1.26 | 2.26 | 2.73 | 3.16 | 3.79 | 4.56 | 5.37 | 8.15 | 9.00 | 9.17 | 9.30 | 9.31 | 9.24 | 9.23 | 9.20 |
| | Tukey | ns | ns | ns | b | b | b | b | b | b | b | b | b | b | b | b | b |

Fig. **46**. Time-course development of Fusarium head blight (FHB) symptoms following *F. graminearum* infection of the transgenic lines ST8-74, J82-23a, the 16B plants and the untransformed *T. aestivum* cv Bobwhite (BW). Mean values (M) standard errors (SE) refer to one FHB assay performed with at least 15 plants per genotype. M ± SE of the three genotypes are graphically represented in **A)**. In **B)**, besides M ± SE values, results of Tukey test at $P<0.05$ (lower case) and $P<0.01$ (upper case) level are reported. ns: not significant.

# 5. Discussion

## 5.1 *HvUGT13248* expression in durum and bread wheat

*Fusarium* species cause threatening diseases both in durum and bread wheat that produced important economic losses and mycotoxin contamination around the world. For successful pathogenesis, during host plant infection *Fusarium* spp. produce mycotoxins, among which deoxynivalenol (DON) is the most detected (Canady et al. 2001; Streit et al. 2012). Among the natural mechanisms occurring in plant to reduce DON accumulation and to counteract its effects, the DON conjugation by specific plant UDP-glycosyltransferases (UGTs) to a glucose molecule, producing the less toxic metabolite D3G, is considered one of the most promising mechanisms in conferring *Fusarium* resistance (Lemmens et al. 2005; Kluger et al. 2015).

To better highlight the DON-detoxification potential, we produced transgenic durum wheat plants constitutively expressing the *HvUGT13248* transgene (Ubi-UGT) and bread wheat plants expressing it in flower tissues (Lem-UGT). We also tried to obtain the same tissue-specific expression in durum wheat, but all the transgenic events underwent silencing phenomena; therefore, these transgenic events will not be further discussed. The HvUGT13248 is a barley UGT that actively detoxifies DON (Gardiner et al. 2010; Schweiger et al. 2010), which was shown to confer FHB resistance when constitutively expressed in bread wheat (Li et al. 2015c). This evidence prompted us to make use of *HvUGT13248* gene for our research purposes. Furthermore, although DON is produced during fungal progression through the stem in FCR disease (Scherm et al. 2011; Powell et al. 2017), the effect of DON detoxification on disease progression was not investigated yet.

In our results, two transgenic Ubi-UGT durum wheat lines, challenged with *F. graminearum* at anthesis stage, exhibited an appreciable reduction of FHB severity (up to 30%), particularly significant between day 6 and 9 post-infection and up to day 15, compared to Svevo untransformed plants. Although seeds of all genotypes were clearly affected by the infection (see, e.g., Figs. **31** and **35**), DON content was significantly reduced in both transgenic lines, which represents a remarkable result, considering the DON effects and toxicity for human and animal health (Pestka 2010; Maresca 2013). In Ubi-UGT plants, more efficient D3G conversion from early infection stages may have reduced fungal progression and, as a consequence, the amount of DON and D3G contamination in kernels. In fact, such lines exhibited a much higher D3G/DON ratio (about 100 times) than the Svevo control, confirming their better DON-to-D3G

conversion ability and the contribution of DON-detoxification in reducing FHB symptoms during disease progression (Li et al. 2015c; Pasquet et al. 2016).

The extent of the UGT-based effect that we observed in a durum wheat context differs from what described by Li et al. (2015c) in bread wheat. In their work, bread wheat lines constitutively expressing *HvUGT13248* exhibited about 60% reduction of disease severity at 21 dpi as compared to untransformed cv Bobwhite when challenged with *F. graminearum* under greenhouse conditions. Results from field trials were more variable; however all transgenic lines exhibited a significant reduction in FHB severity, but were highly variable for DON, D3G and DON+D3G contents, depending on disease pressure. Similar lack of correlation between disease severity and mycotoxin accumulation was also observed in various bread wheat genotypes (Mesterházy et al. 1999). Several possible reasons could contribute to account for the observed differences between our results and those by Li et al. (2015c). First, the genetic background of tetraploid and hexaploid wheat can play a different role in the host-pathogen interaction and in DON-detoxification. Second, the use of different growth conditions (growth chamber *vs* greenhouse) could influence the experimental trend of the infection. Finally, the use of *F. graminearum* strains with different aggressiveness could cause additional response variations. In literature, the influence of different *Fusarium* strains on FHB resistance/susceptibility is debated. Some authors reported an horizontal, non-species/strain specificity of FHB resistance in field trials (van Eeuwijk et al. 1995; Mesterházy et al. 1999), whereas Akinsanmi et al. (2006) demonstrated a strain-specificity for FHB under controlled conditions, thus minimizing environmental effects on pathogen aggressiveness. They also suggested that different wheat genotypes might present distinct mechanisms to control pathogenicity (virulence and aggressiveness of the pathogens). In order to clarify this issue, we performed infection experiments challenging Svevo wild type plants with both the *F. graminearum* strain usually employed in this work (strain 3827) and two other widely used strains, i.e. PH1 and 8/1. Little difference in disease progression was observed, all strains exhibiting a very strong virulence on durum wheat cv Svevo, leading to a complete colonization of the spike between days 9 and 10 post-infection. Moreover, all *F. graminearum* strains caused an initial necrosis on the infected spikelets and in the adjacent ones, followed by a sudden bleaching of the higher part of the spike, typically observed on cv Svevo plants. Since these phenomena were only occasionally detected in bread wheat cv Bobwhite, it suggests that the different reaction is host- and not strain- dependent. This is in line with Bai

and Shaner (1996) observations about a rapid bleaching of the spike top part of highly susceptible cultivars and a variable occurrence of this phenomenon in moderate susceptible cultivars, like cv Bobwhite. The occurrence of spike bleaching is probably associated to vessel occlusion (Bai and Shaner 1996). Our recent investigation (see Fig. **SM-3** and Fig. **SM-4** in Supplementary materials) suggests that vessel occlusion, besides that to plant reaction, can probably be due to the fungal infection as well, since we detected fungal presence in the bleached part of the spike, above the infection point.

Seedlings of the Ubi-UGT lines were also challenged with *F. culmorum* in order to evaluate the contribution of DON-detoxification to FCR resistance. Our results showed a symptom reduction of about 50% at all time-points in the two Ubi-UGT durum wheat lines as compared to Svevo control seedlings. Notably, this is the first evidence of a direct involvement of DON-detoxification by UGT glycosylation in the resistant response toward the FCR disease. By transcriptome analyses, Powell et al. (2017) identified a number of candidate genes differentially regulated after seedling inoculation with *F. pseudograminearum*, another causal agent of FCR. *UGTs* and *ABC-transporter* genes were detected only in infected samples, therefore suggesting a potential involvement in detoxification. However, to date none of these genes has been functionally characterized yet. In addition, Desmond et al. (2008) compared the gene expression changes in the wheat stem base of the partial resistant cv Sunco and the susceptible cv Kennedy, 24 hours after *F. pseudograminearum* inoculation, by using the Affymetrix GeneChip Wheat Genome Array. They found activation of genes encoding anti-microbial proteins, genes involved in ROS metabolism, and genes involved in secondary metabolism, like *cytochrome P450* as well as several *glucosyltransferases* (*GTs*). Once expressed in *A. thaliana*, none of these GTs conferred resistance to DON (Desmond et al. 2008a).

To our knowledge, none of tested genotypes in natural population or in breeding programs exhibited both FHB and FCR resistance, as apparently conferred by our *UTG* transgene. As a remarkable exception, high FHB and FCR resistance was achieved by introgressing into wheat the *Fhb-7EL* and *Fhb-7el$_2$L* QTLs from *Th. elongatum* (Ceoloni et al. 2017) and *Th. ponticum* (Forte et al. 2014), respectively. Although not many researches have been carried out on simultaneous resistance to the two diseases, a genetic correlation between FHB and FCR resistance in bread wheat was not found (Xie et al. 2006; Li et al. 2010).

Concerning the Lem-UGT lines, our results showed that the expression of the *HvUGT13248* in floral tissues enhances FHB resistance in bread wheat, highlighting a differential contribution during disease progression depending on the level of *UGT*-expression. Indeed, a dose-effect result was observed in two transgenic lines with different *HvUGT13248* expression. The higher-expressing line reduced FHB severity throughout the infection, reaching a maximum reduction of 30-40% as compared to the untransformed control, also increasing the infected kernel weight at maturity. The lower-expressing line reduced FHB severity to a lower extent, and not until the end of the infection. In contrast, as recalled above, the constitutive expression of *HvUGT13248* in the same bread wheat cultivar produced a more marked effect on FHB resistance in the work by Li et al. (2015c), in which plants from different transgenic events never exceeded 20% of FHB severity at 21 days post-infection under greenhouse conditions. Disease pressure was higher in our experiments, since the untransformed control Bobwhite always reached complete spike infection (100% diseased spikelets), compared to the 70% in the experiments by Li et al. (2015c). However, although under different experimental conditions, in both studies transgenic UGT contribution to DON-to-D3G conversion was found to significantly increase D3G/DON ratio. In our experiments, the higher-expressing Lem-UGT line reduced DON amount and improved that of D3G, indicating its better DON glycosylation ability due to higher *UGT* expression. By contrast, the lower-expressing Lem-UGT line only increased D3G content, as compared to the control. In the same line, the total DON (DON+D3G) resulted even higher than in the other genotypes, possibly reflecting a stronger aggressiveness and thus DON production by the pathogen in its interaction with this specific genotype.

*Lem1* promoter, initially isolated by Skadsen et al. (2002) from barley, drives the expression in wheat lemma, palea, rachis and anthers (Somleva and Blechl 2005; Tundo et al. 2016a). In wheat, the transcript driven by this promoter is highly expressed during head emergence, before anthesis, whereas the protein activity was found to peak at anthesis stage, both with the reporter GFP protein (Somleva and Blechl 2005) and with the defence PvPGIP2 enzyme (Tundo et al. 2016a). A key factor in DON-sensitivity of the host seems to be represented by the timing of toxin neutralization: the earlier the mycotoxin is neutralized, the higher are the chances of limiting pathogen spread (Li et al. 2015c, 2017). Due to this, the possibility that *Lem1*-driven expression of *HvUGT13248* could not coincide with maximum DON production by the fungus does exist. Indeed, the HvUGT13248 protein might be degraded quickly after its

transcriptional peak, hence being insufficient at later and more critical stages for plant response to DON. In contrast, under a constitutive expression, like that of *Ubi1*-driven HvUGT13248, the transgene activity can be assumed as constant through developmental stages. Direct DON injection in florets, followed by indirect UGT activity evaluation through DON/D3G measurement at different developmental flower stages *in planta*, would be useful to verify whether the *Lem1*-driven HvUGT13248 maximum activity coincides or not with DON peak production at the rachis node (Ilgen et al. 2009).

## 5.2 Pyramiding of *HvUGT13248* and *CWDE inhibitors*

Pyramiding of resistance genes is considered a promising mechanism to improve efficacy against single or multiple diseases, and to extend durability of resistance (Dangl et al. 2013; Brown 2015; Mundt 2014; Li et al. 2016; Pilet-Nayel et al. 2017). In this work, we obtained double transgenic plants expressing *HvUGT13248* and *AcPMEI* or *PvPGIP2* in cross combinations of transgenic lines individually expressing those genes (Volpi et al. 2011; Janni et al. 2008). To our knowledge, no such combinations were previously described in literature. The combination *HvUGT13248* and *AcPMEI* (UGT+PMEI-plants) was achieved in durum wheat, and both transgenes have been constitutively expressed. The *HvUGT13248* and *PvPGIP2* co-presence (UGT+PGIP-plants) was obtained in bread wheat, the first transgene having a floral-specific expression, the latter being constitutively expressed. Both UGT+PMEI- and UGT+PGIP- plants showed an improvement of FHB resistance as compared to the respective parental lines (single transgenics), demonstrating a synergic contribution of DON-detoxification and inhibition of cell wall degrading enzymes (CWDEs) in different backgrounds and combinations. In accordance with our results, pyramiding in transgenic rice of *PR* genes involved in different resistance mechanisms, i.e. a chitinase involved in hydrolyzation of fungal cell wall and an oxalate oxidase that degrades the virulence factor oxalic acid, provided an improved sheath blight resistance against the necrotrophic fungus *Rhizoctonia solani* (Karmakar et al. 2016). In wheat, pyramiding of specific inhibitors of CWDEs by Tundo et al. (2016b) and of specific *Pm3* alleles by Koller et al. (2018), improved FHB and powdery mildew resistance, respectively.

Pyramiding of defence genes was also demonstrated to be a useful tool to broaden resistance to different pathogens and diseases. For instance, Senthilkumar et al. (2010) obtained simultaneous resistance against bacterial and insect diseases in transgenic tobacco

stacking *protease-inhibitor* genes (the potato trypsin inhibitor s*poramin* gene and the taro phytocystatin *CeCPI* gene*)*, driven by a wound and pathogen-responsive promoter. As another example, transgenic potato co-expressing a chitinase from *Streptomyces griseus* and a defensin from *Wasabia japonica* exhibited higher resistance against Fusarium wilt and early blight, caused respectively by the fungal pathogens *F. oxysporum* and *Alternaria solani*, as compared to the untransformed control and the single transgenic lines (Khan et al. 2014). In wheat, improved resistance to FCR of seedlings and FHB was achieved by co-transformation of different anti-fungal peptides (AFPs) (Liu et al. 2012). In particular, these authors co-bombarded four *AFPs* obtaining transgenic lines with all the AFPs combinations, but a consistent resistance throughout various generations was obtained only in two lines carrying *Chi* and *Pep3* or *Chi* and *MsrA1* combinations, highlighting the importance of a proper combination of different transgenes.

In this view, in addition to FHB resistance, we tested also the FCR response of UGT+PMEI plants since the two transgenes are constitutively expressed and therefore both could contribute during seedling infection. However, UGT+PMEI seedlings did not show any further improvement of FCR resistance, as compared to the UGT-parental line. In this case, the parental line expressing the *AcPMEI* transgene was not previously tested against FCR disease. Despite this line provided a broad spectrum of resistance against both *B. sorokiniana* and *F. graminearum* (Volpi et al. 2011), it did not show any resistance upon seedling infection by *F. culmorum*, suggesting a lack of involvement of the pectin de-methylesterification in this interaction. To our knowledge, few works investigated the production of CWDEs during FCR disease and, consequently, the involvement of CWDEs inhibitors. For instance, Urbanek et al. (1976) found that *F. culmorum* is able to produce exo-polygalacturonate (exo-PAL) in culture supplemented with pectin. Moreover, acidic proteases are also produced during maize seedling infection by *F. culmorum* (Urbanek and Yirdaw 1978). Neither Desmond et al. (2008) nor Powell et al. (2017), by using Affymetrix GeneChip Array and RNA-seq approaches, respectively, found CWDEs inhibitors expression in the wheat stem base after *F. pseudograminearum* inoculation. As a general observation, CWDEs are mainly produced during pathogenesis of necrotrophic and hemibiotrophic fungi (Zhao et al. 2013; King et al. 2011). Notably, some observations suggested that, during FCR infection, the pathogen enters the stem without direct penetration, either *via* the point of attachment of the leaf sheath to the stem base (Covarelli et al. 2012), or through the lesions formed during primary root

emergence (Scherm et al. 2013). The absence of direct penetration could explain a possible lack of involvement of CWDEs inhibitors. However, more studies are necessary to confirm such considerations.

Due to the lack of PMEI contribution *per se* to FCR disease, our results on *HvUGT13248* and *AcPMEI* pyramiding cannot be considered conclusive. More studies are necessary to evaluate the involvement of CWDEs during FCR infection, considering for instance CWDEs directly involved in pectin or hemicellulose degradation, like polygalacturonases or xylanases. If any of the CWDEs will be found to be important for *Fusarium* colonization of seedlings, it could be interesting to test the efficacy against FCR-causing pathogens of the combination of the DON-detoxification mechanism conferred by UGTs with a suitable CWDE inhibitor.

# 6. Conclusions

The improvement of natural plant defense mechanisms to control pathogen attacks is one of the most attracting strategies to increase resistance in a sustainable manner. In fact, breeding programs give high value to broad spectrum and durable resistance mechanisms to control different diseases. In this view, contrasting virulence factors, like DON, while simultaneously taking advantage of different resistance mechanisms, is a particularly promising approach.

The present work allowed firstly to elucidate the contribution of DON-detoxification by constitutive *HvUGT13248* expression in durum wheat against FHB and FCR. Both diseases were positively affected by the transgenic UGT expression. The improvement of disease response in a highly susceptible species, like durum wheat, has to be considered as an important result. Concerning the impact on FCR disease, this is the first observation of direct involvement of DON-detoxification in FCR resistance. Moreover, the concomitant efficacy of DON-detoxifying UGT against FHB and FCR makes it interesting for breeding programs addressing broad-spectrum resistance against *Fusarium* pathogens.

The floral specific expression of the barley *HvUGT13248* in bread wheat confirmed the reduction of FHB symptoms, though to a different extent in the two tested lines, suggesting the need for a minimum UGT amount to effectively contribute to resistance. Moreover, if an actual temporal shift between maximum DON production and *Lem1*-driven HvUGT13248 activity will be confirmed, this would support the importance of the "promptness" of the DON-detoxification host response mechanism, in particular under high disease pressure. In such case, despite the *Lem1* promoter is a good choice when considering defence genes important during the initial stages of FHB infection, like PvPGIP2 (Tundo et al. 2016a), it may not represent the most suitable choice for later acting mechanisms/molecules.

Furthermore, since the integration of different mechanisms implicated in response to pathogens could provide a stronger and/or more durable resistance, we investigated the possibility of a synergic contribution of different resistance mechanisms. In particular, the pyramiding of DON-detoxification and CWDE inhibition resulted in additional resistance against FHB, confirming the potential of exploiting simultaneously different mechanisms by stacking resistance genes. On the other hand, since the de-esterification activity of endogenous PMEs does not influence FCR resistance in durum wheat, the specific combination UGT+PMEI did not provide additional resistance against FCR as compared to UGT

alone. This result highlights the importance of a deep knowledge of plant-pathogen interactions for an accurate choice of resistance mechanisms and underlying genes to be combined to best counteract pathogen attacks.

# Bibliography


Akinsanmi, O. A., Backhouse, D., Simpfendorfer, S., and Chakraborty, S. 2006. Pathogenic variation of *Fusarium* isolates associated with head blight of wheat in Australia. J. Phytopathol. 154:513–521

Alexander, N. J., Proctor, R. H., and McCormick, S. P. 2009. Genes, gene clusters, and biosynthesis of trichothecenes and fumonisins in *Fusarium*. Toxin Rev. 28:198–215

Anand, A., Zhou, T., Trick, H. N., Gill, B. S., Bockus, W. W., and Muthukrishnan, S. 2003. Greenhouse and field testing of transgenic wheat plants stably expressing genes for thaumatin-like protein, chitinase and glucanase against *Fusarium graminearum*. J. Exp. Bot. 54:1101–1111

Anderson, J. A., Stack, R. W., Liu, ·S., Waldron, B. L., Fjeld, ·A.D., Coyne, ·C., Moreno-Sevilla, B., Mitchell Fetch, ·J., Song, ·Q.J., Cregan, P. B., and Frohberg, R. C. 2001. DNA markers for Fusarium head blight resistance QTLs in two wheat populations. Theor. Appl. Genet. 102:1164–1168

Bahrini, I., Sugisawa, M., Kikuchi, R., Ogawa, T., Kawahigashi, H., Ban, T., and Handa, H. 2011. Characterization of a wheat transcription factor, TaWRKY45, and its effect on Fusarium head blight resistance in transgenic wheat plants. Breed. Sci. 61:121–129

Bai, G. H., Desjardins, A. E., and Plattner, R. D. 2001. Deoxynivalenol-nonproducing *Fusarium graminerum* causes initial infection, but does not cause disease spread in wheat spikes. Mycopathologia. 153:91–98

Bai, G., and Shaner, G. 2004. Management and resistance in wheat and barley to Fusarium Head Blight. Annu. Rev. Phytopathol. 42:135–161

Bai, G., and Shaner, G. 1996. Variation in *Fusarium graminearum* and cultivar resistance to Wheat Scab. Plant Dis. 80:975–979

Baldoni, R., and Giardini, L. 2000. *Coltivazioni erbacee. cereali e proteaginose.* Pàtron. Bologna.

Balmas, V., Delogu, G., Sposito, S., Rau, D., and Migheli, Q. 2006. Use of a complexation of tebuconazole with β-Cyclodextrin for controlling Foot and Crown Rot of durum wheat incited by *Fusarium culmorum*. J. Agric. Food Chem. 54:480–484

Barabaschi, D., Tondelli, A., Desiderio, F., Volante, A., Vaccino, P., Valè, G., and Cattivelli, L. 2016. Next generation breeding. Plant Sci. 242:3–13

Beccari, G., Covarelli, L., and Nicholson, P. 2011. Infection processes and soft wheat response to root rot and crown rot caused by *Fusarium culmorum*. Plant Pathol. 60:671–684

Beliën, T., Campenhout, S. Van, Robben, J., and Volckaert, G. 2006. Microbial endoxylanases: effective weapons to breach the plant cell-wall barrier or, rather, triggers of plant defense systems? Mol. Plant-Microbe Interact. 19:1072–1081

Berthiller, F., Dall'Asta, C., Schuhmacher, R., Lemmens, M., Adam, G., and Krska, R. 2005. Masked mycotoxins: determination of a deoxynivalenol glucoside in artificially and naturally contaminated wheat by liquid chromatography−tandem mass spectrometry. J. Agric. Food Chem. 53:3421–3425

Berthiller, F., Krska, R., Domig, K. J., Kneifel, W., Juge, N., Schuhmacher, R., and Adam, G. 2011. Hydrolytic fate of deoxynivalenol-3-glucoside during digestion. Toxicol. Lett. 206:264–7

Bhalla, P. L. 2006. Genetic engineering of wheat – current challenges and opportunities. TRENDS Biotechnol. 24:305–311

Birzele, B., Meier, A., Hindorf, H., Krämer, J., and Dehne, H.-W. 2002. Epidemiology of *Fusarium* infection and deoxynivalenol content in winter wheat in the Rhineland, Germany. Pages 667–673in:Mycotoxins in Plant Disease,Springer Netherlands, Dordrecht.

Blandino, M., Haidukowski, M., Pascale, M., Plizzari, L., Scudellari, D., and Reyneri, A. 2012. Integrated strategies for the control of Fusarium head blight and deoxynivalenol contamination in winter wheat. F. Crop. Res. 133:139–149

Boenisch, M. J., and Schäfer, W. 2011. *Fusarium graminearum* forms mycotoxin producing infection structures on wheat. BMC Plant Biol. 11:110

Bommineni, V. R., Jauhar, P. P., and Peterson, T. S. 1997. Transgenic durum wheat by microprojectile bombardment of isolated scutella. J. Hered. 88:475–481

Bowles, D., Lim, E.-K., Poppenberger, B., and Vaistij, F. E. 2006. Glycosyltransferases of lipophilic small molecules. Annu. Rev. Plant Biol. 57:567–597

Bradford, M. M. 1976. A rapid and sensitive method for the quantitation of microgram quantities of protein utilizing the principle of protein-dye binding. Anal. Biochem. 72:248–54

Broekaert, N., Devreese, M., Demeyere, K., Berthiller, F., Michlmayr, H., Varga, E., Adam, G., Meyer, E., and Croubels, S. 2016. Comparative in vitro cytotoxicity of modified deoxynivalenol on porcine intestinal epithelial cells. Food Chem. Toxicol. 95:103–109

Broekaert, N., Devreese, M., De Mil, T., Fraeyman, S., Antonissen, G., De Baere, S., De Backer, P., Vermeulen, A., and Croubels, S. 2015. Oral bioavailability, hydrolysis, and comparative toxicokinetics of 3-acetyldeoxynivalenol and 15-acetyldeoxynivalenol in broiler chickens and pigs. J. Agric. Food Chem. 63:8734–8742

Brown, J. K. M. 2015. Durable resistance of crops to disease: a darwinian perspective. Annu. Rev. Phytopathol. 53:513–539

Buerstmayr, H., Ban, T., and Anderson, J. A. 2009. Review QTL mapping and marker-assisted selection for Fusarium head blight resistance in wheat : a review. Plant Breed. 128:1–26

Buerstmayr, H., Steiner, B., Hartl, L., Griesser, M., Angerer, N., Lengauer, D. ·, Miedaner, T. ·, Schneider, B., and Lemmens, · M. 2003. Molecular mapping of QTLs for Fusarium head blight resistance in spring wheat . II . Resistance to fungal penetration and spread. Theor. Appl. Genet. 107:503–508

Bushnell, W. R., Hazen, B. E., and Pritsch, C. 2003. *Histology and physiology of Fusarium Head Blight*. J.L. Kurt and W. Bushnell, eds. APS Press., St. Paul, MN.

Caffall, K. H., and Mohnen, D. 2009. The structure, function, and biosynthesis of plant cell wall pectic polysaccharides. Carbohydr. Res. 344:1879–1900

Canady, R., Coker, R., Rgan, S., Krska, R., Kuiper-Goodman, T., and Olsen, M. 2001. *WHO Food Additives Series: 47. Safety evaluation of certain mycotoxins in food*. Joint FAO/WHO Expert Committee on Food Additives, ed. Rome: FAO.

Cantarel, B. L., Coutinho, P. M., Rancurel, C., Bernard, T., Lombard, V., and Henrissat, B. 2009. The Carbohydrate-Active EnZymes database (CAZy): an expert resource for Glycogenomics. Nucleic Acids Res. 37:D233–D238

Ceoloni, C., Forte, P., Gennaro, A., Micali, S., Carozza, R., and Bitti, A. 2005. Recent developments in durum wheat chromosome engineering. Cytogenet. Genome Res. 109:328–334

Ceoloni, C., Forte, P., Kuzmanović, L., Tundo, S., Moscetti, I., de Vita, P., Virili, M. E., and D'Ovidio, R. 2017. Cytogenetic mapping of a major locus for resistance to Fusarium head blight and Crown Rot of wheat on *Thinopyrum elongatum* 7EL and its pyramiding with valuable genes from a *Th. ponticum* homoeologous arm onto bread wheat 7DL. Theor. Appl. Genet. :1–20

Ceoloni, C., and Jauhar, P. 2006. *Chromosome Engineering of the Durum Wheat Genome*.

Cesari, S., Bernoux, M., Moncuquet, P., Kroj, T., and Dodds, P. N. 2014. A novel conserved mechanism for plant NLR protein pairs: the "integrated decoy" hypothesis. Front. Plant Sci. 5:606

Chakraborty, S., Liu, C., Mitter, V., Scott, J. B., Akinsanmi, O. A., Ali, S., Dill-Macky, R., Nicol, J.,

Backhouse, D., and Simpfendorfer, S. 2006. Pathogen population structure and epidemiology are keys to wheat crown rot and Fusarium head blight management. Australas. Plant Pathol. 35:643–655

Champeil, A., Fourbet, J.-F., Doré, T., and Rossignol, L. 2004. Influence of cropping system on Fusarium head blight and mycotoxin levels in winter wheat. Crop Prot. 23:531–537

Chen, W. P. ·, Chen, P. D. ·, Liu, D. J. ·, Kynast, R., Friebe, B., Velazhahan, R. ., Muthukrishnan, S., and Gill, B. S. 1999. Development of wheat scab symptoms is delayed in transgenic wheat plants that constitutively express a rice thaumatin-like protein gene. Theor. Appl. Genet. 99:755–760

Chen, X., Steed, A., Travella, S., Keller, B., and Nicholson, P. 2009. *Fusarium graminearum* exploits ethylene signalling to colonize dicotyledonous and monocotyledonous plants. New Phytol. 182:975–983

Cheng, M., Fry, J. E., Pang, S., Zhou, H., Hironaka, C. M., Duncan, D. R., and Conner, T. W. 1997. Genetic Transformation of wheat mediated by *Agrobacterium tumefaciens*. Plant Physiol. 115:971–980

Cheng, W., Song, X.-S., Li, H.-P., Cao, L.-H., Sun, K., Qiu, X.-L., Xu, Y.-B., Yang, P., Huang, T., Zhang, J.-B., Qu, B., and Liao, Y.-C. 2015. Host-induced gene silencing of an essential chitin synthase gene confers durable resistance to Fusarium head blight and seedling blight in wheat. Plant Biotechnol. J. 13:1335–1345

Christensen, A. H., and Quail, P. H. 1996. Ubiquitin promoter-based vectors for high-level expression of selectable and/or screenable marker genes in monocotyledonous plants. Transgenic Res. 5:213–218

Coleman, J. O. D., Blake-Kajff, M. M. A., and Davies, T. G. E. 1997. Detoxification of xenobiotics by plants: chemical modification and vacuolar compartmentation. Trends Plant Sci. 2:144–151

Coll, N., Epple, P., and Dangl, J. 2011. Programmed cell death in the plant immune system Immune Surveillance Systems in Plants and Animals. Cell Death Differ. 18:1247–1256

Cook, J. R. 1980. Fusarium foot rot of wheat and its control in the Pacific Northwest. Plant Dis. 64:1061–1066

Covarelli, L., Beccari, G., Steed, A., and Nicholson, P. 2012. Colonization of soft wheat following infection of the stem base by *Fusarium culmorum* and translocation of deoxynivalenol to the head. Plant Pathol. 61:1121–1129

Cuthbert, P. A., Somers, D. J., and Brulé-Babel, A. 2007. Mapping of *Fhb2* on chromosome 6BS: a gene controlling Fusarium head blight field resistance in bread wheat (Triticum aestivum L.). Theor. Appl. Genet. 114:429–437

D'Mello, J. P. F., Macdonald, A. M. C., and Dijksma, W. T. P. 1998. 3-Acetyl deoxynivalenol and esterase production in a fungicide insensitive strain of *Fusarium culmorum*. Mycotoxin Res. 14:9–18

D'Ovidio, R., and Anderson, O. D. 1994. PCR analysis to distinguish between alleles of a member of a multigene family correlated with wheat bread-making quality. Theor. Appl. Genet. 88:759–63

D'Ovidio, R., Mattei, B., Roberti, S., and Bellincampi, D. 2004. Polygalacturonases, polygalacturonase-inhibiting proteins and pectic oligomers in plant–pathogen interactions. Biochim. Biophys. Acta. 1696:237–244

D'Ovidio, R., and Porceddu, E. 1996. PCR-based assay for detecting IB-genes for low molecular weight glutenin subunits related to gluten quality properties in durum wheat. Plant Breed. 115:413–415

D'Ovidio, R., Tanzarella, O. A., and Porceddu, E. 1992. Isolation of an alpha-type gliadin gene from T*riticum durum* Desf. and genetic polymorphism at the *Gli-2* loci. J. Genet. Breed. 46:41–48

Dal Bello, G. M., Mónaco, C. I., and Simón, M. R. 2002. Biological control of seedling blight of wheat caused by *Fusarium graminearum* with beneficial rhizosphere microorganisms. World J.

Microbiol. Biotechnol. 18:627–636

Dangl, J. L., Horvath, D. M., and Staskawicz, B. J. 2013. Pivoting the plant immune system from dissection to deployment. Science. 341:746–751

Dangl, J. L., and Jones, J. D. 2001. Plant pathogens and integrated defence responses to infection. Nature. 411:826–833

Daniel, R., Simpfendorfer, S., and DPI Tamworth, N. 2008. The impact of crown rot on winter cereal yields. GRDC Grains Res. Updat. Pap.

De Lorenzo, G., D'Ovidio, R., and Cervone, F. 2001. The role of polygalacturonase-inhibiting proteins (PGIPs) in defense against pathogenic fungi. Annu. Rev. Phytopathol. 39:313–335

Debyser, W., Peumans, W. J., Van Damme, E. J. M., and Delcour, J. A. 1999. *Triticum aestivum* Xylanase Inhibitor (TAXI), a new class of enzyme inhibitor affecting breadmaking performance. J. Cereal Sci. 30:39–43

Dellafiora, L., Dall'Asta, C., and Galaverna, G. 2018. Toxicodynamics of Mycotoxins in the Framework of Food Risk Assessment—An In Silico Perspective. Toxins (Basel). 10:e52

Desmond, O. J., Manners, J. M., Schenk, P. M., Maclean, D. J., and Kazan, K. 2008a. Gene expression analysis of the wheat response to infection by *Fusarium pseudograminearum*. Physiol. Mol. Plant Pathol. 73:40–47

Desmond, O. J., Manners, J. M., Stephens, A. E., Maclean, D. J., Schenk, P. M., Gardiner, D. M., Munn, A. L., and Kazan, K. 2008b. The *Fusarium* mycotoxin deoxynivalenol elicits hydrogen peroxide production, programmed cell death and defence responses in wheat. Mol. Plant Pathol. 9:435–445

Di, R., Blechl, A., Dill-Macky, R., Tortora, A., and Tumer, N. E. 2010. Expression of a truncated form of yeast ribosomal protein L3 in transgenic wheat improves resistance to Fusarium head blight. Plant Sci. 178:374–380

Diamond, M., Reape, T. J., Rocha, O., Doyle, S. M., Kacprzyk, J., Doohan, F. M., and Mccabe, P. F. 2013. The *Fusarium* mycotoxin deoxynivalenol can inhibit plant apoptosis-like programmed cell death. PLoS ONE 8: e69542

DONcast Europe. Available at: http://www.doncast.eu/intro.cfm

Dornez, E., Croes, E., Gebruers, K., Carpentier, S., and Swennen, R. 2010a. 2-D DIGE reveals changes in wheat xylanase inhibitor protein families due to *Fusarium graminearum ΔTri5* infection and grain development. Proteomics 10:2303–2319

Dornez, E., Croes, E., Gebruers, K., De Coninck, B., Cammue, B. P. A., Delcour, J. A., and Courtin, C. M. 2010b. Accumulated evidence substantiates a role for three classes of wheat xylanase inhibitors in plant defense. CRC. Crit. Rev. Plant Sci. 29:244–264

Downie, B., Dirk, L. M., Hadfield, K. A., Wilkins, T. A., Bennett, A. B., and Bradford, K. J. 1998. A gel diffusion assay for quantification of pectin methylesterase activity. Anal. Biochem. 264:149–57

Dunwell, J. M. 2014. Transgenic cereals: current status and future prospects. J. Cereal Sci. 59:419–434

Dvorak, J., and Zhang, H.-B. 1990. Variation in repeated nucleotide sequences sheds light on the phylogeny of the wheat B and G genomes. PNAS. 87:9640–9644

Dweba, C. C., Figlan, S., Shimelis, H. A., Motaung, T. E., Sydenham, S., Mwadzingeni, L., and Tsilo, T. J. 2017. Fusarium head blight of wheat: pathogenesis and control strategies. Crop Prot. 91:114–122

Dyer, A. T., Johnston, R. H., Hogg, A. C., and Johnston, J. A. 2009. Comparison of pathogenicity of the Fusarium crown rot (FCR) complex (*F. culmorum, F. pseudograminearum* and *F. graminearum*) on hard red spring and durum wheat. Eur. J. Plant Pathol. 125:387–395

Ehrlich, K. C., and Daigle, K. W. 1987. Protein synthesis inhibition by 8-oxo-12,13-epoxytrichothecenes. Biochim. Biophys. Acta. 923:206–213

European Commission. 2006. Setting Maximum Levels for Certain Contaminants in Foodstuffs. Comm. Regul. No. 1881/2006.

FAO. 2017. *Food Outlook - Biannual report on global food markets*. Food and Agriculture Organization of the United Nations.

FAO. 2016. *Save and grow in practice: maize, rice and wheat. A guide to sustainable*.

FAOSTAT. 2014. FAOSTAT. Available at: http://www.fao.org/faostat/en/#data/QC/visualize.

Ferrari, S., Savatin, D. V, Sicilia, F., Gramegna, G., Cervone, F., and Lorenzo, G. De. 2013. Oligogalacturonides: plant damage-associated molecular patterns and regulators of growth and development. Front. Plant Sci. 4:49

Ferrari, S., Sella, L., Janni, M., Lorenzo, G. De, Favaron, F., and Ovidio, R. D. 2012. Transgenic expression of polygalacturonase-inhibiting proteins in *Arabidopsis* and wheat increases resistance to the flower pathogen *Fusarium graminearum*. 14:31–38

Fierens, E., Rombouts, S., Gebruers, K., Goesaert, H., Brijs, K., Beaugrand, J., Volckaert, G., Van Campenhout, S., Proost, P., Courtin, C. M., and Delcour, J. a. 2007. TLXI, a novel type of xylanase inhibitor from wheat (*Triticum aestivum*) belonging to the thaumatin family. Biochem. J. 403:583–91

Flor, H. H. 1971. Current status of the gene-for-gene.pdf. Annu. Rev. Phytopathol. 9:275–296

Foroud, N., and Eudes, F. 2009. Trichothecenes in Cereal Grains. Int. J. Mol. Sci. 10:147–173

Forte, P., Virili, M. E., Kuzmanović, L., Moscetti, I., Gennaro, A., D'Ovidio, R., and Ceoloni, C. 2014. A novel assembly of *Thinopyrum ponticum* genes into the durum wheat genome: pyramiding Fusarium head blight resistance onto recombinant lines previously engineered for other beneficial traits from the same alien species. Mol. Breed. 34:1701–1716

Fusaprog. Available at: http://www.fusaprog.ch/fusa-start-f.html.

Fusarium Risk Assessment Tool. Available at: http://www.wheatscab.psu.edu/.

Gao, C. S., Kou, X. J., Li, H. P., Zhang, J. B., Saad, A. S. I., and Liao, Y. C. 2013. Inverse effects of *Arabidopsis NPR1* gene on Fusarium seedling blight and Fusarium head blight in transgenic wheat. Plant Pathol. 62:383–392

Gardiner, D. M., McDonald, M. C., Covarelli, L., Solomon, P. S., Rusu, A. G., Marshall, M., Kazan, K., Chakraborty, S., McDonald, B. A., and Manners, J. M. 2012. Comparative pathogenomics reveals horizontally acquired novel virulence genes in fungi infecting cereal hosts. PLoS Pathog. 8:e1002952

Garvey, G. S., Mccormick, S. P., and Rayment, I. 2007. Structural and functional characterization of the TRI101 trichothecene 3-o-acetyltransferase from *Fusarium sporotrichioides* and *Fusarium graminearum*. J. Biol. Chem. 283:1660–1669

Gebruers, K., Brijs, K., Courtin, C. M., Fierens, K., Goesaert, H., Rabijns, A., Raedschelders, G., Robben, J., Sansen, S., Sørensen, J. F., Van Campenhout, S., and Delcour, J. A. 2004. Properties of TAXI-type endoxylanase inhibitors. Biochim. Biophys. Acta. 1696:213–221

Gerhardt, S., Balconi, C., and Sherwood, J. 2002. Control of Fusarium scab with puroindoline-containing transgenic wheat. 2002 Annu. Meet., Milwaukee.

Gunnaiah, R., Kushalappa, A. C., Duggavathi, R., Fox, S., and Somers, D. J. 2012. Integrated metabolo-proteomic approach to decipher the mechanisms by which wheat QTL (*Fhb1*) contributes to resistance against *Fusarium graminearum*. PLoS One. 7:e40695

Han, J., Lakshman, D. K., Galvez, L. C., Mitra, S., Baenziger, P. S., and Mitra, A. 2012. Transgenic expression of lactoferrin imparts enhanced resistance to head blight of wheat caused by *Fusarium graminearum*. BMC Plant Biol. 12:33

Horevaj, P., Milus, E. A., and Bluhm, B. H. 2011. A real-time *q*PCR assay to quantify *Fusarium graminearum* biomass in wheat kernels. J. Appl. Microbiol. 111:396-406.

Huang, S., Sirikhachornkit, A., Su, X., Faris, J., Gill, B., Haselkorn, R., and Gornicki, P. 2002. Genes encoding plastid acetyl-CoA carboxylase and 3-phosphoglycerate kinase of the *Triticum/Aegilops* complex and the evolutionary history of polyploid wheat. PNAS. 99:8133–8

Igawa, T., Ochiai-Fukuda, T., Takahashi-Ando, N., Ohsato, S., Shibata, T., Yamaguchi, I., and Kimura, M. 2004. New TAXI-type xylanase inhibitor genes are inducible by pathogens and wounding in hexaploid wheat. Plant Cell Physiol. 45:1347–1360

Igawa, T., Tokai, T., Kudo, T., Yamaguchi, I., and Kimura, M. 2005. A wheat xylanase inhibitor gene, Xip-I, but not Taxi-I, is significantly induced by biotic and abiotic signals that trigger plant defense. Biosci. Biotechnol. Biochem. 69:1058–63

Ilgen, P., Hadeler, B., Maier, F. J., and Schäfer, W. 2009. Developing kernel and rachis node induce the trichothecene pathway of *Fusarium graminearum* during wheat head infection. Mol. Plant-Microbe Interact. 22:899–908

ISAAA. 2016. *Global Status of Commercialized Biotech/GM Crops: 2016*. ISAAA Brie. ISAAA, ed. ISAAA, Ithaca, NY.

Ishida, Y., Tsunashima, M., Hiei, Y., and Komari, T. 2015. Wheat (*Triticum aestivum* L.) transformation using immature embryos. Pages 189–198in:Springer, New York, NY.

Janni, M., Bozzini, T., Moscetti, I., Volpi, C., and D'Ovidio, R. 2013. Functional characterisation of wheat *Pgip* genes reveals their involvement in the local response to wounding. Plant Biol. 15:1019–1024

Janni, M., Di Giovanni, M., Roberti, S., Capodicasa, C., and D'Ovidio, R. 2006. Characterization of expressed *Pgip* genes in rice and wheat reveals similar extent of sequence variation to dicot PGIPs and identiWes an active PGIP lacking an entire LRR repeat. Theor. Appl. Genet. 113:1233–1245

Janni, M., Sella, L., Favaron, F., Blechl, A. E., Lorenzo, G. De, and Ovidio, R. D. 2008. The expression of a bean PGIP in transgenic wheat confers increased resistance to the fungal pathogen *Bipolaris sorokiniana*. Mol. Plant-Microbe Interact. 21:171–177

Jansen, C., von Wettstein, D., Schäfer, W., Kogel, K.-H., Felk, A., and Maier, F. J. 2005. Infection patterns in barley and wheat spikes inoculated with wild-type and trichodiene synthase gene disrupted *Fusarium graminearum*. Proc. Natl. Acad. Sci. U. S. A. 102:16892–16897

Jia, Y., Mcadams, S. A., Bryan, G. T., Hershey, H. P., and Valent, B. 2000. Direct interaction of resistance gene and avirulence gene products confers rice blast resistance. EMBO J. 19:4004–4014

Johansson, P. M., Johnsson, L., and Gerhardson, B. 2003. Suppression of wheat-seedling diseases caused by *Fusarium culmorum* and *Microdochium nivale* using bacterial seed treatment. Plant Pathol. 52:219–227

Jones, J. D. G., and Dangl, J. L. 2006. The plant immune system. Nature. 444:323–329

Joubert, D. A., Kars, I., Wagemakers, L., Bergmann, C., Kemp, G., Vivier, M. A., and Van Kan, J. A. L. 2007. A Polygalacturonase-inhibiting protein from grapevine reduces the symptoms of the endopolygalacturonase BcPG2 from *Botrytis cinerea* in *Nicotiana benthamiana* leaves without any evidence for *in vitro* interaction. Mol. Plant-Microbe Interact. 392:392–402

Kage, U., Yogendra, K. N., and Kushalappa, A. C. 2017. TaWRKY70 transcription factor in wheat *QTL-2DL* regulates downstream metabolite biosynthetic genes to resist *Fusarium graminearum* infection spread within spike. Sci. Rep. 7:42596

Kalunke, R. M., Cenci, A., Volpi, C., O'Sullivan, D. M., Sella, L., Favaron, F., Cervone, F., De Lorenzo, G., and D'Ovidio, R. 2014. The pgip family in soybean and three other legume species: evidence for a birth-and-death model of evolution. BMC Plant Biol. 14:189

Karlovsky, P. 2011. Biological detoxification of the mycotoxin deoxynivalenol and its use in genetically engineered crops and feed additives. Appl. Microbiol. Biotechnol. 91:491–504

Karmakar, S., Molla, K. A., Chanda, P. K., Sarkar, S. N., Datta, S. K., and Datta, K. 2016. Green tissue-specific co-expression of chitinase and oxalate oxidase 4 genes in rice for enhanced resistance against sheath blight. Planta. 243:115–130

Kazan, K., and Gardiner, D. 2017. Fusarium Crown Rot Caused By *Fusarium pseudograminearum* in cereal crops: recent progress and future prospects. Mol. Plant Pathol. doi: 10.1111/mpp.12639

Keen, N. T. 1990. Plant -pathogen interactions.

Khan, M. R., Fischer, S., Egan, D., and Doohan, F. M. 2006. Biological control of Fusarium Seedling Blight disease of wheat and barley. Phytopathology. 96:386–394

Khan, R. S., Darwish, N. A., Khattak, B., Ntui, V. O., Kong, K., Shimomae, K., Nakamura, I., and Mii, M. 2014. Retransformation of marker-free potato for enhanced resistance against fungal pathogens by pyramiding chitinase and wasabi defensin genes. Mol. Biotechnol. 56:814–823

Kikot, G. E., Hours, R. A., and Alconada, T. M. 2009. Contribution of cell wall degrading enzymes to pathogenesis of *Fusarium graminearum:* a review. J. Basic Microbiol. 49:231–241

Kilian, B., Özkan, H., Deusch, O., Effgen, S., Brandolini, A., Kohl, J., Martin, W., and Salamini, F. 2007. Independent wheat B and G genome origins in outcrossing *Aegilops* progenitor haplotypes. Mol. Biol. Evol. 24:217–227

King, B. C., Waxman, K. D., Nenni, N. V, Bergstrom, G. C., and Gibson, D. M. 2011. Arsenal of plant cell wall degrading enzymes reflects host preference among plant pathogenic fungi. Biotechnol. Biofuels. 4:4

King, R., Urban, M., Hammond-Kosack, M. C. U., Hassani-Pak, K., and Hammond-Kosack, K. E. 2015. The completed genome sequence of the pathogenic ascomycete fungus *Fusarium graminearum*. BMC Genomics. 16:544

Kirby, E. J. M., and Appleyard, M. 1987. *Cereal development guide*. N.A.C. Arable Unit, ed. Kenilworth, England.

Kluger, B., Bueschl, C., Lemmens, M., Berthiller, F., Häubl, G., Jaunecker, G., Adam, G., Krska, R., and Schuhmacher, R. 2013. Stable isotopic labelling-assisted untargeted metabolic profiling reveals novel conjugates of the mycotoxin deoxynivalenol in wheat. Anal. Bioanal. Chem. 405:5031–5036

Kluger, B., Bueschl, C., Lemmens, M., Michlmayr, H., Malachova, A., Koutnik, A., Maloku, I., Berthiller, F., Adam, G., Krska, R., and Schuhmacher, R. 2015. Biotransformation of the mycotoxin deoxynivalenol in *Fusarium* resistant and susceptible near isogenic wheat lines. PLoS One. 10:e0119656

Koller, T., Brunner, S., Herren, G., Hurni, S., and Keller, B. 2018. Pyramiding of transgenic *Pm3* alleles in wheat results in improved powdery mildew resistance in the field. Theor. Appl. Genet. :1–11

Kumar, M., Campbell, L., and Turner, S. 2016. Secondary cell walls: biosynthesis and manipulation. J. Exp. Bot. 67:515–531

Kushiro, M. 2008. Effects of Milling and cooking processes on the deoxynivalenol content in wheat. Int. J. Mol. Sci. 9:2127–2145

Laemmli, U. K. 1970. Cleavage of structural proteins during the assembly of the head of bacteriophage T4. Nature. 227:680–685

Lemmens, M., Scholz, U., Berthiller, F., Dall'Asta, C., Koutnik, A., Schuhmacher, R., Adam, G.,

Buerstmayr, H., Mesterházy, Á., Krska, R., and Ruckenbauer, P. 2005. The ability to detoxify the mycotoxin deoxynivalenol colocalizes with a major quantitative trait locus for Fusarium Head Blight resistance in wheat. Mol. Plant-Microbe Interact. 18:1318–1324

Li, C., Martinez, F., and Delmotte, F. 2016. Combining selective pressures to enhance the durability of disease resistance genes. Front. Plant Sci. 7:1916

Li, H. P., Zhang, J.-B., Shi, R.-P., Huang, T., Fischer, R., and Liao, Y.-C. 2008. Engineering Fusarium Head Blight Resistance in wheat by expression of a fusion protein containing a *Fusarium*-specific antibody and an antifungal peptide. Mol. Plant-Microbe Interact. 21:1242–1248

Li, H. B., Xie, G. Q., Ma, J., Liu, G. R., Wen, S. M., Ban, T., Chakraborty, S., and Liu, C. J. 2010. Genetic relationships between resistances to Fusarium head blight and crown rot in bread wheat (*Triticum aestivum* L.). Theor. Appl. Genet. 121:941–950

Li, L. F., Liu, B., Olsen, K. M., and Wendel, J. F. 2015a. A re-evaluation of the homoploid hybrid origin of *Aegilops tauschii*, the donor of the wheat D-subgenome. New Phytol. 208:4–8

Li, L. F., Liu, B., Olsen, K. M., and Wendel, J. F. 2015b. Multiple rounds of ancient and recent hybridizations have occurred within the *Aegilops-Triticum* complex. New Phytol. 208:11–12

Li, X., Michlmayr, H., Schweiger, W., Malachova, A., Shin, S., Huang, Y., Dong, Y., Wiesenberger, G., Mccormick, S., Lemmens, M., Fruhmann, P., Hametner, C., Berthiller, F., Adam, G., and Muehlbauer, G. J. 2017. A barley UDP-glucosyltransferase inactivates nivalenol and provides Fusarium Head Blight resistance in transgenic wheat. J. Exp. Bot. 68:2187–2197

Li, X., Shin, S., Heinen, S., Dill-Macky, R., Berthiller, F., Nersesian, N., Clemente, T., McCormick, S., and Muehlbauer, G. J. 2015c. Transgenic wheat expressing a barley UDP-glucosyltransferase detoxifies deoxynivalenol and provides high levels of resistance to *Fusarium graminearum*. Mol. Plant-Microbe Interact. 28:1237–1246

Li, Z., Zhou, M., Zhang, Z., Ren, L., Du, L., Zhang, B., Xu, H., and Xin, Z. 2011. Expression of a radish defensin in transgenic wheat confers increased resistance to *Fusarium graminearum* and *Rhizoctonia cerealis*. Funct. Integr. Genomics. 11:63–70

Lionetti, V., Cervone, F., and Bellincampi, D. 2012. Methyl esterification of pectin plays a role during plant-pathogen interactions and affects plant resistance to diseases. J. Plant Physiol. 169:1623–1630

Liu, S., Zhang, X., Pumphrey, M. O., Stack, R. W., Gill, B. S., and Anderson, J. A. 2006. Complex microcolinearity among wheat, rice, and barley revealed by fine mapping of the genomic region harboring a major QTL for resistance to Fusarium head blight in wheat. Funct. Integr. Genomics. 6:83–89

Liu, Z. W., Li, H. P., Cheng, W., Yang, P., Zhang, J. B., Gong, A. D., Feng, Y. N., Fernando, W. G. D., and Liao, Y. C. 2012. Enhanced overall resistance to Fusarium seedling blight and Fusarium head blight in transgenic wheat by co-expression of anti-fungal peptides. Eur. J. Plant Pathol. 134:721–732

Lulin, M., Yi, S., Aizhong, C., Zengjun, Q., Liping, X., Peidu, C., Dajun, L., and Xiu-E, W. 2010. Molecular cloning and characterization of an up-regulated UDP-glucosyltransferase gene induced by DON from *Triticum aestivum* L. cv. Wangshuibai. Mol. Biol. Rep. 37:785–795

Lutz, M. P., Feichtinger, G., and Défago, G. 2003. Mycotoxigenic Fusarium and deoxynivalenol production repress chitinase gene expression in the biocontrol agent *Trichoderma atroviride* P1. Appl. Environ. Microbiol. 69:3077–3084

Ma, J., Li, H. B., Zhang, C. Y., Yang, X. M., Liu, Y. X., Yan, G. J., and Liu, C. J. 2010. Identification and validation of a major QTL conferring crown rot resistance in hexaploid wheat. Theor. Appl. Genet. 120:1119–1128

Ma, L. J., Geiser, D. M., Proctor, R. H., Rooney, A. P., O'Donnell, K., Trail, F., Gardiner, D. M., Manners,

J. M., and Kazan, K. 2013. *Fusarium* Pathogenomics. Annu. Rev. Microbiol. 67:399–416

Mackintosh, C. A., Lewis, J., Lorien, ·, Radmer, E., Shin, S., Heinen, S. J., Smith, L. A., Wyckoff, M. N., Dill-Macky, R., Evans, C. K., Kravchenko, S., Baldridge, G. D., Zeyen, R. J., Muehlbauer, G. J., Dill-Macky, R., Baldridge, G. D., Zeyen, R. J., Kravchenko, S., and Evans, C. K. 2007. Overexpression of defense response genes in transgenic wheat enhances resistance to Fusarium head blight. Plant Cell Rep. 26:479–488

Makandar, R., Essig, J. S., Schapaugh, M. A., Trick, H. N., and Shah, J. 2006. Genetically engineered resistance to Fusarium Head Blight in wheat by expression of *Arabidopsis* NPR1. Mol. Plant-Microbe Interact. 19:123–129

Malinovsky, F. G., Fangel, J. U., and Willats, W. G. T. 2014. The role of the cell wall in plant immunity. Front. Plant Sci. 5:178

Marcussen, T., Sandve, S. R., Heier, L., Spannagl, M., Pfeifer, M., Jakobsen, K. S., Wulff, B. B. H., Steuernagel, B., Mayer, K. F. X., Olsen, O. A., et al. 2014. Ancient hybridizations among the ancestral genomes of bread wheat. Science. 345:1250092

Maresca, M. 2013. From the gut to the brain: Journey and pathophysiological effects of the food-associated trichothecene mycotoxin deoxynivalenol. Toxins (Basel). 5:784–820

Martin, A., Bovill, W. D., Percy, C. D., Herde, D., Fletcher, S., Kelly, · A, Neate, S. M., and Sutherland, M. W. 2015. Markers for seedling and adult plant crown rot resistance in four partially resistant bread wheat sources. Theor. Appl. Genet. 128:377–385

Masuda, D., Ishida, M., Yamaguchi, K., Yamaguchi, I., Kimura, M., and Nishiuchi, T. 2007. Phytotoxic effects of trichothecenes on the growth and morphology of *Arabidopsis thaliana*. J. Exp. Bot. 58:1617–1626

McLauchlan, W. R., Garcia-Conesa, M. T., Williamson, G., Roza, M., Ravestein, P., and Maat, J. 1999. A novel class of protein from wheat which inhibits xylanases1. Biochem. J. 338:441

Melamud, E., Vastag, L., and Rabinowitz, J. D. 2010. Metabolomic analysis and visualization engine for LC–MS Data. Anal. Chem. 82:9818–9826

Mengiste, T. 2012. Plant immunity to necrotrophs. Annu. Rev. Phytopathol. 50:267–294

Mesterházy, Á., Bartók, T., Mirocha, C. G., and Komoróczy, R. 1999. Nature of wheat resistance to Fusarium head blight and the role of deoxynivalenol for breeding. Plant Breed. 118:97–110

Micheli, F. 2001. Pectin methylesterases: cell wall enzymes with important roles in plant physiology. Trends Plant Sci. 6:414-419

Michlmayr, H., Malachova, A., Varga, E., Kleinova, J., Lemmens, M., Newmister, S., Rayment, I., Berthiller, F., and Adam, G. 2015. Biochemical characterization of a recombinant UDP-glucosyltransferase from rice and enzymatic production of Deoxynivalenol-3-O-beta-D-glucoside. Toxins (Basel). 7:2685–2700

Miller, S. S., Chabot, D. M. P., Ouellet, T., Harris, L. J., and Fedak, G. 2004. Use of a Fusarium graminearum strain transformed with green fluorescent protein to study infection in wheat (*Triticum aestivum*). Can. J. Plant Pathol. 26:453–463

Mitter, V., Zhang, M. C., Liu, C. J., Ghosh, R., Ghosh, M., and Chakraborty, S. 2006. A high-throughput glasshouse bioassay to detect crown rot resistance in wheat germplasm. Plant Pathol. 55:433–441

Moscetti, I., Tundo, S., Janni, M., Sella, L., Gazzetti, K., Tauzin, A., Giardina, T., Masci, S., Favaron, F., and D'Ovidio, R. 2013. Constitutive expression of the xylanase inhibitor TAXI-III delays Fusarium head blight symptoms in durum wheat transgenic plants. Mol. Plant-Microbe Interact. 26:1464–1472

Moustacas, A.-M., Nari, J., Borel, M., Noat, G., and Ricard, J. 1991. Pectin methylesterase, metal ions and plant cell-wall extension: The role of metal ions in plant cell-wall extension. Biochem. J. 279:351–354

Mudge, A. M., Dill-Macky, R., Dong, Y., Gardiner, D. M., White, R. G., and Manners, J. M. 2006. A role for the mycotoxin deoxynivalenol in stem colonisation during crown rot disease of wheat caused by *Fusarium graminearum* and *Fusarium pseudograminearum*. Physiol. Mol. Plant Pathol. 69:73–85

Mundt, C. C. 2014. Durable resistance: A key to sustainable management of pathogens and pests. Infect. Genet. Evol. 0:446–455

Okubara, P. A., Blechl, A. E., McCormick, S. P., Alexander, N. J., Dill-Macky, R., and Hohn, T. M. 2002. Engineering deoxynivalenol metabolism in wheat through the expression of a fungal trichothecene acetyltransferase gene. Theor. Appl. Genet. 106:74–83

Osorio, S., Bombarely, A., Giavalisco, P., Usadel, B., Stephens, C., Aragüez, I., Medina-Escobar, N., Botella, M. A., Fernie, A. R., and Valpuesta, V. 2011. Demethylation of oligogalacturonides by *FaPE1* in the fruits of the wild strawberry *Fragaria vesca* triggers metabolic and transcriptional changes associated with defence and development of the fruit. J. Exp. Bot. 62:2855–2873

Osorio, S., Castillejo, C., Quesada, M. A., Medina-Escobar, N., Brownsey, G. J., Suau, R., Heredia, A., Botella, M. A., and Valpuesta, V. 2008. Partial demethylation of oligogalacturonides by pectin methyl esterase 1 is required for eliciting defence responses in wild strawberry (*Fragaria vesca*). Plant J. 54:43–55

Paccanaro, M. C., Sella, L., Castiglioni, C., Giacomello, F., Martinez-Rocha, A. L., D'Ovidio, R., Schäfer, W., and Favaron, F. 2017. Synergistic effect of different plant cell wall degrading enzymes is important for virulence of *Fusarium graminearum*. Mol. Plant-Microbe Interact. 30: 886-895

Pasquet, J.-C., Changenet, V., Macadré, C., Boex-Fontvieille, E., Soulhat, C., Bouchabké-Coussa, O., Dalmais, M., Atanasova-Pénichon, V., Bendahmane, A., Saindrenan, P., and Dufresne, M. 2016. A *Brachypodium* UDP-glycosytransferase confers root tolerance to deoxynivalenol and resistance to *Fusarium* infection. Plant Physiol. 172:559–574

Paul, P. A., Lipps, P. E., and Madden, L. V. 2005. Relationship between visual estimates of Fusarium Head Blight intensity and deoxynivalenol accumulation in harvested wheat grain: a meta-analysis.

Payros, D., Alassane-Kpembi, I., Pierron, A., Loiseau, N., Pinton, P., and Oswald, I. P. 2016. Toxicology of deoxynivalenol and its acetylated and modified forms. Arch. Toxicol. 90:2931–2957

Pereyra, S. A., Dill-Macky, R., and Sims, A. L. 2004. Survival and inoculum production of *Gibberella zeae* in wheat residue. Plant Dis. 88:724–730

Pestka, J. J. 2010. Deoxynivalenol: Mechanisms of action, human exposure, and toxicological relevance. Arch. Toxicol. 84:663–679

Pierron, A., Mimoun, S., Murate, L. S., Loiseau, N., Lippi, Y., Bracarense, A. P., Liaubet, L., Schatzmayr, G., Berthiller, F., Moll, W.-D., and Oswald, I. P. 2016. Intestinal toxicity of the masked mycotoxin deoxynivalenol-3-β-D-glucoside. Arch. Toxicol. 90:2037–2046

Pilet-Nayel, M. L., Moury, B., Caffier, V., Montarry, J., Kerlan, M. C., Fournet, S., Durel, C. E., and Delourme, R. 2017. Quantitative resistance to plant pathogens in pyramiding strategies for durable crop protection. Front. Plant Sci. 8:1838

Ponts, N., Pinson-Gadais, L., Barreau, C., Richard-Forget, F., and Ouellet, T. 2007. Exogenous $H_2O_2$ and catalase treatments interfere with *Tri* genes expression in liquid cultures of *Fusarium graminearum*. FEBS Lett. 581:443–447

Ponts, N., Pinson-Gadais, L., Verdal-Bonnin, M. N., Barreau, C., and Richard-Forget, F. 2006. Accumulation of deoxynivalenol and its 15-acetylated form is significantly modulated by oxidative

stress in liquid cultures of *Fusarium graminearum*. FEMS Microbiol. Lett. 258:102–107

Poole, G. J., Smiley, R. W., Walker, C., Huggins, D., Rupp, R., Abatzoglou, J., Garland-Campbell, K., and Paulitz, T. C. 2013. Effect of climate on the distribution od *Fusarium* spp. causing crown rot of wheat in the Pacific Northwest of the United States. Phytopathology. 103:1130–40

Poppenberger, B., Berthiller, F., Lucyshyn, D., Sieberer, T., Schuhmacher, R., Krska, R., Kuchler, K., Glössl, J., Luschnig, C., and Adam, G. 2003. Detoxification of the *Fusarium* Mycotoxin Deoxynivalenol by a UDP-glucosyltransferase from *Arabidopsis thaliana*. J. Biol. Chem. 278:47905–47914

Poppenberger, B., Fujioka, S., Soeno, K., George, G. L., Vaistij, F. E., Hiranuma, S., Seto, H., Takatsuto, S., Adam, G., Yoshida, S., and Bowles, D. 2005. The UGT73C5 of *Arabidopsis thaliana* glucosylates brassinosteroids. Proc. Natl. Acad. Sci. 102:15253–15258

Powell, J. J., Carere, J., Fitzgerald, T. L., Stiller, J., Covarelli, L., Xu, Q., Gubler, F., Colgrave, M. L., Gardiner, D. M., Manners, J. M., Henry, R. J., and Kazan, K. 2017. The Fusarium crown rot pathogen *Fusarium pseudograminearum* triggers a suite of transcriptional and metabolic changes in bread wheat (*Triticum aestivum* L.). Ann. Bot. 119:853–867

Pritsch, C., Muehlbauer, G. J., Bushnell, W. R., Somers, D. A., and Vance, C. P. 2000. Fungal development and induction of defense response genes during early infection of wheat spikes by *Fusarium graminearum*. Mol. Plant-Microbe Interact. 13:159–169

Ramirez, M. L., Chulze, S., and Magan, N. 2004. Impact of environmental factors and fungicides on growth and deoxinivalenol production by *Fusarium graminearum* isolates from Argentinian wheat. Crop Prot. 23:117–125

Rathjen, J. R., Strounina, E. V., and Mares, D. J. 2009. Water movement into dormant and non-dormant wheat (*Triticum aestivum* L.) grains. J. Exp. Bot. 60:1619–1631

Rauh, D. Grasses. Am. Soc. Bot. Artist. Available at: https://www.asba-art.org/article/science-botanical-art-grasses.

Rawat, N., Pumphrey, M. O., Liu, S., Zhang, X., Tiwari, V. K., Ando, K., Trick, H. N., Bockus, W. W., Akhunov, E., Anderson, J. A., and Gill, B. S. 2016. Wheat *Fhb1* encodes a chimeric lectin with agglutinin domain:s and a pore-forming toxin-like domain conferring resistance to Fusarium head blight. Nat. Genet. 1576-1580

Reddy, M. V. B., Arul, J., Angers, P., and Couture, L. 1999. Chitosan treatment of wheat seeds induces resistance to *Fusarium graminearum* and improves seed quality. J. Agric. Food Chem. 47:1208–1216

Ridley, B. L., O'Neill, M. A., and Mohnen, D. 2001. Pectins: structure, biosynthesis, and oligogalacturonide-related signaling. Phytochemistry. 57:929–967

Rotter, B. A. 1996. Toxicology of deoxynivalenol (Vomitoxin). J. Toxicol. Environ. Health. 48:1–34

Le Roux, C., Huet, G., Jauneau, A., Camborde, L., Trémousaygue, D., Kraut, A., Zhou, B., Levaillant, M., Adachi, H., Yoshioka, H., Raffaele, S., Berthomé, R., Couté, Y., Parker, J. E., and Deslandes, L. 2015. A receptor pair with an integrated decoy converts pathogen disabling of transcription factors to immunity. Cell. 161:1074–1088

Sambrook, J., Fritsch, E. F., and Maniatis, T. 1989. *Molecular cloning : a laboratory manual*. Cold Spring Harbor Laboratory.

Sandve, S. R., Marcussen, T., Mayer, K., Jakobsen, K. S., Heier, L., Steuernagel, B., Wulff, B. B. H., and Olsen, O. A. 2015. Chloroplast phylogeny of *Triticum/Aegilops* species is not incongruent with an ancient homoploid hybrid origin of the ancestor of the bread wheat D-genome. New Phytol. 208:9–10

Scheller, H. V., and Ulvskov, P. 2010. Hemicelluloses. Annu. Rev. Plant Biol. 61:263–289

Scherm, B., Balmas, V., Spanu, F., Pani, G., Delogu, G., Pasquali, M., and Migheli, Q. 2013. Pathogen profile *Fusarium culmorum*: causal agent of foot and root rot and head blight on wheat. Mol. Plant Pathol. 14:323–341

Scherm, B., Orrù, M., Balmas, V., Spanu, F., Azara, E., Delogu, G., Hammond, T. M., Keller, N. P., and Migheli, Q. 2011. Altered trichothecene biosynthesis in TRI6 -silenced transformants of fusarium culmorum influences the severity of crown and foot rot on durum wheat seedlings. Mol. Plant Pathol. 12:759–771

Schweiger, W., Boddu, J., Shin, S., Poppenberger, B., Berthiller, F., Lemmens, M., Muehlbauer, G. J., and Adam, G. 2010. Validation of a candidate deoxynivalenol-inactivating UDP-glucosyltransferase from barley by heterologous expression in yeast. Mol. Plant-Microbe Interact. 23:977–986

Schweiger, W., Pasquet, J.-C., Nussbaumer, T., Paris, M. P. K., Wiesenberger, G., Macadré, C., Ametz, C., Berthiller, F., Lemmens, M., Saindrenan, P., Mewes, H.-W., Mayer, K. F. X., Dufresne, M., and Adam, G. 2013a. Functional characterization of two clusters of *Brachypodium distachyon* UDP-glycosyltransferases encoding putative deoxynivalenol detoxification genes. Mol. Plant-Microbe Interact. 26:781–92

Schweiger, W., Steiner, B., Ametz, C., Siegwart, G., Wiesenberger, G., Berthiller, F., Lemmens, M., Jia, H., Adam, G., Muehlbauer, G. J., Kreil, D. P., and Buerstmayr, H. 2013b. Transcriptomic characterization of two major *Fusarium* resistance quantitative trait loci (QTLs), *Fhb1* and *Qfhs.ifa-5A*, identifies novel candidate genes. Mol. Plant Pathol. 14:772–785

Sears, R. G., and Deckard, E. L. 1982. Tissue culture variability in wheat: callus induction and plant regeneration. Crop Sci. 22:546

Sella, L., Castiglioni, C., Paccanaro, M. C., Janni, M., Schafer, W., D'Ovidio, R., and Favaron, F. 2016. Involvement of fungal pectin methylesterase activity in the interaction between *Fusarium graminearum* and wheat. Mol. Plant-Microbe Interact. 29:258–267

Senthilkumar, R., Cheng, C. P., and Yeh, K. W. 2010. Genetically pyramiding protease-inhibitor genes for dual broad-spectrum resistance against insect and phytopathogens in transgenic tobacco. Plant Biotechnol. J. 8:65–75

Shang, Y., Xiao, J., Ma, L., Wang, H., Qi, Z., Chen, P., Liu, D., and Wang, X. 2009. Characterization of a PDR type ABC transporter gene from wheat (*Triticum aestivum* L.). Chinese Sci. Bull. 54:3249—3257

Shin, S., Torres-Acosta, J. A., Heinen, S. J., McCormick, S., Lemmens, M., Kovalsky Paris, M. P., Berthiller, F., Adam, G., and Muehlbauer, G. J. 2012. Transgenic *Arabidopsis thaliana* expressing a barley methylation and chromatin patterning UDP-glucosyltransferase exhibit resistance to the mycotoxin deoxynivalenol. J. Exp. Bot. 63:4731–4740

Simmons, S., Oelke, E., and Anderson, P. Growth and development guide for spring wheat. Univ. Minnesota Ext. Available at: http://www.extension.umn.edu/agriculture/small-grains/growth-and-development/spring-wheat/index.html

Sitton, J. W., and Cook, R. J. 1981. Comparative morphology and survival of chlamydospores of *Fusarium roseum "culmorum" and "graminearum*". Phytopathology. 71:85– 90

Skadsen, R. W., Sathish, P., Federico, M. L., Abebe, T., Fu, J., and Kaeppler, H. F. 2002. Cloning of the promoter for a novel barley gene, *Lem1*, and its organ-specific promotion of Gfp expression in lemma and palea. Plant Mol. Biol. 49:545–555

Smiley, R. W., Gourlie, J. A., Easley, S. A., Patterson, L.-M., and Whittaker, R. G. 2005. Crop damage estimates for crown rot of wheat and barley in the Pacific Northwest.

Somleva, M. N., and Blechl, A. E. 2005. The barley *Lem1* gene promoter drives expression specifically in outer floret organs at anthesis in transgenic wheat. Cereal Res. Commun. 33:665–671

SortInfo. Available at: https://sortinfo.dk/

Stack, R. W., Elias, E. M., Mitchell Fetch, J., Miller, J. D., and Joppa, L. R. 2002. Fusarium Head Blight reaction of langdon durum-*Triticum dicoccoides* chromosome substitution lines. Crop Sci. 42:637–642

Stephens, A. E., Gardiner, D. M., White, R. G., Munn, A. L., and Manners, J. M. 2008. Phases of infection and gene expression of *Fusarium graminearum* during crown rot disease of wheat. Mol. Plant-Microbe Interact. 21:1571–1581

Strange, R. N., and Smith, H. 1971. A fungal growth stimulant in anthers which predisposes wheat to attack by *Fusarium graminearum*. Physiol. Plant Pathol. 1:141–150

Streit, E., Schatzmayr, G., Tassis, P., Tzika, E., Marin, D., Taranu, I., Tabuc, C., Nicolau, A., Aprodu, I., Puel, O., and Oswald, I. P. 2012. Current situation of mycotoxin contamination and co-occurrence in animal feed focus on Europe. Toxins. 4:788–809

Tai, T. H., and Tanksley, S. D. 1990. A rapid and inexpensive method for isolation of total DNA from dehydrated plant tissue. Plant Mol. Biol. Report. 8:297–303

Taylor, R. J., and Secor, G. A. 1988. An improved diffusion assay for quantifying the polygalacturonase content of *Erwinia* culture filtrates. Phytopathology. 8:1101–1103

Tian, Y., Tan, Y., Liu, N., Liao, Y., Sun, C., Wang, S., and Wu, A. 2016. Functional agents to biologically control deoxynivalenol contamination in cereal grains. Front. Microbiol. 7:395

Tomassini, A., Sella, L., Raiola, A., D'Ovidio, R., and Favaron, F. 2009. Characterization and expression of *Fusarium graminearum* endo-polygalacturonases *in vitro* and during wheat infection. Plant Pathol. 58:556–564

Tunali, B., Obanor, F., Erginbas, G., Westecott, R. A., and Nicol, J. 2012. Fitness of three *Fusarium* pathogens of wheat. FEMS Microbiol. Ecolology. 81:596–609

Tundo, S. 2015. Exploitation of cell wall glycosidase inhibitors to improve wheat resistance against *Fusarium graminearum*. Dr. Thesis Diss. Univ. della Tuscia, Aix-Marseille Univ.

Tundo, S., Janni, M., Moscetti, I., Mandalá, G., Savatin, D., Blechl, A., Favaron, F., and D'Ovidio, R. 2016a. PvPGIP2 accumulation in specific floral tissues but not in the endosperm limits *Fusarium graminearum* infection in wheat. Mol. Plant-Microbe Interact. 29: 815-821

Tundo, S., Kalunke, R., Janni, M., Volpi, C., Lionetti, V., Bellincampi, D., Favaron, F., and Ovidio, R. D. 2016b. Pyramiding PvPGIP2 and TAXI-III but not PvPGIP2 and PMEI enhances resistance against *Fusarium graminearum*. Mol. Plant-Microbe Interact. 29:629–639

Tundo, S., Moscetti, I., Faoro, F., Lafond, M., Giardina, T., Favaron, F., Sella, L., and D'Ovidio, R. 2015. *Fusarium graminearum* produces different xylanases causing host cell death that is prevented by the xylanase inhibitors XIP-I and TAXI-III in wheat. Plant Sci. 240:161–169

U.S. Food and Drug Administration. 2010. Guidance for Industry and FDA: Advisory Levels for Deoxynivalenol (DON) in Wheat Finished Products for Human Consumption and Grains and Grain By-Products used for Animal Feed. Available at: https://www.fda.gov/Food/GuidanceRegulation/GuidanceDocumentsRegulatoryInformation/ChemicalContaminantsMetalsNaturalToxinsPesticides/ucm120184.htm

Ueno, Y., Nakajima, M., Sakai, K., Ishii, K., Sato, N., and Shimada, N. 1973. Comparative toxicology of trichothec mycotoxins : inhibition of protein synthesis in animal cells. J. Biochem. 74:285–296

Urban, M., Daniels, S., Mott, E., and Hammond-Kosack, K. 2002. *Arabidopsis* is susceptible to the cereal ear blight fungal pathogens *Fusarium graminearum* and *Fusarium culmorum*. Plant J. 32:961–73

Urban, M., King, R., Andongabo, A., Maheswari, U., Pedro, H., Kersey, P., and Hammond-Kosack, K. 2016. First draft genome sequence of a UK Strain (UK99) of *Fusarium culmorum*. Genome Announc. 4:e00771-16

Urbanek, H., and Yirdaw, G. 1978. Acid proteases produced and in infected seedlings. Physiol. Plant Pathol. 13:81–87

Urbanek, H., Zalewska-Sobczak, J., and Krzechowska, M. 1976. Exo-polygalacturonate Lyase of *Fusarium culmorum*. Bullettin l'Academie Pol. des Sci. 24:635–639

van Eeuwijk, F., Mesterhazy, A., Kling, C., Ruckenbauer, P., Saur, L., Bürstmayr, H., Lemmens, M., Keizer, L., Maurin, N., and Snijders, C. 1995. Assessing non specificity of resistance in wheat to head blight caused by inoculation with European strains of *Fusarium culmorum*, *F. graminearum* and *F. nivale* using a multiplicative model for interaction. Theor. Appl. Genet. 90:221–228

Van Der Hoorn, R. A. L., and Kamoun, S. 2008. From guard to decoy: a new model for perception of plant pathogen effectors. Plant Cell. 20:2009–2017

Van der Lee, T., Zhang, H., van Diepeningen, A., and Waalwijk, C. 2015. Biogeography of *Fusarium graminearum* species complex and chemotypes: a review. Food Addit. Contam. Part A. 32:453–460

Vasil, V., Srivastava, V., Castillo, A. M., Fromm, M. E., and Vasil, I. K. 1993. Rapid production of transgenic wheat plants by direct bombardment of cultured immature embryos. Nat. Biotechnol. 11:1553–1558

Vogel, J. 2008. Unique aspects of the grass cell wall. Curr. Opin. Plant Biol. 11:301–307

Voigt, C. A., Schäfer, W., and Salomon, S. 2005. A secreted lipase of *Fusarium graminearum* is a virulence factor required for infection of cereals. Plant J. 42:364–375

Voigt, C. A., Von Scheidt, B., Gàcser, A., Kassner, H., Lieberei, R., Schafer, W., and Salomon, S. 2007. Enhanced mycotoxin production of a lipase-deficient *Fusarium graminearum* mutant correlates to toxin-related gene expression. Eur. J. Plant Pathol. 117:1–12

Volpi, C., Janni, M., Lionetti, V., Bellincampi, D., Favaron, F., and Ovidio, R. D. 2011. The ectopic expression of a pectin methyl esterase inhibitor increases pectin methyl esterification and limits fungal diseases in wheat. Mol. Plant-Microbe Interact. 24:1012–1019

Wagacha, J. M., and Muthomi, J. W. 2007. *Fusarium culmorum* : Infection process , mechanisms of mycotoxin production and their role in pathogenesis in wheat. Crop Prot. 26:877–885

Waldron, B. L., Moreno-Sevilla, B., Anderson, J. A., Stack, R. W., and Frohberg, R. C. 1999. RFLP mapping of QTL for Fusarium head blight resistance in wheat. Crop Sci. 39:805–811

Walter, S., Brennan, J. M., Trognitz, F., Trognitz, B., Leonard, G., Egan, D., and Doohan, F. M. 2008. Components of the gene network associated with genotype-dependent response of wheat to the *Fusarium* mycotoxin deoxynivalenol. Funct. Integr. Genomics. 8:421–427

Walter, S., Kahla, A., Arunachalam, C., Perochon, A., Khan, M. R., Scofield, S. R., and Doohan, F. M. 2015. A wheat ABC transporter contributes to both grain formation and mycotoxin tolerance. J. Exp. Botany 66:2583-93

Wang, X., Jiang, N., Liu, J., Liu, W., and Wang, G.-L. 2014. The role of effectors and host immunity in plant-necrotrophic fungal interactions. Virulence. 5:722–32

Wanjiru, W. M., Zhensheng, K., and Buchenauer, H. 2002. Importance of cell wall degrading enzymes produced by *Fusarium graminearum* during infection of wheat heads. Eur. J. Plant Pathol. 108:803–810

Weeks, J. T., Anderson, O. D., and Blechl, A. E. 1993. Rapid production of multiple lndependent lines of fertile transgenic wheat (*Triticum aestivum*). Plant Physiol. 102:1077–1084

Wei, C.-M., Hansent, B. S., Vaughan, M. H., and Mclaughlin, C. S. 1974. Mechanism of action of the mycotoxin trichodermin, a 1 2,13-epoxytrichothecene. PNAS USA. 71:713–717

Wetterhorn, K. M., Newmister, S. A., Caniza, R. K., Busman, M., McCormick, S. P., Berthiller, F., Adam, G., and Rayment, I. 2016. Crystal Structure of Os79 (Os04g0206600) from *Oryza sativa*: A UDP-glucosyltransferase involved in the detoxification of deoxynivalenol. Biochemistry. 55:6175–6186

Willyerd, K. T., Li, C., Madden, L. V, Bergstrom, G. C., Ransom, J. K., Wegulo, S. N., Hershman, D. E., and Esker, P. D. 2012. Efficacy and stability of integrating fungicide and cultivar resistance to manage Fusarium head blight and deoxynivalenol in wheat. Plant Dis. 96:957–967

Windels, C. E. 2000. Economic and social impacts of Fusarium Head Blight: Changing farms and rural communities in the northern great plains. Phytopathology. 90:17–21

Xie, G., Zhang, M., Magner, T., Ban, T., Chakraborty, S., and Liu, C. 2006. Evidence that resistance to Fusarium head blight and crown rot are controlled by different genes in wheat. Pages 15–19 in: The Global Fusarium Initiative for International Collaboration: A Strategic Planning Workshop,T. Ban, J.M. Lewis, and E.E. Phipps, eds.CIMMYT, Batan, Mexico.

Xing, L., Qian, C., Cao, A., Li, Y., Jiang, Z., Li, M., Jin, X., Hu, J., Zhang, Y., Wang, X., Chen, P., and Picard, D. 2013. The *Hv-SGT1* Gene from *Haynaldia villos*a contributes to resistances towards both biotrophic and hemi-biotrophic pathogens in common wheat (*Triticum aestivum* L.). PLoS One. 8: e72571

Xue, S., Xu, F., Tang, M., Zhou, Y., Li, G., An, X., Lin, F., Xu, H., Jia, H., Zhang, L., Kong, Z., and Ma, Z. 2011. Precise mapping *Fhb5*, a major QTL conditioning resistance to *Fusarium* infection in bread wheat (*Triticum aestivum* L.). Theor Appl Genet. 123:1055–1063

Yang, Z. P., Gilbert, J., Somers, D. J., Fedak, G., Procunier, J. D., and Mckenzie, I. H. 2003. Marker assisted selection of Fusarium head blight resistance genes in two doubled haploid populations of wheat. Mol. Breed. 12:309–317

Yuen, G. Y., and Schoneweis, S. D. 2007. Strategies for managing Fusarium head blight and deoxynivalenol accumulation in wheat. Int. J. Food Microbiol. 119:126–130

Zadoks, J. C., Chang, T. T., and Konzak, C. F. 1974. A decimal code for the growth stages of cereals. Weed Res. 14:415–421

Zhao, Z., Liu, H., Wang, C., and Xu, J.-R. 2013. Comparative analysis of fungal genomes reveals different plant cell wall degrading capacity in fungi. BMC Genomics. 14:274

Zheng, Z., Kilian, A., Yan, G., and Liu, C. 2014. QTL conferring Fusarium crown rot resistance in the elite bread wheat variety EGA Wylie. PLoS One. 9:e96011

Zhu, X., Li, Z., Xu, H., Zhou, M., Du, L., and Zhang, Z. 2012. Overexpression of wheat lipid transfer protein gene *TaLTP5* increases resistances to *Cochliobolus sativus* and *Fusarium graminearum* in transgenic wheat. Funct. Integr. Genomics. 12:481–488

Zhuang, Y., Gala, A., and Yen, Y. 2013. Identification of functional genic components of major Fusarium Head Blight resistance quantitative trait loci in wheat cultivar Sumai 3. Mol. Plant-Microbe Interact. 442:442–450

# Supplementary materials

Fig. **SM-1**. Nucleotide sequence alignment of the coding sequence *HvUGT13248* optimized for wheat codon usage (upper line, in black) and original *HvUGT13248* (Accession number: GU170355; lower line, in blue). Sequences share an identity of 78.50% (1121/1428 bp). |represents nucleotide identity. *Bam*HI restriction site and the FLAG®-tag sequences are highlighted in grey and green, respectively, in the optimized sequence.

```
1      GGATCCATGGAGACCACCGTCACCGCCGTGTCGGGCACCACCTCATCGTCAGTCGGGCAT
       BamHI |||||||||||| |||||||| ||||| ||||||||    |||   ||||| |||
1      ......ATGGAGACCACGGTCACCGCGGTGTCAGGCACCACGAGCTCGAGCGTCGGCCAT

61     GGGGCGGGGGGGGGGGGCGGCCAGGGTCCTGCTGCTCCCATCCCCAGGCGCCCAGGGGCAC
       || || || || || || || || || ||||| || |||||   ||| || || ||||| |||
55     GGAGCCGGCGGCGGTGCTGCGAGAGTCCTCCTCCTCCCGAGCCCGGGAGCGCAGGGCCAC

121    ACCAACCCAATGCTGCAACTCGGCAGGAGGCTCGCGTACCATGGGCTGAGGCCAACCCTC
       |||||||| ||||| ||  | ||| |  | || |||||||| || ||  | || || |||
115    ACCAACCCGATGCTCCAGTTGGGCCGCCGCCTGGCGTACCACGGCCTCCGCCCCACACTC

181    GTGGCCACCCGCTACGTGCTGTCGACCACCCCAGCCCCAGGCGCGCCATTCGACGTGGCC
       || |||||||||||||||| || |||||||| ||||| || ||||| ||||||||||||
175    GTCGCCACCCGCTACGTGCTCTCCACCACCCCGGCCCCCGGTGCGCCCTTCGACGTGGCC

241    GCGATCTCAGACGGGTTCGACGCCGGCGGGATGGCGCTGTGCCCAGACCCGGCGGAGTAC
       |||||||| ||||| |||||||||||| || |||||  ||||||| |||||||||||||||
235    GCGATCTCCGACGGCTTCGACGCCGGTGGCATGGCCTTGTGCCCCGACCCGGCGGAGTAC

301    TTCTCCAGGCTCGAGGCCGTCGGCAGCGAGACCCTGAGGGAGCTCCTGCTCTCCGAGGCC
       |||||| |||| |||||||| |||  |||||| ||| |||||||||| || || |||||
295    TTCTCCCGGCTGGAGGCCGTGGGCTCCGAGACGCTGCGGGAGCTCCTCCTGTCGGAGGCG

361    AGGGCGGGCAGGCCAGTGCGGGTCCTCGTGTACGACGCCCACCTGGCCTGGGCGCGGAGG
        | |||||  |||| ||||| || || |||||||||| |||||||| ||||| ||| ||
355    CGCGCGGGGCGGCCCGTGCGCGTGCTGGTGTACGACGCTCACCTGGCGTGGGCACGGCGG

421    GTGGCCCAGGCGAGCGGCGTCGCCGCGGCCGCGTTCTTCTCCCAACCATGCAGCGTGGAC
       ||||| |||||   ||||||||| || || || |||||||||| || |||   ||||||
415    GTGGCACAGGCATCCGGCGTCGCGGCCGCGGCCTTCTTCTCCCAGCCGTGCTCGGTGGAC

481    GTGGTCTACGGCGAGCTCTGGGCCGGGAGGCTGGCCCTCCCAGCGACCGACGGCCGGGCC
       || |||||||| ||||| ||||| ||| ||||||| || || || || ||||| || ||
475    GTCGTCTACGGGGAGCTGTGGGCGGGGCGGCTGGCGCTGCCGGCCACGGACGGGCGCGCG

541    CTGCTCGCGAGGGGCGTCCTGGGGGTGGAGCTGGGCCTCGAGGACATGCCACCATTCGCC
       |||||||| || || || ||||| |||||||||| || |||||||||| || |||||
535    CTGCTCGCAAGAGGAGTGCTGGGCGTGGAGCTGGGGCTGGAGGACATGCCGCCGTTCGCA

601    GCGGTGCCAGAGTCCCAACCCGCGTTCCTCCAGGTCAGCGTGGGCCAATTCGAGGGGCTC
       |||||||| ||||| || || ||||||||||||||    || || || ||||||||||
595    GCGGTGCCGGAGTCGCAGCCGGCGTTCCTCCAGGTGTCAGTTGGGCAGTTCGAGGGGCTG

661    GACTACGCCGACGACGTCCTGGTGAACTCCTTCCGGGACATCGAGCCAAAGGAGGTGGAG
       |||||||||||||||| || || ||||| ||||| ||||||||||||||||||| |||
655    GACTACGCCGACGACGTGCTCGTCAACTCATTCCGTGACATCGAGCCAAAGGAGGTAGAG

721    TACATGGAGCTGACCTGGAGGGCCAAGATGGTCGGCCCAACCCTGCCATCGTACTACCTC
       |||||||| | || ||||| || |||||||| || |||||| ||||||| |||||||||
715    TACATGGAATTAACATGGAGAGCGAAGATGGTTGGACCAACCTTGCCATCATACTACCTC

781    GGCGACGGGAGGCTGCCGTCGAACAAGTCATACGGCCTGGACCTCTTCAACAGCGAGGTG
```

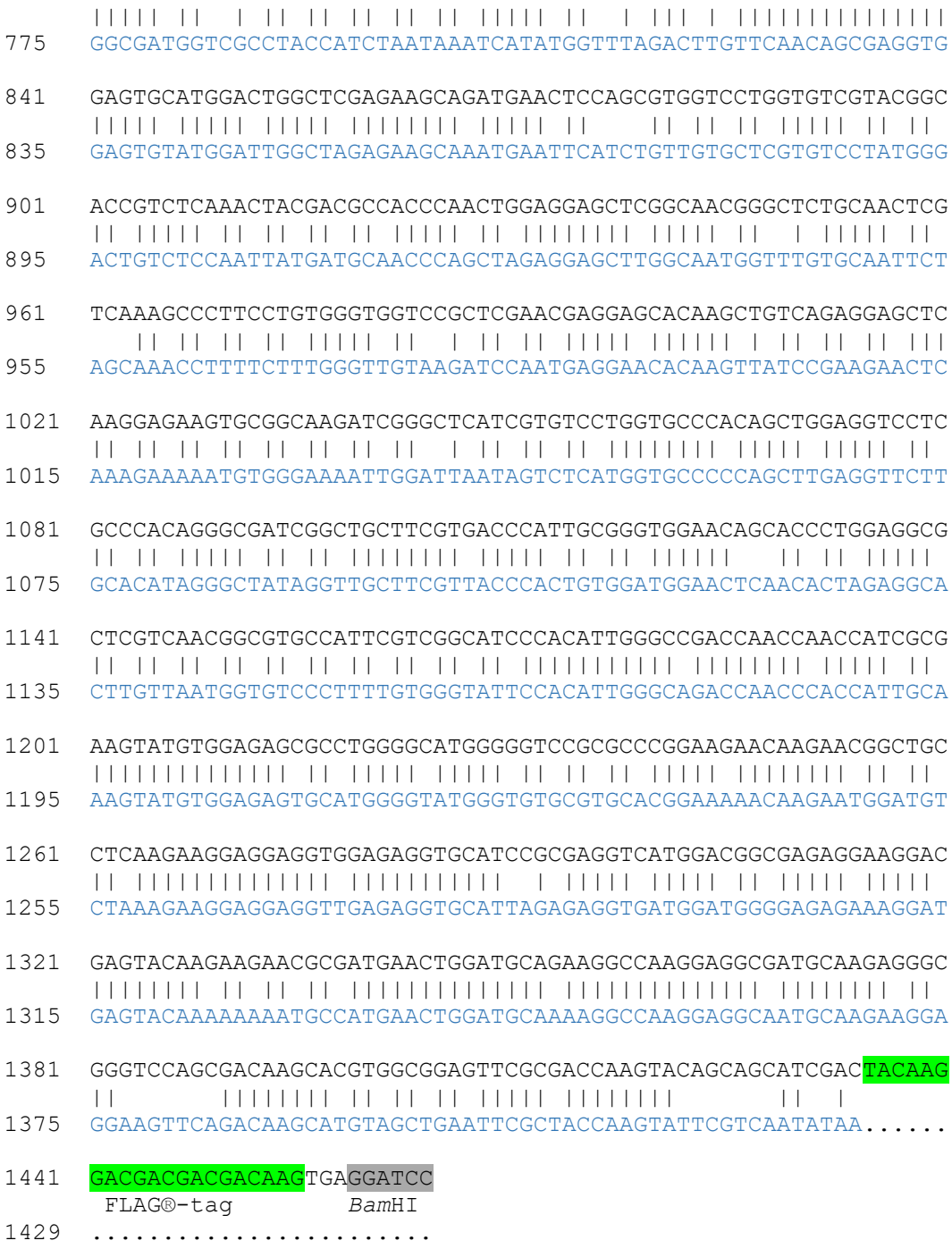
GGCGATGGTCGCCTACCATCTAATAAATCATATGGTTTAGACTTGTTCAACAGCGAGGTG
GAGTGCATGGACTGGCTCGAGAAGCAGATGAACTCCAGCGTGGTCCTGGTGTCGTACGGC
GAGTGTATGGATTGGCTAGAGAAGCAAATGAATTCATCTGTTGTGCTCGTGTCCTATGGG
ACCGTCTCAAACTACGACGCCACCCAACTGGAGGAGCTCGGCAACGGGCTCTGCAACTCG
ACTGTCTCCAATTATGATGCAACCCAGCTAGAGGAGCTTGGCAATGGTTTGTGCAATTCT
TCAAAGCCCTTCCTGTGGGTGGTCCGCTCGAACGAGGAGCACAAGCTGTCAGAGGAGCTC
AGCAAACCTTTTCTTTGGGTTGTAAGATCCAATGAGGAACACAAGTTATCCGAAGAACTC
AAGGAGAAGTGCGGCAAGATCGGGCTCATCGTGTCCTGGTGCCCACAGCTGGAGGTCCTC
AAAGAAAAATGTGGGAAAATTGGATTAATAGTCTCATGGTGCCCCCAGCTTGAGGTTCTT
GCCCACAGGGCGATCGGCTGCTTCGTGACCCATTGCGGGTGGAACAGCACCCTGGAGGCG
GCACATAGGGCTATAGGTTGCTTCGTTACCCACTGTGGATGGAACTCAACACTAGAGGCA
CTCGTCAACGGCGTGCCATTCGTCGGCATCCCACATTGGGCCGACCAACCAACCATCGCG
CTTGTTAATGGTGTCCCTTTTGTGGGTATTCCACATTGGGCAGACCAACCCACCATTGCA
AAGTATGTGGAGAGCGCCTGGGGCATGGGGGTCCGCGCCCGGAAGAACAAGAACGGCTGC
AAGTATGTGGAGAGTGCATGGGGTATGGGTGTGCGTGCACGGAAAAACAAGAATGGATGT
CTCAAGAAGGAGGAGGTGGAGAGGTGCATCCGCGAGGTCATGGACGGCGAGAGGAAGGAC
CTAAAGAAGGAGGAGGTTGAGAGGTGCATTAGAGAGGTGATGGATGGGGAGAGAAAGGAT
GAGTACAAGAAGAACGCGATGAACTGGATGCAGAAGGCCAAGGAGGCGATGCAAGAGGGC
GAGTACAAAAAAAATGCCATGAACTGGATGCAAAAGGCCAAGGAGGCAATGCAAGAAGGA
GGGTCCAGCGACAAGCACGTGGCGGAGTTCGCGACCAAGTACAGCAGCATCGACTACAAG
GGAAGTTCAGACAAGCATGTAGCTGAATTCGCTACCAAGTATTCGTCAATATAA.....
GACGACGACGACAAGTGAGGATCC
FLAG®-tag
BamHI
.....

Fig. **SM-2.** Amino acidic sequence alignment of the optimized HvUGT13248 (upper line, in black) and original HvUGT13248 (Accession number: GU170355; lower line, in blue). Sequences share an identity of 100% (474/474 aa).
|represents amino acidic identity. The FLAG®-tag sequence is highlighted in green in the optimized sequence.

```
1      METTVTAVSGTTSSSVGHGAGGGAARVLLLPSPGAQGHTNPMLQLGRRLAYHGLRPTLVA
       ||||||||||||||||||||||||||||||||||||||||||||||||||||||||||||
1      METTVTAVSGTTSSSVGHGAGGGAARVLLLPSPGAQGHTNPMLQLGRRLAYHGLRPTLVA

61     TRYVLSTTPAPGAPFDVAAISDGFDAGGMALCPDPAEYFSRLEAVGSETLRELLLSEARA
       ||||||||||||||||||||||||||||||||||||||||||||||||||||||||||||
61     TRYVLSTTPAPGAPFDVAAISDGFDAGGMALCPDPAEYFSRLEAVGSETLRELLLSEARA

121    GRPVRVLVYDAHLAWARRVAQASGVAAAAFFSQPCSVDVVYGELWAGRLALPATDGRALL
       ||||||||||||||||||||||||||||||||||||||||||||||||||||||||||||
121    GRPVRVLVYDAHLAWARRVAQASGVAAAAFFSQPCSVDVVYGELWAGRLALPATDGRALL

181    ARGVLGVELGLEDMPPFAAVPESQPAFLQVSVGQFEGLDYADDVLVNSFRDIEPKEVEYM
       ||||||||||||||||||||||||||||||||||||||||||||||||||||||||||||
181    ARGVLGVELGLEDMPPFAAVPESQPAFLQVSVGQFEGLDYADDVLVNSFRDIEPKEVEYM

241    ELTWRAKMVGPTLPSYYLGDGRLPSNKSYGLDLFNSEVECMDWLEKQMNSSVVLVSYGTV
       ||||||||||||||||||||||||||||||||||||||||||||||||||||||||||||
241    ELTWRAKMVGPTLPSYYLGDGRLPSNKSYGLDLFNSEVECMDWLEKQMNSSVVLVSYGTV

301    SNYDATQLEELGNGLCNSSKPFLWVVRSNEEHKLSEELKEKCGKIGLIVSWCPQLEVLAH
       ||||||||||||||||||||||||||||||||||||||||||||||||||||||||||||
301    SNYDATQLEELGNGLCNSSKPFLWVVRSNEEHKLSEELKEKCGKIGLIVSWCPQLEVLAH

361    RAIGCFVTHCGWNSTLEALVNGVPFVGIPHWADQPTIAKYVESAWGMGVRARKNKNGCLK
       ||||||||||||||||||||||||||||||||||||||||||||||||||||||||||||
361    RAIGCFVTHCGWNSTLEALVNGVPFVGIPHWADQPTIAKYVESAWGMGVRARKNKNGCLK

421    KEEVERCIREVMDGERKDEYKKNAMNWMQKAKEAMQEGGSSDKHVAEFATKYSSIDYKDD
       |||||||||||||||||||||||||||||||||||||||||||||||||||| FLAG®-tag
421    KEEVERCIREVMDGERKDEYKKNAMNWMQKAKEAMQEGGSSDKHVAEFATKYSS......

481    DDK

475    ...
```

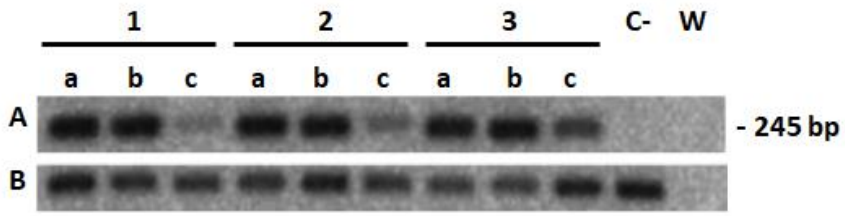


Fig. **SM-3.** PCR amplification products of DNA extracted from different spikelets of Ubi-UGT and control spike, point-inoculated with *F. graminearum* strain 3827, at the end of infection. **A)** Amplification of fungal *Tri6* gene; **B)** Amplification of plant *Actin* gene.
(1) *T. durum* cv Svevo; (2) ST7-56II; (3) ST7-47I; (C-) not infected spikelets; (W) water.
(a) Lower spikelet of the spike; (b) central spikelet of the spike (site of infection); (c) upper spikelet of the spike.

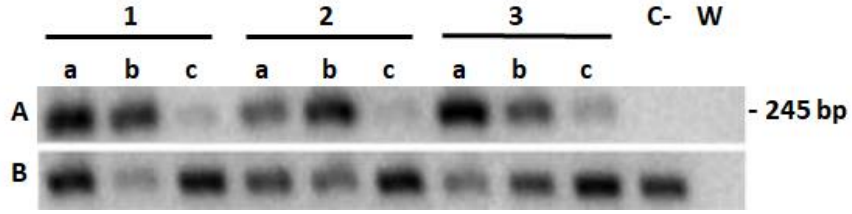


Fig. **SM-4.** PCR amplification products of DNA extracted from different spikelets of Lem-UGT and control spike, point-inoculated with *F. graminearum* strain 3827, at the end of infection. **A)** Amplification of fungal *Tri6* gene; **B)** Amplification of plant *Actin* gene.
(1) *T. aestivum* cv Bobwhite; (2) ST8-74; (3) ST8-49; (C-) not infected spikelets; (W) water.
(a) Lower spikelet of the spike; (b) central spikelet of the spike (site of infection); (c) upper spikelet of the spike.

# 7. Annex

In this section, results produced from a different work conducted at ISM2's laboratory (Aix-Marseille Université) during my PhD, will be illustrated.

## 7.1 Effect of the *Fusarium* mycotoxin deoxynivalenol on host innate immunity: modulation of the expression of defensins

### 7.1.1 Introduction

Mycotoxins are secondary metabolites produced by fungi. Among them, deoxynivalenol (DON) is of particular importance due to its prevalence and toxicity (see § 1.4). Fungi belonging to the *Fusarium* genus produce DON mainly on wheat, barley and corn, in order to contribute to phyto-pathogenesis (see § 1.4.1). One of the best known effect of DON is the inhibition of protein synthesis (Ueno et al. 1973; Wei et al. 1974; Payros et al. 2016) but, depending on dose and time of exposure, it could alter immune response and cause cell death, both on human/animal and plant cells (Desmond et al. 2008; Pestka 2010; Maresca 2013; Arunachalam and Doohan 2013; Payros et al. 2016).

The so-called innate immune system, the complex response that plants implement to counteract pathogens (see § 1.2), includes an important strategy for an active offense against invading pathogens: production of peptides and proteins with antimicrobial activities. The main groups of antimicrobial peptides (AMPs) are thionins, defensins and lipid transfer proteins (Castro and Fontes 2005). A database of plant AMPs is available (PhytAMP Database; Hammami et al. 2009). Plant defensins (PDFs) are small (~5 kDa), basic, cysteine-rich peptides with a widespread distribution in eukaryotes (Lay and Anderson 2005; Aerts et al. 2008). Although the amino acidic sequences present high variation among different PDFs, the global fold is conserved and is characterized by a cysteine-stabilized αβ (CSαβ) motif, formed with a βαββ configuration, and a ϒ-core motif GXC($X_{3-9}$)C; four disulfide bonds stabilize the structure and bind together the N- and C-terminal regions creating a pseudo-cyclic protein (Lay and Anderson 2005). Despite the precise mode of PDFs action is still not completely known, in general PDFs exhibit mainly an anti-fungal activity, acting by interaction with host membrane and induction of signaling cascades, i.e. to increase potassium efflux, calcium uptake and membrane permeabilization (Aerts et al. 2008; De Coninck et al. 2013). Usually, PDFs are constitutively expressed in storage and reproductive organs and/or induced upon pathogenic

attack, injuries, environmental stress and by signaling molecules, like hormones (reviewed by De Coninck et al. 2013).

In *Arabidopsis thaliana*, the *PDF* family is composed of more than 300 defensin-like genes (Silverstein et al. 2005). To date, however, about 15 *PDFs* encoding genes have been documented in *A. thaliana* (Thomma et al. 2002; Sels et al. 2008). According to phylogenetic analysis, *A. thaliana* PDFs (*AtPDFs*) can be classified into three families: *AtPDF-1*, *-2* and *-3.* Previous studies have shown that *AtPDF* genes are differentially expressed in different plant tissues and can be induced following infection by a number of pathogens (Sels et al. 2008). A summary of the *AtPDF* genes, location and mode of expression in provided in Table **A-1**. Although some of these PDFs demonstrated antifungal activity *in vitro* (in particular AtPDF 1.1, 1.2, 1.3 - Terras et al. 1993; Sels et al. 2007) and therefore can be involved in plant-pathogen interaction, the impact of mycotoxins like DON on PDFs expression has little been investigated so far. Nishiuchi et al. (2006) observed, by leaf infiltration of *Arabidopsis* plants, the effect of different trichothecenes on *PR1* and *AtPDF1.2* gene expression, respectively regulated by SA and JA/ET signaling pathways (Glazebrook 2001). Whereas type-A trichothecenes, like T-2 toxin, induced both pathways 48h after infusion, DON at 1 µM concentration failed the induction (Nishiuchi et al. 2006). In addition, increased doses of DON, tested up to 100 µM, did not up-regulate *PR1* expression. However, *AtPDF1.2* expression was not investigated in these conditions (Nishiuchi et al. 2006).

Table **A-1.** Overview of documented *A. thaliana* defensin genes with respective expression profile.

| **Defensin gene** | **Expression** | | **References** |
|---|---|---|---|
| | Constitutive | Inducible | |
| ***AtPDF1.1*** | **YES**<br>• Seed | **YES**<br>• Paraquat (ROS)<br>• MeJA + ET<br>• SA<br>• *Botrytis cinerea*<br>• *Cercospora beticola* (non-host)<br>• *Blumeria graminis*<br>• *Pectobacterium carotovorum* | Penninckx et al. 1996; Zimmerli et al. 2004; De Coninck et al. 2010; Hsiao et al. 2017 |
| ***AtPDF1.2a*** [+] | **NO** | **YES** (leaf)<br>• Paraquat (ROS)<br>• MeJA + ET<br>• *B. cinerea* | Penninckx et al. 1996; Epple et al. 1997; Penninckx et al. 1998; Zimmerli et al. 2004; De Coninck et al. 2010 |

| Defensin gene | Expression | | References |
|---|---|---|---|
| | Constitutive | Inducible | |
| | | • *Alternaria brassicicola*<br>• *F. oxysporum*<br>• *B. graminis* | |
| ***AtPDF1.2b*** [+] | **YES**<br>• leaf<br>• seed | **YES**<br>• *B. graminis* | Zimmerli et al. 2004; Sels et al. 2008 |
| ***AtPDF1.2c*** [+] | **nd** | **nd** | |
| ***AtPDF1.3*** | **NO** | **YES**<br>• *B. graminis* | Zimmerli et al. 2004; Sels et al. 2008 |
| ***AtPDF1.4*** | **YES**<br>• Seed | **NO** | Sels et al. 2008 |
| ***AtPDF1.5*** | **nd** | **nd** | Sels et al. 2008 |
| ***AtPDF2.1*** | **YES**<br>• root<br>• silique<br>• seed | **NO** | Thomma and Broekaert 1998 |
| ***AtPDF2.2*** | **YES**<br>• root<br>• silique<br>• flower<br>• leaf | **NO**<br>(downregulation upon *A. brassicicola* infection) | Thomma and Broekaert 1998 |
| ***AtPDF2.3*** | **YES**<br>• seedling<br>• flower<br>• siliques<br>• seed<br>• leaf<br>• stem | **NO** | Epple et al. 1997 |
| ***AtPDF2.4*** | **YES**<br>• flower | **NO** | Sels et al. 2008 |
| ***AtPDF2.5*** | **YES**<br>• root | **NO** | Sels et al. 2008 |
| ***AtPDF2.6*** | **YES**<br>• flower | **NO** | Sels et al. 2008 |
| ***AtPDF3.1*** | **YES**<br>(very low) | **NO** | Sels et al. 2008 |
| ***AtPDF3.2*** | **YES**<br>(very low) | **YES**<br>• SA | Sels et al. 2008 |

[+] *AtPDF1.2a*, *b* and *c* encode the same mature peptide.
nd: not detemined. MeJa: methyl jasmonate; ET: ethylene; SA: salicidic acid.

Persistence of DON in wheat based products causes several deleterious effects in human and animals, also depending on chronic or acute exposures (Pestka 2010; Maresca 2013;

see § 1.4). Moreover, DON exposure could lead to paradoxical effects being either immunostimulant or immunosuppressant, depending on dose, time and exposure frequency (Pestka et al. 2004). As an example, Wan et al. (2013) demonstrated that the *in vitro* exposition of porcine IPEC-J2 cell line to different *Fusarium* toxins among which DON, induces the *pBD-1* and *pBD-2* defensins after 48 hours, although the antibacterial activity of toxin-exposed supernatant reduced against *Escherichia coli*, as compared to the un-exposed supernatant. Moreover, recent findings suggested that DON exerts a role also in suppressing human and animal's innate immunity, as demonstrated by the inhibition of the intestinal expression of AMPs (unpublished results from ISM2's laboratory, Aix-Marseille Université). In particular, depending also on its concentration, DON elicits AMPs expression just after exposure, but, in consecutive time, it is able to inhibit the expression and secretion of constitutive or inducible AMPs, such as defensins and LL-37, both in *in vitro* Caco-2 human cells, in *ex vivo* pig explants and in pigs *in vivo* (Mandalà et al. 2016). In addition, DON inhibitory effect seemed to prevail on elicitor effect of immunostimulatory molecules. Indeed, *in vitro* cell exposed to DON for an extended time, failed to induce *AMPs* expression (M. Maresca, personal communication). These findings might explain the increased susceptibility to infections observed in DON-exposed animals (reviewed by Bondy and Pestka 2000; Payros et al. 2016).

Reflecting on animals and humans as beside/collateral targets of mycotoxins, and plants as primary target, we investigated if DON may have similar effect on plant innate immunity. Indeed, alteration of plant basal immune system could be an effective pathogens strategy for leading to an easier infection. To this aim, in the model plant *A. thaliana*, and in particular T87 cell line derived from it, the expression of a set of *AtPDF* genes was evaluated upon exposition to sub-lethal doses of DON. Furthermore, *Arabidopsis* cultures were also co-exposed to homogenate of *F. graminearum* and to DON, in order to investigate if DON can alter the plant response to *Fusarium* infection in term of defensin's expression.

### 7.1.2 Materials and Methods

#### 7.1.2.1 Cell cultures

*A. thaliana* T87 cell line (from Riken BRC Experimental Plant Division; Koyadai, Japan) were grown in 100 ml Gamborg's B5 with minimal organics medium (Sigma-Aldrich) supplemented with 1 mM NAA, 1.5% sucrose and 0.05% MES (final pH adjusted to 5.7) in sterile 250 ml Erlenmeyer flasks with continuous orbital shaking at 100 rpm under 18/6 h light at 22°C.

Subcultures were performed each 7 days by transferring 10 ml of 7-days old T87 culture to 90 ml of fresh medium. The 10 ml were collected by using a 10 ml serological pipette after waiting big aggregate setting down (about 1 min).

#### 7.1.2.2 Mycotoxin/*F. graminearum* treatments

DON (from Romer Lab) stock solution was prepared in ethanol as well as the serial dilutions. Homogenate of *F. graminearum* mycelium (Fg) was prepared as follow: 3 mg of 7-day old *F. graminearum* strain 3827 grown on PDA was moved to 2 ml lysing matrix D tube (MP Biomedicals) with 1 ml of sterilized water. Tube was homogenized by FastPrep 120 instrument (Thermo Scientific) by 3 cycles of 15 seconds shaking. Platting on PDA agar plates was used to confirm that *F. graminearum* did not survive to lysis and that homogenate do not contain any living fungi but only fungal constituents. DON or Fg, or both, were added to 3 ml of T87 cell suspension in 6-wells microplates, previously resuspended in fresh medium (see § 7.1.2.1). Cells were incubated for 1, 6, 24, or 72 h before evaluation of cell viability, using the Alamar blue assay, or quantification of gene expression, by quantitative real-time PCR (*q*RT-PCR).

#### 7.1.2.3 Cell viability assay

Alamar Blue (AB) assay was used to evaluate T87 cell viability upon DON treatments using the method described by Byth et al. (2001). Briefly, 1 ml of T87 cells, incubated with 0 M, 10 nM, 100 nM, 1 µM, 10 µM and 100 µM of DON, was collected in 1.5 ml Eppendorf tube after 1, 6, 24 and 72 h from the beginning of incubation. Tubes were centrifuged for 1 min at 2000 rpm and supernatant was discarded. Cells were washed twice in 1 ml of Phosphate Buffer Solution (PBS; 0.05 M, pH 7.45) and finally incubate for 1 h in 200 µl of PBS + 10% AB. Eppendorf tubes were then sonicated for 30 s, and centrifuged for 10 min at 12,000 rpm. Surnatant (100 µl) was transferred on 96-wells microplate for fluorimetric reading, performed with excitation at 560 nm and emission at 590 nm. Experiments were performed in duplicate. PBS + 10% AB was used as blank. Surnatants from T87 cell suspensions showed no significant auto-fluorescence.

#### 7.1.2.4 Quantification of *AtPDF* expression

Cells were lysed on ice using 500 ml of Tri reagent (Molecular Research Center). Total RNA was extracted using the RNeasy mini Kit (Qiagen) following the manufacturer's protocol. RNA

concentrations were quantified at 260 nm using NanoDrop™ (Thermo Scientific) spectrophotometer and purity was assessed by the $A_{260}/A_{280}$nm ratio. Reverse transcription was performed on 1 µg of total RNA by using SuperScript VILO cDNA synthesis kit (Invitrogen) according to the manufacturer's instructions. Gene expression analysis was carried out using *q*RT-PCR on a LightCycler 480 instrument II (Roche Applied Science). One µL of cDNA was incubated in the presence of LightCycler 480 SYBR Green I Master (Roche Applied Science) and 0.5 µM of each primer (Table **A-2**). Amplification program was performed as follows: initial denaturation at 94°C for 5min; 45 cycles consisting of denaturation at 94°C for 10 s, annealing at the selected temperature (see Table **A-2**) for 10 s, and extension at 72°C for 30 s. Data were collected using the Light Cycler 480 software (Roche Applied Science), and all experiments were performed in triplicate. Target mRNA levels were normalized to *AtACT2* mRNA level (housekeeping gene) and the relative quantification was performed using the comparative $2^{-\Delta\Delta Ct}$ method (Livak and Schmittgen 2001).

Table **A-2.** Primer list used for *q*RT-PCR.

| **Gene** (Accession no.) | **Primer name** | **Sequence 5'-3'** | **Annealing temp.** | **Amplicon size (bp)** |
|---|---|---|---|---|
| ***AtAct2*** (AT3G18780.2) | ACT2F | CCGCTCTTTCTTTCCAAGC | 60°/63° | 78 |
| | ACT2R | CCGGTACCATTGTCACACAC | | |
| ***AtPDF1.1*** (AT1G75830.1) | PDF1.1F | TTGTTTTCTTTGCTGCTCTTGA | 63° | 112 |
| | PDF1.1R | TTCTTGCACGCGTTACTGTT | | |
| ***AtPDF1.4*** (AT1G19610.1) | PDF1.4F | GCTCTTCCTTTGCCTCTCCA | 63° | 136 |
| | PDF1.4R | GCACGTTCCCATCTCTTACAC | | |
| ***AtPDF1.5*** (AT1G55010.1) | PDF1.5F | TTGAAGCACCGACAATTGTG | 63° | 140 |
| | PDF1.5R | CCACCAGCGCAATATCCATC | | |
| ***AtPDF2.2*** (AT2G02100.1) | PDF2.2F | TATTCGTCGCCACTGGGATG | 60° | 78 |
| | PDF2.2R | ACTCACGCATGTACCCTTGA | | |
| ***AtPDF2.3*** (AT2G02130.1) | PDF2.3F | CATTGCCACAGGGATGGGTC | 60° | 151 |
| | PDF2.3R | ACGGAATCCACGGCATTTACC | | |

#### 7.1.2.5 Statistical analyses

Statistical analyses were performed using SYSTAT12 software (Systat Software Incorporated, San Jose, CA, USA). All data were subjected to analysis of variance (ANOVA) followed by pairwise analysis, carried out by the Tukey Honestly Significant Difference test (Tukey test) at 0.95 confidence level.

### 7.1.3 Results

*A. thaliana* T87 cell culture was exposed to 1, 10 and 100 µM of DON and/or to homogenate of *F. graminearum*, for 24 hours (h). The mentioned DON concentration are not lethal for *A. thaliana* T87 cells, at least until 72 h in the case of DON 100 µM (Fig. **A-1**). The duration of the treatment was chosen since all the analyzed genes resulted differently expressed 24 h after DON-treatments (data not shown).

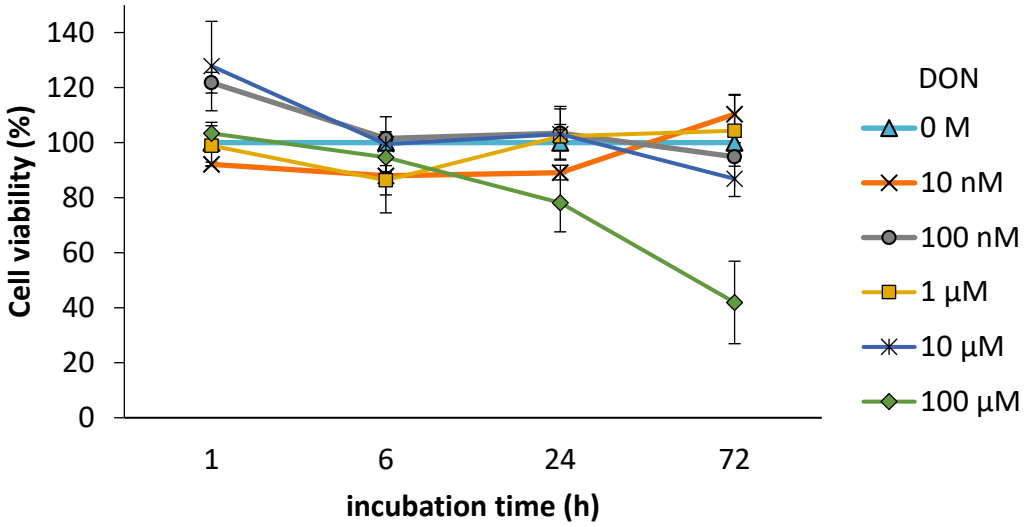


Fig. **A-1.** T87 cell viability (%) upon treatment with DON at different concentrations.
Data represent fluorescent unit normalized with 0 M DON incubation, considered as 100 %.

Relative expression of the different plant defensins *AtPDF1.1*, *AtPDF1.4*, *AtPDF1.5*, *AtPDF2.2* and *AtPDF2.3* (Fig. **A-2**) showed that all the analyzed defensins underwent variation in their expression depending on the different exposures compared to the respective mock treatments. Differential expression response of *AtPDFs* was observed within the different DON concentration (Fig. **A-2**A), except for *AtPDF1.5* that showed an high variability of induction between 1 and 10 µM of DON exposure, but a clear induction at 100 µM. The lowest DON concentration did not cause repression of the other analyzed genes, as compared to the respective mock treatments, whereas *AtPDF1.1*, *AtPDF1.4* and *AtPDF2.2* were progressively repressed with increasing DON concentrations (Fig. **A-2**A). On the other hand, *AtPDF2.3* showed variability of response to the various DON concentrations; indeed it resulted repressed in presence of 10 µM DON but again little overexpressed in presence of 100 µM DON, as compared to the mock treatments (Fig. **A-2**A).

The incubation of homogenate of *F. graminearum* mycelium (Fg) triggered in *A. thaliana* cells a clear induction of class 1 defensins, a small response in *AtPDF2.2* expression and the repression of *AtPDF2.3* (Fig. **A-2**B).

The co-exposure of T87 cells to homogenate of Fg and different doses of DON (Fg+DON) for 24 hours reveals a different response of *AtPDF* expression (Fig. **A-2**C), as compared to the cells exposed individually to the Fg homogenate (Fig. **A-2**B) or DON (Fig. **A-2**A). In general, little difference of expression can be observed with the combination Fg+DON 1 µM, except for *AtPDF2.3*, as compare to DON 1 µM exposure alone. Greater differences can be observed with the co-exposure of Fg+DON 10 µM and Fg+DON 100 µM, as follows reported: i) *AtPDF1.1* overexpression caused by Fg alone is enhanced by DON presence. ii) *AtPDF1.4* followed the same pattern of expression caused by the DON exposure alone, not exhibiting the high up-regulation followed by Fg incubation. iii) *AtPDF1.5* response to Fg+DON is similar to the respective single exposure until 10 µM DON concentration. Fg+DON 100 µM caused a complete new response down-regulating the *AtPDF1.5* expression. iv) *AtPDF2.2* expression showed a progressive overexpression, increasing DON concentration with Fg, oppositely to the individual DON exposures. v) Finally, *AtPDF2.3* resulted again clearly repressed between DON 1 and 10 µM, as for Fg individual incubation, but almost not variable from the mock treatment with Fg+DON 100 µM co-incubation.

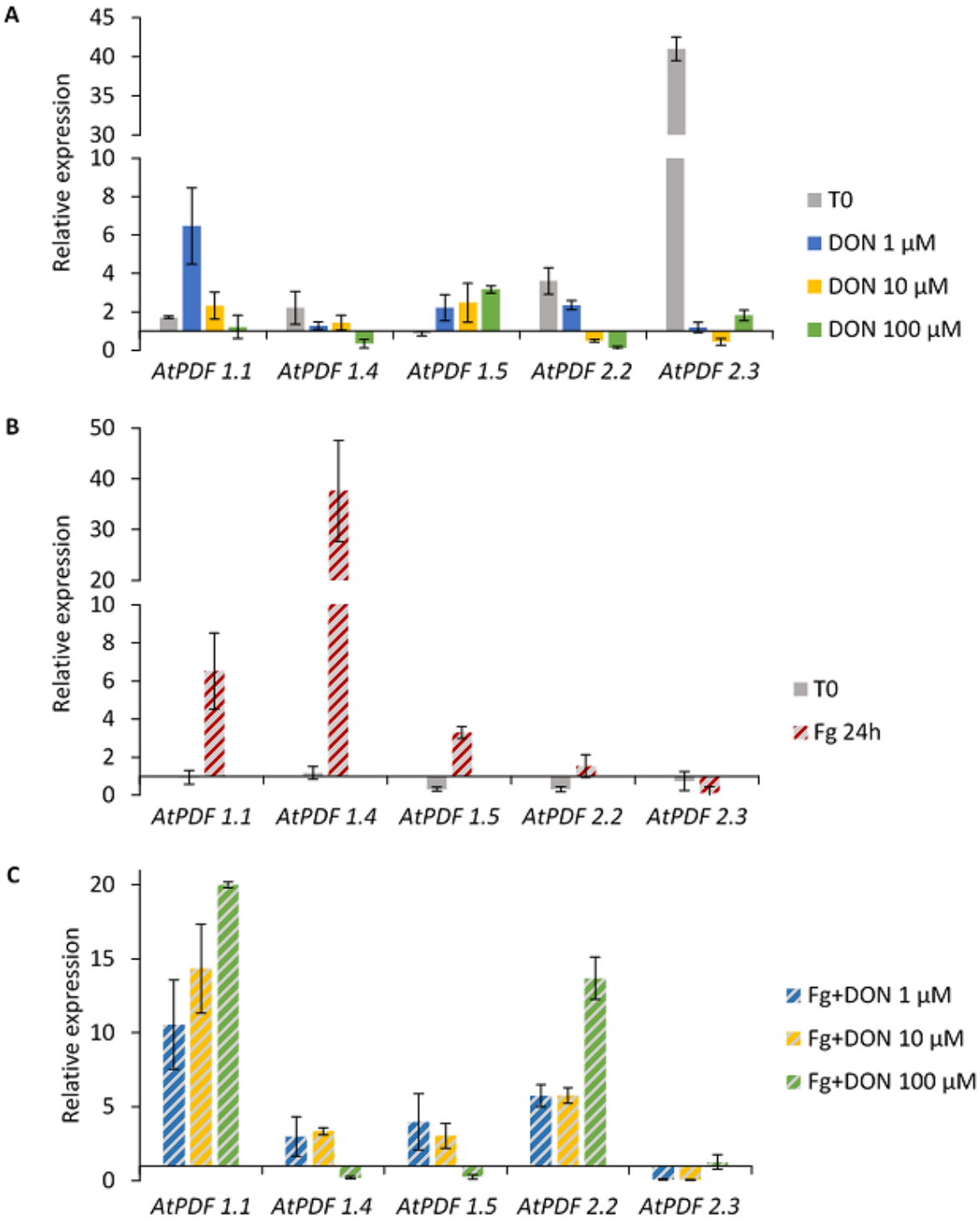


Fig. **A-2.** Relative expression of plant defensins (*AtPDF*) in *A. thaliana* T87 cell line exposed for 24 h to **A)** DON at 1, 10 or 100 µM; **B)** 3 mg of homogenized mycelium of *F. graminearum* (Fg); **C)** the combination of treatments performed in A) and B).
Bars represent means ± standard deviation of three independent experiment. All data were normalized with the housekeeping *AtACT2* gene expression. T0 represents the differential expression at the beginning of the experiment compared to: A) the mock treatment after 24 h; B) the Fg exposure. All graphs represent the relative expression as compared to the corresponding mock buffer: ethanol for DON; sterile water for Fg; the combination of the two previous mock buffer for Fg+DON

### 7.1.4 Discussion and conclusions

Living organisms are continuously exposed to attacks from pathogens. Their interaction mainly consist of a complex network of preventive measures, attacks, responses and contro-reactions. The failure even of one of their actions may lead to death both of the sides. An ancient defense mechanism shared by plants, invertebrate and vertebrate animals is innate immunity. It consists of both constitutive and inducible mechanisms against pathogens, among which AMPs, and in particular defensins, consist in a direct offence to pathogens. The use of *in vitro* system is a useful and simple method to verify and to demonstrate perturbation of cell response to different molecules, like hormones, xenobiotic, effectors, etc.

In this work, we investigated defensin response of *A. thaliana* T87 cell line to the *Fusarium* mycotoxin DON, alone and with fungal presence. Our results showed that *F. graminearum* mycelium triggers a host immunity response, in particular up-regulating family *AtPDF-1* genes. In accordance to this result, previous works showed an induction of several *AtPDF-1* genes (Penninckx et al. 1996; Zimmerli et al. 2004; De Coninck et al. 2010; Sels et al. 2008) but not of *AtPDF-2* ones (Thomma and Broekaert 1998; Sels et al. 2008) upon different pathogen infections.

On the other hand, defensin genes resulted in general down-regulated by the presence of DON, but the response differed in relation to different doses. However, not all *AtPDF* genes were suppressed, revealing possible attempt of plant cell counteraction against mycotoxin presence.

Finally, the reaction to the co-presence of *F. graminearum* and DON at 10 and 100 µM, differed between the various genes as compared singly to fungal or DON respectively. Indeed, in some cases the induction or repression of *AtPDFs* was amplified by the co-exposure, suggesting a synergic DON-fungal action on host immune system. In other cases, DON-modulated expression seemed to prevail on fungal-related one, suggesting the occurrence of a specific response to the mycotoxin. In accordance to latter observation, it is known that DON contributes to fungal infection (see § 1.4.1) and the impairment of immune response to fungal presence, caused by DON, might be involved in causing host susceptibility.

Taken all together, our results demonstrate that plant innate immunity, here represented by defensin expression, is altered upon pathogen and DON exposure, singly or in combination. Therefore, this work provides evidences of DON role in suppressing innate immunity mechanism in plant and therefore in contributing to infection progress. Further studies using

*in vivo* expression analysis on model plants and on commodity crops, susceptible to *Fusarium* diseases, will be useful to confirm our preliminary observation and to uncover possible additional targets for increasing pathogen resistance.

### 7.1.5 Bibliography


Aerts, A. M., Francois, I. E. J. A., Cammue, B. P. A., and Thevissen, K. 2008. The mode of antifungal action of plant, insect and human defensins. Cell. Mol. Life Sci. 65:2069–2079

Arunachalam, C., and Doohan, F. M. 2013. Trichothecene toxicity in eukaryotes: Cellular and molecular mechanisms in plants and animals. Toxicol. Lett. 217:149–158

Bondy, G. S., and Pestka, J. J. 2000. Immunomodulation by fungal toxins. J. Toxicol. Environ. Health. 3:109–143

Byth, H. A., Mchunu, B. I., Dubery, I. A., and Bornman, L. 2001. Assessment of a simple, non-toxic Alamar Blue cell survival assay to monitor tomato cell viability. Phytochem. Anal. 12:340–346

Castro, M. S., and Fontes, W. 2005. Plant Defense and Antimicrobial Peptides. Protein Pept. Lett. 12:11–16

De Coninck, B. D. E., Cammue, B. P. A., and Thevissen, K. 2013. Modes of antifungal action and in planta functions of plant defensins and defensin-like peptides. Fungal Biol. Rev. 26:109–120

De Coninck, B. M. A., Sels, J., Venmans, E., Thys, W., Goderis, I. J. W. M., Carron, D., Delaure, S. L., Cammue, B. P. A., De Bolle, M. F. C., and Mathys, J. 2010. *Arabidopsis thaliana* plant defensin AtPDF1.1 is involved in the plant response to biotic stress. New Phytol. 187:1075–1088

Desmond, O. J., Manners, J. M., Stephens, A. E., Maclean, D. J., Schenk, P. M., Gardiner, D. M., Munn, A. L., and Kazan, K. 2008. The *Fusarium* mycotoxin deoxynivalenol elicits hydrogen peroxide production, programmed cell death and defence responses in wheat. Mol. Plant Pathol. 9:435–445

Epple, P., Apel, K., and Bohlmann, H. 1997. ESTs reveal a multigene family for plant defensins in *Arabidopsis thaliana*. FEBS Lett. 400:168–172

Glazebrook, J. 2001. Genes controlling expression of defense responses in *Arabidopsis* — 2001 status. Curr. Opin. Plant Biol. 4:301–308

Hammami, R., Ben Hamida, J., Vergoten, G., and Fliss, I. 2009. PhytAMP: a database dedicated to antimicrobial plant peptides. Nucleic Acids Res. 37:D963–D968

Hsiao, P. Y., Cheng, C. P., Wee Koh, K., and Chan, M. T. 2017. The *Arabidopsis* defensin gene, *AtPDF1.1*, mediates defence against *Pectobacterium carotovorum* subsp. *carotovorum* via an iron-withholding defence system. Sci. Rep. 23:9175

Lay, F., and Anderson, M. 2005. Defensins - Components of the Innate Immune System in Plants. Curr. Protein Pept. Sci. 6:85–101

Livak, K. J., and Schmittgen, T. D. 2001. Analysis of relative gene expression data using real-time quantitative PCR and the $2^{-\Delta\Delta Ct}$ method. Methods. 25:402–408

Mandalà, G., Pinton, P., Giardina, T., D'Ovidio, R., Oswald, I., and Maresca, M. 2016. Modulation de l'expression des peptides antimicrobiens intestinaux chez l'Homme et le porc par le déoxynivalénol. in: 6ème journée Mycotoxines, Toulouse 15-16 Mars 2016.

Maresca, M. 2013. From the gut to the brain: Journey and pathophysiological effects of the food-associated trichothecene mycotoxin deoxynivalenol. Toxins (Basel). 5:784–820

Nishiuchi, T., Masuda, D., Nakashita, H., Ichimura, K., Shinozaki, K., Yoshida, S., Kimura, M., Yamaguchi, I., and Yamaguchi, K. 2006. *Fusarium* phytotoxin trichothecenes have an elicitor-like activity in *Arabidopsis thaliana*, but the activity differed significantly among their molecular species. Mol. Plant-Microbe Interact. 19:512–520

Payros, D., Alassane-Kpembi, I., Pierron, A., Loiseau, N., Pinton, P., and Oswald, I. P. 2016. Toxicology of deoxynivalenol and its acetylated and modified forms. Arch. Toxicol. 90:2931–2957

Penninckx, I. A. M. A., Eggermont, K., Terras, F. R. G., Thomma, B. P. H. J., De Samblanx, G. W., Buchala, A., Métraux, Jean-Pierre, Manners, J. M., and Broekaert, W. F. 1996. Pathogen-Induced systemic activation of a plant defensin gene in *Arabidopsis* follows a salicylic acid-independent pathway. Plant Cell. 8:2309–2323

Penninckx, I. A. M. A., Thomma, B. P. H. J., Buchala, A., Métraux, J., and Broekaert, W. F. 1998. Concomitant activation of jasmonate and ethylene response pathways is required for induction of a plant defensin gene in *Arabidopsis*. Plant Cell. 10:2103–2113

Pestka, J. J. 2010. Deoxynivalenol: Mechanisms of action, human exposure, and toxicological relevance. Arch. Toxicol. 84:663–679

Pestka, J. J., Zhou, H. R., Moon, Y., and Chung, Y. J. 2004. Cellular and molecular mechanisms for immune modulation by deoxynivalenol and other trichothecenes: unraveling a paradox. Toxicol. Lett. 153:61–73

PhytAMP Database. Available at: http://phytamp.hammamilab.org/main.php

Sels, J., Delairé, S. L., Aarts, A. M., Proost, P., Cammue, B. P. A., and De Bolle, M. F. C. 2007. Use of a PTGS-MAR expression system for efficient in planta production of bioactive Arabidopsis thaliana plant defensins. Transgenic Res. 16:531–538

Sels, J., Mathys, J., De Coninck, B. M. A., Cammue, B. P. A., and De Bolle, M. F. C. 2008. Plant pathogenesis-related (PR) proteins : A focus on PR peptides. Plant Physiol. Biochem. 46:941–950

Silverstein, K. A. T., Graham, M. A., Paape, T. D., and Vandenbosch, K. A. 2005. Genome organization of more than 300 defensin-like genes in *Arabidopsis*. Plant Physiol. 138:600–610

Terras, F. R. G., Torrekens, S., Van Leuven, F., Osborn, R. W., Vanderleyden, J., Cammue, B. P. A., and Broekaert, W. F. 1993. A new family of basic cysteine-rich plant antifungal proteins from *Brassicaceae* species. FEBS Lett. 316:233–240

Thomma, B. P. H. J., and Broekaert, W. F. 1998. Tissue-specific expression of plant defensin genes *PDF2.1* and *PDF2.2* in *Arabidopsis thaliana*. Plant Physiol. Biochem. 36:533–537

Thomma, B. P. H. J., Bruno, A., Cammue, P. A., and Thevissen, K. 2002. Plant defensins. Planta. 216:193–202

Ueno, Y., Nakajima, M., Sakai, K., Ishii, K., Sato, N., and Shimada, N. 1973. Comparative toxicology of trichothec mycotoxins : inhibition of protein synthesis in animal cells. J. Biochem. 74:285–296

Wan, M. L. Y., Woo, C.-S. J., Allen, K. J., Turner, P. C., and El-Nezami, H. 2013. Modulation of porcine β-defensins 1 and 2 upon individual and combined *Fusarium* toxin exposure in a swine jejunal epithelial cell line. Appl. Environ. Microbiol. 79:2225–32

Wei, C. M., Hansent, B. S., Vaughan, M. H., and Mclaughlin, C. S. 1974. Mechanism of action of the mycotoxin trichodermin, a 1 2,13-epoxytrichothecene. PNAS USA. 71:713–717

Zimmerli, L., Stein, M., Lipka, V., Schulze-Lefert, P., and Somerville, S. 2004. Host and non-host pathogens elicit different jasmonate/ethylene responses in *Arabidopsis*. Plant J. 40:633–646